

Experimental and computational studies of calcium-triggered transmitter release

by

Soyoun Cho

BS, Seoul National University, 1997

MS, Seoul National University, 1999

Submitted to the Graduate Faculty of
Arts and Sciences in partial fulfillment
of the requirements for the degree of
Doctor of Philosophy

University of Pittsburgh

2007

UNIVERSITY OF PITTSBURGH
SCHOOL OF ARTS AND SCIENCES

This dissertation was presented

by

Soyoun Cho

It was defended on

August 2, 2007

and approved by

Committee Chairperson: Nathaniel N. Urban, Ph.D.

German Barrionuevo, M.D.

Guo-Qiang Bi, Ph.D.

Karl Kandler, Ph.D.

Joel R. Stiles, M.D. Ph.D.

Harold L. Atwood, Ph.D., D.Sc., F.R.S.C.

Dissertation Advisor: Stephen D. Meriney, Ph.D.

Experimental and computational studies of calcium-triggered transmitter release

Soyoun Cho, PhD

University of Pittsburgh, 2007

Calcium influx through presynaptic calcium channels triggers transmitter release, but many of the details that underlie calcium-triggered secretion are not well understood. In an attempt to increase our understanding of this process, synaptic transmission at the frog neuromuscular junction has been investigated using physiological experiments and computational modeling. Pharmacological manipulations ((R)-roscovitine and DAP) were used as tools to modulate presynaptic calcium influx and study effects on transmitter release. I showed that (R)-roscovitine predominately slowed deactivation kinetics of calcium current (by 427%), and as a result, increased the integral of calcium channel current evoked by a physiological action potential waveform (by 44%). (R)-roscovitine also increased the quantal content of acetylcholine released from the motor nerve terminals (by 149%) without changing paired-pulse facilitation under low calcium conditions. In contrast, exposure to 3,4-diaminopyridine (which affects transmitter release evoked by partially blocking potassium channels, altering the amplitude of the presynaptic action potential, and indirectly increasing calcium entry) increased paired-pulse facilitation (by 23%). In normal calcium conditions, both pharmacological treatments showed relatively similar effects on paired-pulse facilitation. I used a computational model, constrained by previous reports in the literature and my physiological measurements, to simulate my experimental data. This model faithfully reproduced calcium current with a single action potential, the average number of released synaptic vesicles, and the effects of (R)-

roscovitine and DAP on calcium influx and vesicle release. Using this model, I made several predictions about the mechanisms underlying transmitter release. First, calcium ions originating from one or two voltage-gated calcium channels most often contributed to cause the fusion of each vesicle. Second, the calcium channel closest to a vesicle that fuses, provides 77% of calcium ions. My simulation of paired-pulse facilitation using the present model needed more adjustments, and in the process of adjusting the model parameters, various hypotheses that might explain observed short-term synaptic plasticity, including the effects of changes in buffer conditions, the effects of uneven calcium channel distribution, reducing terminal volume by adding vesicles to a storage pool, changes in the second action potential waveform, and possible persistent changes in vesicle release machinery were explored.

TABLE OF CONTENTS

1. INTRODUCTION	1
1.1 OVERVIEW	1
1.2 CALCIUM INFLUX AND TRANSMITTER RELEASE	2
1.2.1 Neurotransmitter release at the nerve terminal.....	2
1.2.2 Quantitative relationship between calcium and transmitter release.....	8
1.3 VOLTAGE-GATED CALCIUM CHANNELS	10
1.3.1 Classification, structures, and functions.....	10
1.3.2 Channelopathy involving the voltage-gated calcium channel.....	11
1.4 SHORT-TERM SYNAPTIC PLASTICITY	15
1.5 FROG NEUROMUSCULAR JUNCTION MODEL SYSTEM	16
1.6 ROSCOVITINE	19
1.7 GOALS OF THE DISSERTATION	22
2. ROSCOVITINE EFFECTS ON CALCIUM CHANNEL ACTIVITIES	23
2.1 INTRODUCTION	23
2.2 METHODS	26
2.2.1 Cell culture of frog motoneurons and muscle cells.....	26
2.2.2 Recording and analysis of currents through calcium channels.....	26
2.2.3 Reagents.....	29

2.3	RESULTS	29
2.4	DISCUSSION	39
3.	ROSCOVITINE EFFECTS ON TRANSMITTER RELEASE AND SHORT-TERM PLASTICITY	43
3.1	INTRODUCTION	43
3.2	METHODS	45
3.2.1	Tissue preparation.....	45
3.2.2	Recording and analysis of transmitter release.	45
3.2.3	Reagents.....	46
3.3	RESULTS	46
3.3.1	Roscovitine effects on neurotransmitter release.....	46
3.3.2	Roscovitine effects on short-term plasticity.....	52
3.4	DISCUSSION	57
4.	COMPUTATIONAL MODELING OF THE ADULT FROG NEUROMUSCULAR JUNCTION	63
4.1	INTRODUCTION	64
4.1.1	Overview of Monte Carlo simulation of cellular microphysiology	64
4.1.2	MCell input and output files	64
4.1.3	Three dimensional model of a frog neuromuscular junction active zone..	66
4.1.4	Temporal and spatial resolution of the active zone model.....	72
4.1.5	Excessive number of calcium binding sites on each vesicle.....	72
4.2	METHODS	74
4.2.1	Tissue preparation.....	74

4.2.2	Confocal microscopy	74
4.2.3	Two-electrode voltage clamp experiments.....	75
4.2.4	Modeling of calcium channel activity and vesicle release	76
4.2.5	Simulation and data analysis	82
4.3	RESULTS	82
4.3.1	Physiology and anatomy of the adult frog neuromuscular junction	82
4.3.2	Modeling of calcium influx.....	88
4.3.3	Modeling of vesicle release during a single action potential	91
4.3.4	MCell simulation of paired-pulse stimulation at the frog neuromuscular junction.....	100
4.4	DISCUSSION	110
5.	GENERAL DISCUSSION	121
5.1	ROSCOVITINE, AS A NOVEL TOOL TO STUDY PRESYNAPTIC CALCIUM CHANNELS AND SYNAPTIC TRANSMISSION	121
5.2	ROSCOVITINE EFFECTS ON CA _v 2 CHANNELS ARE REMINISCENT OF BAYK 8644 EFFECTS ON CA _v 1 CHANNELS.....	123
5.3	CLINICAL ASPECTS REGARDING NEUROMUSCULAR WEAKNESS.....	124
5.4	GLYCEROTOXIN.....	125
5.5	COMPLEMENTARY EXPERIMENTAL AND COMPUTATIONAL STUDIES OF THE SYNAPSE	126
	BIBLIOGRAPHY	132

LIST OF TABLES

Table 1 Summary of voltage-gated calcium channel nomenclature, pharmacological blockers, distribution and functions.	14
Table 2 MCell simulation reproduced transmitter release by single action potential.....	95
Table 3 Manipulations of active zone parameters and their resulting paired-pulse ratio.	109

LIST OF FIGURES

Figure 1 The synaptic vesicle cycle.....	7
Figure 2 Structure and subunit composition of voltage-gated calcium channels.	13
Figure 3 Frog neuromuscular junction.....	18
Figure 4 Structures of (R)-, (S)- roscovitine and olomoucine.....	21
Figure 5 Effects of 100 μ M (R)-roscovitine on calcium channel current recorded from the somata of cultured frog motoneurons.	34
Figure 6 Changes in the proportion of calcium current activated following action potentials of various durations at half amplitude in cultured motoneurons.	36
Figure 7 1 μ M DAP effects on calcium influx and the proportion of calcium current activated following action potentials of various durations at half amplitude in cultured motoneurons.	38
Figure 8 Effects of (R)-roscovitine on EPP amplitude at the adult frog neuromuscular junction.	49
Figure 9 Comparison of the effects of (R)-roscovitine, (S)-roscovitine, and olomoucine on neurotransmitter release at the adult frog neuromuscular junction.....	50
Figure 10 Effects of (R)-roscovitine and DAP on the paired-pulse ratio at the adult frog neuromuscular junction recorded in 0.3 mM Ca^{2+}	54
Figure 11 The effects of (R)-roscovitine on paired-pulse ratio in 1.8mM Ca^{2+}	55

Figure 12 The effects of DAP on paired-pulse ratio in 1.8mM Ca ²⁺	56
Figure 13 Schematic diagram of calcium entry and vesicle release with a single action potential before (control) and after roscovitine and DAP treatment.	61
Figure 14 Multiple views of active zone model.	70
Figure 15 Close-up view from within the synaptic cleft.....	71
Figure 16 Calcium channel gating model and rate parameters.....	80
Figure 17 Vesicle release schemes.....	81
Figure 18 Projections of confocal image stacks of a frog neuromuscular junction.....	84
Figure 19 Frequency distribution for the number of active zones per nerve terminal.....	85
Figure 20 Two-electrode voltage clamp recordings of EPCs and mEPCs.....	86
Figure 21 Frequency distribution for quantal content per nerve terminal per single action potential in 1.8 mM Ca ²⁺	87
Figure 22 MCell simulated presynaptic calcium currents.....	89
Figure 23 Comparison of MCell simulated variability in control synaptic delay with experimental measurements.....	96
Figure 24 The percentage of vesicle fusion events triggered by calcium ions originating from the indicated numbers of calcium channels in the active zone.	97
Figure 25 Relative location of calcium channel contribution to vesicle release.	99
Figure 26 The action potential waveforms used for the action potential broadening manipulations.....	106
Figure 27 Vesicle release schemes for persistent conformational change of SNARE complexes.	107
Figure 28 Effect of 1 µg/ml glycerotoxin on calcium currents.	131

1. INTRODUCTION

1.1 OVERVIEW

Voltage-gated calcium channels open when an action potential invades the presynaptic nerve terminal and depolarizes the membrane. Subsequent calcium influx through the open channel triggers neurotransmitter release. Presynaptic calcium influx is the critical signal that controls communication throughout the nervous system. Although this process has been studied for a long time, many details still remain unclear. Due to the importance of this basic aspect of synaptic physiology, the study of the calcium regulation of transmitter release remains an active research area.

In this thesis, calcium regulation of transmitter release at the frog neuromuscular junction has been investigated using electrophysiology and computational modeling. To manipulate presynaptic calcium influx, two pharmacological tools were used. Previous work has shown that roscovitine, an inhibitor of cyclin-dependent kinase (cdk), might directly affect calcium channels in a cdk-independent way. Thus, I characterized the effects of roscovitine on calcium entry through voltage-gated calcium channels and on transmitter release. Using roscovitine as a tool, additional underlying mechanisms that control calcium entry, transmitter release, and short-term synaptic plasticity were elucidated further at the frog neuromuscular junction. The effect of 3,4-diaminopyridine (DAP), a potassium channel blocker, was also investigated as a contrasting

drug. DAP increased presynaptic calcium influx indirectly by altering the action potential waveform and DAP has been shown to increase transmitter release in many preparations (Hue et al., 1976; Jankowska et al., 1977; Guerrero and Novakovic, 1980; Kim et al., 1980; Matsumoto and Riker, 1983; Augustine GJ, 1990; Barish et al., 1996; Seo et al., 1999; Gu et al., 2004). Because DAP showed similar effects on transmitter release to roscovitine at the adult frog neuromuscular junction, but works by different underlying mechanisms, DAP was chosen as a contrasting drug in this study.

The work described in this dissertation is focused on exploring underlying mechanisms of neurotransmission and short-term plasticity. The physiological and theoretical questions I have addressed will increase our understanding of the neuromuscular junction synapse.

1.2 CALCIUM INFLUX AND TRANSMITTER RELEASE

1.2.1 Neurotransmitter release at the nerve terminal

The essential role of calcium ions in triggering neurotransmitter release has been studied for many years (Katz and Miledi, 1965b; Dodge and Rahamimoff, 1967; Katz and Miledi, 1970). The influx of calcium through voltage-gated calcium channels in the presynaptic terminal is the transduction mechanism that links the action potential with neurotransmitter release (Augustine et al., 1987). As such, voltage-gated calcium channels at active zone regions of the adult frog nerve terminal play an important role as one of the elements of the vesicle release machinery (Stanley, 1997).

Calcium entry through voltage-gated calcium channels increases the intracellular calcium

concentration (to approximately $\sim 10 \mu\text{M}$) in a spatially restricted area near the intracellular face of the calcium channel. This area is known as a microdomain (Stanley, 1997; Llinas and Moreno, 1998; Bertram et al., 1999; Schneggenburger and Neher, 2005). Because the calcium sensor for neurotransmitter release is thought to be positioned very close to these calcium channels, the presynaptic action potential triggers transmitter release within a millisecond (Borst and Sakmann, 1996). In fact, the delay between calcium influx and the fusion of synaptic vesicles can be as little as 60-350 μsec and this suggests that calcium ions diffuse less than 100 nm to trigger the exocytosis of synaptic vesicles (Llinas et al., 1981; Heidelberger et al., 1994; Sabatini and Regehr, 1996; Neher, 1998). Given the homeostatic calcium handling mechanisms present within the nerve terminal, free ionic calcium cannot diffuse great distances in this environment. The spatially-restricted and temporally-confined local calcium signal is thought to interact with a nearby vesicular membrane protein (synaptotagmin) that initiates the process that leads to the fusion of neurotransmitter-containing vesicles.

The movement of vesicles through the neuron's cytoplasm is highly regulated and most vesicles are not immediately available for release. Vesicles must be tethered, docked and primed before release occurs with action potential stimulation (Figure 1). Vesicles are thought to reside in distinct pools, such as the readily releasable pool and the reserve pool, though the terminology can be different (Zucker and Regehr, 2002; Rizzoli and Betz, 2005). Vesicles in the readily releasable pool seem to be docked and primed for release and immediately available upon stimulation. Only about 1% of all vesicles reside in the readily releasable pool (Mennerick and Matthews, 1996; Neves and Lagnado, 1999; Schneggenburger et al., 1999; Delgado et al., 2000; Rettig and Neher, 2002; Richards et al., 2003; Rizzoli and Betz, 2004). There is also a pool of recycling vesicles (10-20% of total vesicles) that can be quickly prepared for fusion (Rizzoli and

Betz, 2004, 2005). The reserve pool generally makes up about 80-90% of total vesicles. Vesicles in the reserve pool only can be released during intense stimulation (Neves and Lagnado, 1999; Delgado et al., 2000; Richards et al., 2000). In my computational model (chapter 4), each active zone has 26 docked and primed vesicles.

Cytoskeletal elements, such as actin, myosin and motor proteins, play important roles in the transport of vesicles. The disassembly of the actin network controls the transit of vesicles from the reserve pool to the readily releasable pool and this process can be regulated by calcium and ATP (Mulholland et al., 1997; Prekeris and Terrian, 1997; Trifaro et al., 1997; Bajjalieh, 1999; Ryan, 1999). A complex of proteins, called the “exocyst” interacts with the cytoskeleton to target vesicles to the active zone. Rab-3 may regulate the alignment of vesicles in the active zone and assist in the displacement of n-sec-1 from syntaxin (this step is often called tethering). Then, syntaxin and SNAP25 bind to VAMP to form the CORE complex. This step “docks” a vesicle to the release site, which contains the presynaptic calcium channels. Priming is a preparing step in which the CORE complex binds synaptotagmin (the calcium sensor) and provides a calcium-sensitive clamp that holds vesicle back from fusion until calcium influx occurs. Calcium binding to synaptotagmin is thought to cause cytoplasmic domains of synaptotagmin to insert into the plasma membrane, promoting vesicle fusion (Martens et al., 2007). After fusion of vesicles, cytoplasmic NSF/ α -SNAP are thought to dissociate the CORE complex so that vesicles and their associated membrane proteins can be recycled (see Figure 1; Bajjalieh, 1999; Chapman 2002; O’Conner and Lee, 2002).

Based on its ability to bind to calcium, and to link calcium influx and vesicle fusion, the best candidate calcium sensor for transmitter release is synaptotagmin. Synaptotagmin is a vesicle membrane protein with two cytoplasmic calcium-binding motifs, called C2 domains (the

C2A and C2B domains; Perin et al., 1990; Geppert et al., 1991). Among 16 identified vertebrate isoforms, the most abundant isoform is synaptotagmin 1, which is thought to function as a calcium sensor regulating fast exocytosis of synaptic vesicles (Geppert et al., 1991; Brose et al., 1992; Ullrich et al., 1994; Davis et al., 1999; Craxton, 2004; Hui et al., 2005). The functions of the remaining synaptotagmin isoforms are less well understood and they are differentially expressed in the nervous system. Despite incomplete information, synaptotagmin 2 seems functionally similar to synaptotagmin 1 (Sugita et al., 2002; Hui et al., 2005; Xu et al., 2007) but synaptotagmin 5-7, 10 appear to be related with asynchronous release of transmitter (Hui et al., 2005). Synaptotagmin 4 is predominantly expressed postsynaptically and functions as a postsynaptic calcium sensor to release retrograde signals that enhance presynaptic release (Adolfson et al., 2004; Yoshihara et al., 2005).

Synaptotagmin 1 has 5 calcium binding sites; the C2A domain binds 3 calcium ions and the C2B domain binds 2 calcium ions (Sudhof and Rizo, 1996; Ubach et al., 1998; Fernandez et al., 2001) and a recent study suggests that each docked vesicle has 5 to 8 SNARE complexes and associated synaptotagmin molecules (Han et al., 2004). Both C2 domains have low intrinsic affinity for calcium ions. In synaptotagmin 1, K_D values for C2A are $\sim 60 \mu\text{M}$, $400 \mu\text{M}$, and more than 1 mM and K_D values for C2B are $\sim 300\text{-}400 \mu\text{M}$ and $\sim 500\text{-}600 \mu\text{M}$ (Ubach et al., 1998; Davis et al., 1999; Fernandez et al., 2001). The affinity for calcium ions of C2 domains strongly increases into physiological ranges when the C2 domains bind to phospholipids in plasma membrane. Under these phospholipid binding conditions, the overall calcium affinity of the C2 domains increases up to 5000 fold ($K_D = 5\text{-}50 \mu\text{M}$) because additional coordination sites for calcium ions are probably provided by the negatively charged phospholipid headgroups (Brose et al., 1992; Davletov and Sudhof, 1993; Zhang et al., 1998; Fernandez-Chacon et al.,

2001; Gerber et al., 2002; Sugita et al., 2002). Other synaptic molecules binding with synaptotagmin, such as syntaxin, SNAP-25, and intracellular domains of the voltage-gated calcium channel, also affect calcium binding affinity of C2 domains (Chapman et al., 1995, 1998; Li et al., 1995; Kee and Scheller, 1996; Schiavo et al., 1997). The calcium binding affinities described above may be relative values rather than absolute, because they depend on the composition of the phospholipid membranes (Zhang et al., 1998; Fernandez-Chacon et al., 2001; Sugita et al., 2002). Depending on the exact lipid composition of the fusion sites, which is unclear, the real affinities may vary by a factor of 2-4 (Sugita et al., 2002). Calcium binding and unbinding rates have been less studied than calcium binding affinity (K_D value). A previous study (Davis et al., 1999) measured the response time of the synaptotagmin C2 domain and demonstrated that the synaptotagmin C2A domains could respond rapidly to both increases and decreases in calcium concentration; rapidly enough to fit known rates for calcium-triggered vesicle fusion. They also showed that calcium binding triggered synaptotagmin penetration into membrane, and led to simultaneous binding to the SNARE complex (Davis et al., 1999). In this dissertation, I used predicted calcium binding and unbinding rates to synaptotagmin in modeling the calcium sensors on synaptic vesicles in my computational model.

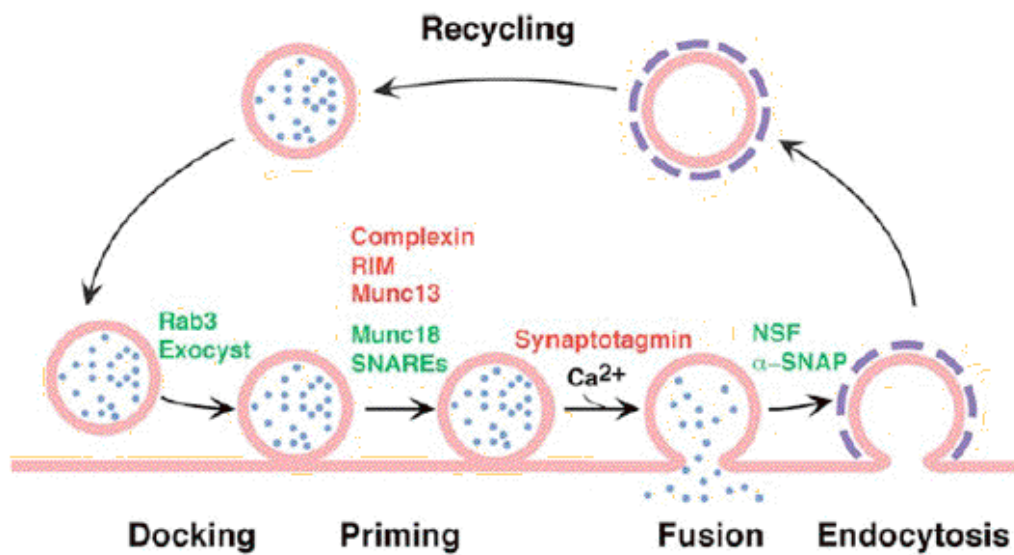


Figure 1 The synaptic vesicle cycle.

Protein components of the vesicle release machinery participate in the steps of docking, priming, fusion, endocytosis, and recycling. This thesis is focused on the calcium-dependent mechanisms that occur between priming and fusion. From Li and Chin (2003).

1.2.2 Quantitative relationship between calcium and transmitter release

The precise order of the dependence of transmitter release on calcium concentration varies among different synapses and different measuring methods. However, a nonlinear relationship between calcium concentration and transmitter release is consistently observed across various synapses and species, including the squid giant synapse (Lester, 1970; Llinas et al., 1981; Smith et al., 1985; Augustine et al., 1985; Stanley, 1986), the crayfish neuromuscular junction (Dudel, 1981; Parnas et al., 1982), the calyx of Held (Barnes-Davis et al., 1995; Schneggenberger and Neher, 2000) and hippocampal CA3-CA1 synapses (Wu and Saggau, 1994). The frog neuromuscular junction shows a 4th order cooperative relationship between the postsynaptic response, which is measured as endplate potential (EPP) amplitude, and the extracellular calcium concentration. That is, doubling calcium influx results in a 16-fold increase in transmitter release (Jenkinson, 1957; Katz and Miledi, 1965b; Dodge and Rahamimoff, 1967; Andreu and Barrett, 1980; Barton et al., 1983). Based on these observations, it has been inferred that 3 to 5 calcium ions trigger the release of a synaptic vesicle (Dodge and Rahamimoff, 1967; Stanley, 1986; Heidelberger et al., 1994; Bollmann et al., 2000; Schneggenberger and Neher, 2000; Shahrezaei et al., 2006). However, this conclusion has been called into question by modeling work suggesting that measured calcium cooperativity for transmitter release may not reflect the exact number of calcium binding sites (Barton et al., 1983; Zucker et al., 1991; Pattillo, 2002; Pattillo et al., 2007). That is, 4 calcium-binding sites may not be sufficient to explain the 4th order relationship. At this point, it is probably safer to say that the non-linear relationship between calcium and transmitter release requires that multiple calcium ions bind to cause fusion, but that number might be greater than previously predicted. Though synaptotagmin

is the leading candidate for the calcium sensor that triggers transmitter release, synaptotagmin may not be the only determinant of the cooperative relationship between calcium and transmitter release. Manipulations of VAMP and syntaxin expression levels have also been shown to alter the calcium-release cooperativity (Stewart et al., 2000). These data suggest that SNARE proteins, as well as synaptotagmin, are important for determining the cooperative relationship between calcium and transmitter release. However, it may be that by altering the expression levels of SNARE proteins, the number of synaptotagmin molecules associated with those SNARE complexes has been altered. In this case, changes in cooperativity may still be governed by the number of synaptotagmin molecules associated with each docked vesicle.

The number of calcium channels that contribute to the release of a single vesicle also seems different among various synapses (Llinas et al., 1981; Adler et al., 1991; Quastel et al., 1992; Stanley, 1993, 1997; Borst and Sakmann, 1996; Neher, 1998; Mulligan et al., 2001; Fedchyshyn and Wang, 2005) but still remains unclear. The “single-channel domain” hypothesis, which suggests that calcium influx through a single calcium channel triggers the release of a vesicle, and the “overlapping domain” hypothesis, which suggests that multiple calcium channels contribute to the fusion of a single vesicle and overlapping calcium domains is required to trigger release, are competing. At the frog neuromuscular junction, a recent study showed that one or two calcium channels contribute to fusion of a single synaptic vesicle (Shahrezaei et al., 2006), which supports previous predictions (Yoshikami et al., 1989).

Based on the non-linear dependence of transmitter release on calcium entry as well as the tight temporal and spatial relationship between calcium and transmitter release, even slight modifications of presynaptic calcium influx would be expected to significantly affect transmitter release.

1.3 VOLTAGE-GATED CALCIUM CHANNELS

1.3.1 Classification, structures, and functions

Voltage-gated calcium channels can be classified as high-voltage activated (HVA) or low-voltage activated (LVA) calcium channels (Hagiwara et al., 1975; Llinas and Yarom, 1981). HVA calcium channels are activated by more depolarized membrane voltages (e.g. -20 mV) and these channel types can be involved in the regulation of neurotransmitter release and muscle contraction. L-type, N-type, P/Q-type, and R-type calcium channels are included in the HVA class of calcium channels. In contrast, LVA calcium channels activate at more hyperpolarized membrane voltages (e.g. -70 mV). LVA calcium channels (predominantly the T-type) play an important role in generating repetitive electrical activity (Tsien et al., 1988).

At the adult frog neuromuscular junction, the N-type channel is thought to exclusively control transmitter release (Kerr and Yoshikami, 1984; Robitaille et al., 1990). In developing synapses of the *Xenopus* frog neuromuscular junction preparation, additional types of channels, such as L-type, may also contribute to the control of transmitter release (Yazejian et al., 1997; Thaler et al., 2001; Sand et al., 2001).

Voltage-gated calcium channels are comprised of the principal pore-forming $\alpha 1$ subunit, and auxiliary subunits β , $\alpha 2\delta$, and γ (Figure 2; Hofmann et al., 1999; Catterall, 2000; Spafford and Zamponi, 2003). The electrophysiological and pharmacological characteristics of calcium channels are determined by the pore-forming $\alpha 1$ subunit. The basic structure of voltage-gated calcium channels is homologous with voltage-gated sodium and potassium channels. In all of these cases, the pore-forming subunit contains 4 transmembrane domains and each domain has 6 transmembrane segments. The fourth segment (S4), which is positively charged, works as a

voltage sensor (Guy and Conti, 1990; Dewaard et al., 1996) and a pore loop is created between the fifth (S5) and the sixth (S6) segments (Heinemann et al., 1992). Genes that code for the $\alpha 1$ subunit are also used to classify channel types. The Ca_v1 family is composed of the various L-type channels. $Ca_v2.1$ is P/Q-type, $Ca_v2.2$ is N-type, and $Ca_v2.3$ is the R-type calcium channel. T-type calcium channels are in the Ca_v3 family (Table 1; Ertel et al., 2000). All of the work in this thesis is focused on the N-type ($Ca_v2.2$) calcium channel. This channel is associated closely with the proteins on vesicles that regulate calcium-triggered secretion by a synaptic integration site on the cytoplasmic loop between domains 2 and 3 (see Figure 2).

1.3.2 Channelopathy involving the voltage-gated calcium channel

Dysfunctions of many kinds of ion channels result in diseases, also called channelopathies. Channelopathies involving calcium channels include Lambert Eaton Myasthenic syndrome (LEMS). LEMS is an autoimmune disorder of the neuromuscular junction characterized by a reduced number of normally functioning presynaptic calcium channels (Lambert et al., 1956; Flink and Atchison, 2002). Antibodies in patients with LEMS seem to target, among other proteins, the P/Q-type channels that trigger release at mammalian neuromuscular junctions (Lennon et al., 1995; Pinto et al., 2002). Patients with LEMS have symptoms such as skeletal muscle weakness, decreased tendon reflexes, and various dysautonomias. Electrophysiological studies have identified a presynaptic decrease in the quantal content of evoked transmitter release from presynaptic nerve terminals as the cause of skeletal muscle weakness (Vincent et al., 1989). Freeze fracture electron microscopy has revealed that the functional decrease in quantal content in this disorder is associated with a decrease in the

number and organization of active zone particles that are thought to include presynaptic calcium channels (Fukunaga et al., 1982; 1983). The mechanism underlying the disruption of active zone structure and the decrease in quantal content is hypothesized to be removal of calcium channels from the cell membrane by antibody-mediated cross-linking of calcium channel proteins followed by cellular endocytosis (Lambert et al., 1988; Kim and Neher, 1988; Smith et al., 1995; Peers et al., 1993; Meriney et al., 1996).

In terms of therapy, one strategy is to increase the magnitude of transmitter release with each action potential. Guanidine hydrochloride, that blocks selectively presynaptic potassium channels, broadens the presynaptic action potential, and thus increases calcium influx and transmitter release, is occasionally prescribed in the United States (Matthews and Wickelgren, 1977; Anderson and Harvey, 1988). While guanidine has been shown to be effective in treating LEMS, it has many side-effects (Silbert et al., 1990; Sanders, 1995; Oh et al., 1997). Aminopyridines (such as DAP) are also selective potassium channel blockers and have been used to treat LEMS. However, DAP has been shown to have side effects including fatigue and/or deterioration of muscle strength (Lundh et al., 1993). It is expected that a selective calcium channel agonist (perhaps a derivative of (R)-roscovitine), if it can be developed, might provide the best treatment for LEMS. In this context, some of the data in this study might be helpful in the exploration of potential treatment strategies for channelopathy involving voltage-gated calcium channels and neuromuscular weakness, including LEMS.

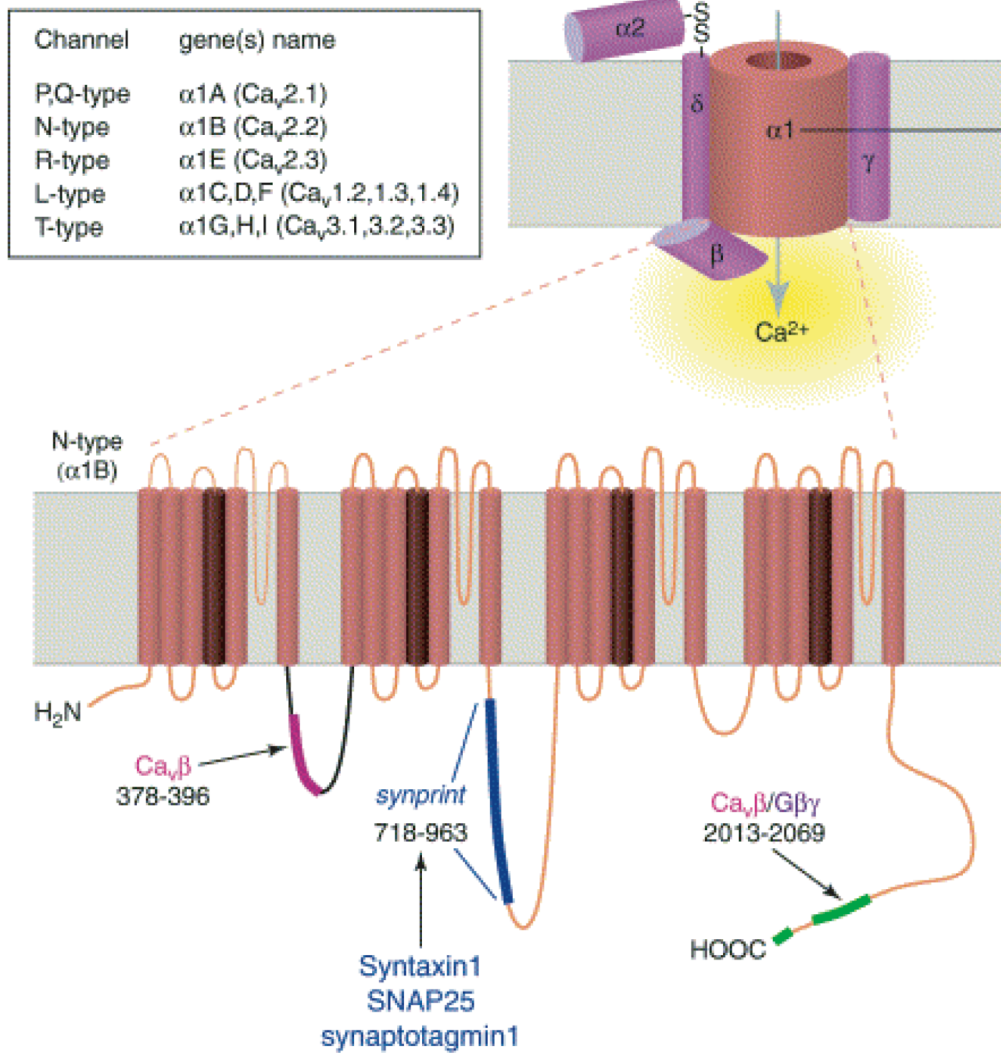


Figure 2 Structure and subunit composition of voltage-gated calcium channels.

Voltage-gated calcium channels consist of pore-forming $\alpha 1$ subunit, and auxiliary subunits β , $\alpha 2\delta$, and γ . The $\alpha 1$ subunit contains 4 transmembrane domains, and N-type calcium channel is tightly associated with SNARE proteins involved in vesicle fusion by their binding to the amino acid sequences in the cytoplasmic loop between the 3rd and 4th domain (a synaptic protein interaction site; synprint). Modified from Spafford and Zamponi (2003).

Nomenclature		Primary localization	Functions	Specific blocker	
HVA	L	Ca _v 1.1	Skeletal muscle	Excitation-contraction coupling Calcium homeostasis Gene regulation	Di-hydropyridine
		Ca _v 1.2	Cardiac muscle Endocrine cells Neurons	Excitation-contraction coupling Hormone secretion Gene regulation	
		Ca _v 1.3	Endocrine cells Neurons	Hormone secretion Gene regulation	
		Ca _v 1.4	Retina	Tonic neurotransmitter release	
	P/Q	Ca _v 2.1	Nerve terminals Dendrites	Neurotransmitter release Dendritic Ca ²⁺ transients	ω-Agatoxin
	N	Ca _v 2.2	Nerve terminals Dendrites		ω-Conotoxin GVIA
	R	Ca _v 2.3	Cell bodies Dendrites Nerve terminals	Ca ²⁺ dependent action potentials Neurotransmitter release	SNX-482
LVA	T	Ca _v 3.1	Cardiac muscle Skeletal muscle Neurons	Repetitive firing Dendritic signaling	None
		Ca _v 3.2	Cardiac muscle Neurons		
		Ca _v 3.3	Neurons		

Table 1 Summary of voltage-gated calcium channel nomenclature, pharmacological blockers, distribution and functions.

Adapted from Lacinova (2005), and Catterall (2000).

1.4 SHORT-TERM SYNAPTIC PLASTICITY

Communication between cells, or synaptic transmission, is not fixed in strength. Physiological activity patterns lead to changes in synaptic strength at all types of synapses. Some synapses show increased neurotransmitter release with repeated stimulation. At other synapses, a reduction in neurotransmitter release occurs. These alterations in synaptic strength are often termed “facilitation” for increases, or “depression” for decreases. The mechanisms that underlie all of these processes probably occur at every synapse, but the observed behavior is a mix of the offsetting strengths of these influences. In general, at synapses with a high probability of release, depression dominates, while synapses with a low release probability tend to show facilitation (Thomson, 2000; Xu-Friedman and Regehr, 2004).

While manipulating the release probability by changing the extracellular calcium concentration can alter the form of short-term plasticity that dominates at synapses, there are also physiologically relevant manipulations that can change these plastic events as well. Possible physiologically relevant regulation sites for short-term synaptic plasticity include changes in the waveform of the presynaptic action potential (Jackson et al., 1991; Borst et al., 1995; Borst and Sakmann, 1999; Poage and Zengel, 2002), changes in calcium influx (Borst and Sakmann, 1998; Cuttle et al., 1998; Forsythe et al., 1998; Patil et al., 1998), the size of readily releasable pool (Betz, 1970; Ryan et al., 1993; Ryan and Smith, 1995), neuromodulators (Stefani et al., 1996; Takahashi et al., 1996; Scanziani et al., 1997; Wang and Lambert, 2000), internal calcium storage within mitochondria (Magnus and Keizer, 1997; Levy et al., 2003; Talbot et al., 2003; Tong, 2007) , and postsynaptic receptors (Katz and Thesleff, 1957; Trussell et al., 1993). It is widely accepted that intra-terminal residual calcium from previous action potentials causes activity-dependent synaptic enhancement, though underlying mechanisms of these dynamic

changes in synaptic strength are not well understood. One possible mechanism for this is saturation of local calcium buffers during the first action potential in a pair on train (Klingauf and Neher, 1997; Neher, 1998; Matveev et al., 2004). In contrast, depletion of the vesicles within the readily releasable pool can cause synaptic depression (Betz, 1970; Glavinovic and Narahashi, 1988; von Gersdorff and Matthews, 1997; Delgado et al., 2000). In addition, postsynaptic receptors can be desensitized by long exposure to neurotransmitter and this reduces synaptic responses (Trussell and Fischbach, 1989; Trussell et al., 1993; Mennerick and Zorumski, 1996; Otis et al., 1996; Oleskevich et al., 2000)

Many presynaptic proteins including synaptotagmin, synapsin, synaptophysin, and munc 13-1, and native calcium binding proteins, such as frequenin, and piccolo, can influence short-term plasticity (Rivosecchi et al., 1994; Pieribone et al., 1995; Rosahl et al., 1995; Ryan et al., 1996; Hilfiker et al., 1998; Stevens and Wesseling, 1999; Gerber et al., 2001). Despite our current detailed molecular understanding of presynaptic events surrounding transmitter release, there is no consensus as to the molecular mechanisms that underlie any particular phase of short-term plasticity. Most attention is focused on trying to implicate various calcium binding proteins found in synaptic terminals. As there are many mechanisms that may lead to short-term synaptic plasticity, at most synapses multiple mechanisms probably interact in complex ways to generate the plastic physiological patterns of synaptic transmission (Zucker and Regehr 2002).

1.5 FROG NEUROMUSCULAR JUNCTION MODEL SYSTEM

The frog neuromuscular junction has been studied for more than 60 years because of its usefulness for understanding synaptic function, and thus provides a wealth of background

information upon which to build. This preparation has unique presynaptic active zone structure, including the regularly spaced, long linear arrays of synaptic particles in the active zone (Figure 3). Freeze fracture electron micrographs of the frog active zone are characterized by distinctive double rows of synaptic particles that are thought to include voltage-gated calcium channels. Each active zone is $\sim 1 \mu\text{m}$ long and they are separated from one another by about $1 \mu\text{m}$ (Heuser et al., 1974; Lester, 1977; Pumplin et al., 1981; Robitaille et al., 1990; Cohen et al., 1991; Harlow et al., 2001). Confocal microscopy has demonstrated that presynaptic active zone proteins and postsynaptic acetylcholine receptors are colocalized very tightly (Pumplin et al., 1981; Robitaille et al., 1990, 1993; Cohen et al., 1991).

The frog neuromuscular junction is a fast synapse that releases acetylcholine with high fidelity. Though the entire nerve terminal releases more than 300 vesicles per single action potential, each active zone releases less than 1 vesicle in response to a single action potential. Therefore, strong communication between motoneurons and muscle cells results from the summed activity of hundreds of individual low probability active zones positioned along whole length of the nerve terminal. These detailed studies of neuromuscular transmission have provided many insights into our general understanding of central synapses.

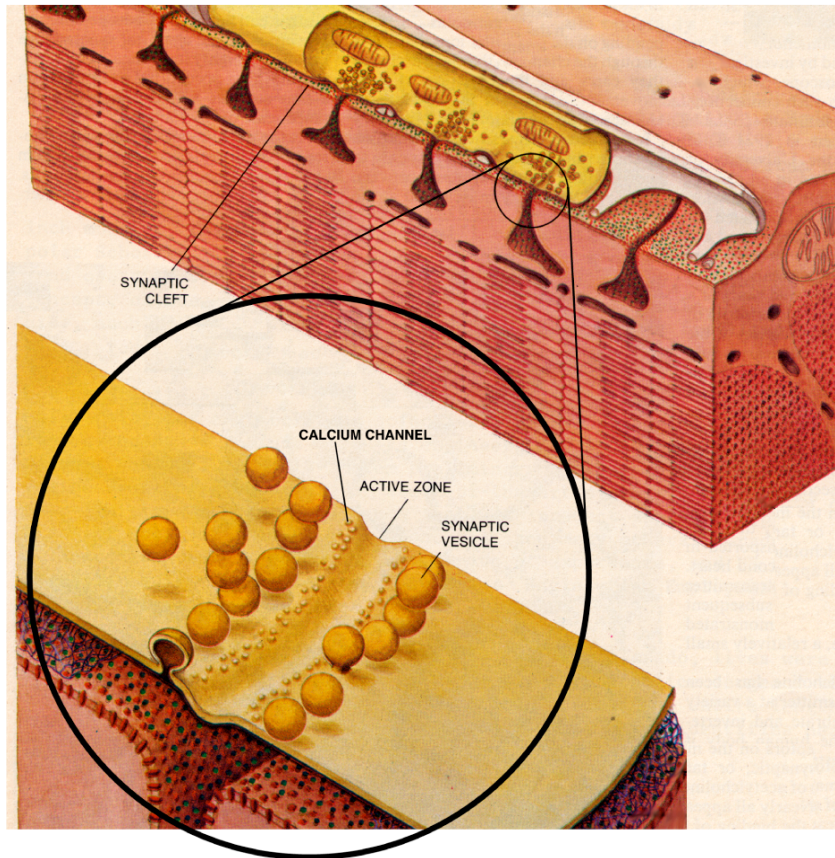


Figure 3 Frog neuromuscular junction

Top. Schematic diagram of frog neuromuscular junction and the active zones that organize the transmitter release machinery. Adapted from Lester (1977). **Bottom.** Freeze fracture electron micrograph of the frog neuromuscular junction. Double rows of intramembrane particles surround the active zone (Heuser and Reese, 1977).

1.6 ROSCOVITINE

Roscovitine was originally identified as an inhibitor of cyclin-dependent kinases (cdks). Cdks have been shown to be important in neuronal development (Dhavan and Tsai, 2001), synaptic transmission (Cheng and Ip, 2003), cytoskeletal control (Smith, 2003), neurodegeneration (Shelton and Johnson, 2004), and cell cycle control (Murray, 2004). With respect to clinical use, some inhibitors of cdks affecting the cell cycle are being tested for use as anticancer drugs (Sausville, 2002).

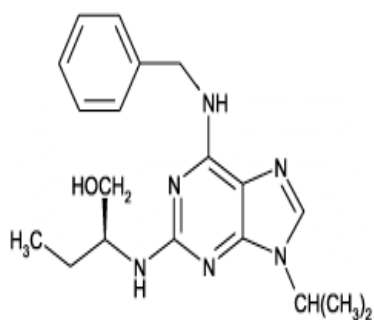
Roscovitine exists as (R)- and (S)- enantiomers, each of which can be obtained in pure form. Interestingly, one of these enantiomers ((R)-roscovitine) has also been shown to have other effects that may be cdk-independent (Yan et al., 2002; Buraei et al., 2005, 2007). For example, (R)-roscovitine has been shown to act on P/Q- and N-type calcium channels altering directly their deactivation kinetics with fast onset of action (1~2 sec), and to increase transmitter release at CNS synapses (Yan et al., 2002; Tomizawa et al., 2002; Buraei et al., 2005). However, (R)-roscovitine does not affect L-type calcium channels (Yan et al., 2002; Buraei et al., 2005, 2007).

(R)-roscovitine appears to slow deactivation of calcium channels by binding to the open state of channels and decreasing transition rates between two open states (Buraei et al., 2005, 2007). In contrast to strongly slowed deactivation, the effect of (R)-roscovitine on activation kinetics was small. At higher concentrations, (R)-roscovitine slowly inhibited peak currents activated by a step voltage command (Buraei et al., 2005). A slower time course and the requirement for a higher concentration suggested a separate mechanism of action than that mediating slow deactivation kinetics. A recent study (Buraei et al., 2007) showed that (R)-roscovitine also slowed deactivation of expressed R-type calcium channels and inhibited expressed putative A-type potassium currents. Effects were also noted on delayed rectifier and

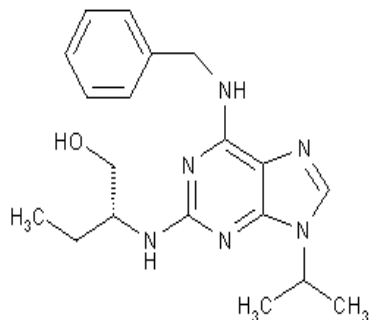
Shaker-type potassium currents, the Kv4.2, Kv2.1 and Kv1.3 channels. (R)-roscovitine does not appear to affect sodium channels (Buraei et al., 2007).

(S)-roscovitine is also known as a cdk inhibitor, but has no acute effects on calcium currents or transmitter release (see section 2.3 and 3.3; Cho and Meriney, 2006); this enantiomer can be used as a control for calcium channel effects. Another control used in this thesis is olomoucine, which also inhibits cdks and has a similar structure to roscovitine (Figure 4), but has no effect on calcium currents or calcium-triggered transmitter release (see section 2.3 and 3.3; Yan et al., 2002; Buraei et al., 2005; Cho and Meriney, 2006).

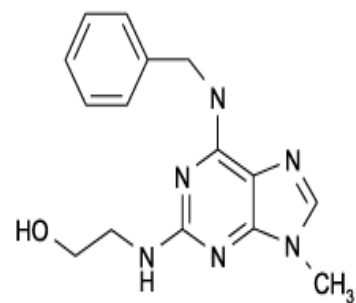
In this thesis, I have designed experimental work around the most prominent effect of (R)-roscovitine: slowing of deactivation kinetics of calcium channels. This drug is seen here as a tool to manipulate calcium channels and study subsequent effects on transmitter release. However, these direct effects of (R)-roscovitine on calcium channels may inspire the development of roscovitine derivatives that lack cdk activity, and only have actions on calcium channel deactivation. Unless specified, I will use the term “roscovitine” elsewhere in this dissertation to refer to only the (R)- enantiomer.



(R)-roscovitrine



(S)-roscovitrine



Olomoucine

Figure 4 Structures of (R)-, (S)- roscovitrine and olomoucine.

1.7 GOALS OF THE DISSERTATION

Neurotransmitter release is tightly regulated by presynaptic calcium influx through voltage-gated calcium channels. Using two pharmacological manipulations (roscovitine and DAP), the calcium regulation of transmitter release was investigated. My study consists of (1) clarifying the underlying mechanism of these two pharmacological treatments by recording calcium currents and presynaptic action potential waveforms, (2) evaluating the effects of such manipulations on synaptic transmission and short-term synaptic plasticity at the adult frog neuromuscular junction by measuring postsynaptic responses, and (3) computational modeling to investigate synaptic molecular mechanisms at a sub-active zone level.

This study allowed me to understand the specific relationship between calcium entry and transmitter release at the synapse further and provided interesting insights into short-term plasticity. This work also may spark further interest in examining the possibility that roscovitine derivatives might be effective as potential tools to change presynaptic calcium channel function at the neuromuscular junction.

2. ROSCOVITINE EFFECTS ON CALCIUM CHANNEL ACTIVITIES

In this chapter, the effects of roscovitine on calcium currents have been characterized in frog motoneurons. As a comparison, the effects of 3,4-diaminopyridine (DAP), a potassium channel blocker, were also investigated. DAP is known to enhance transmitter release because it increases presynaptic calcium influx indirectly by altering the action potential waveform. The underlying mechanisms of these two pharmacological treatments in frog motoneurons were clarified by recording calcium currents and presynaptic action potential waveforms. The possibility that these two treatments may be effective as tools to investigate calcium entry and subsequent transmitter release at the frog neuromuscular junction was examined.

2.1 INTRODUCTION

Calcium entry through voltage-gated calcium channels in the motor nerve terminal is known to trigger neurotransmitter release. Voltage-gated calcium channels have been shown to be localized at active zone regions of the adult frog neuromuscular junction where they play a critical role in regulating vesicle fusion (Robitaille et al. 1990; Cohen et al. 1991). Among several types of voltage-gated calcium channels (L-, N-, P/Q-, T- and R- type), the N-type

channel has been shown to mediate transmitter release at the adult frog neuromuscular junction (Kerr & Yoshikami, 1984).

Studying the effects of agents that directly alter presynaptic calcium channel function may provide insight into the details underlying calcium-triggered secretion. In addition, a specific agonist of an ion channel is a very useful tool for characterizing ion channels. For example, L-type calcium channels have been investigated productively using BayK 8644, a specific agonist of L-type calcium channels (Brown et al., 1984; Kokubun and Reuter, 1984; Nowycky et al., 1985; Sanguinetti et al., 1986; Fox et al., 1987; Jones and Jacobs, 1990; Bargas et al., 1994). So far, the absence of a similar agonist for N-type calcium channels has hampered investigation in this area.

Roscovotine, an inhibitor of cyclin-dependent kinases (cdks), has been demonstrated to have effects that may be cdk-independent (Yan et al. 2002; Buraei et al. 2005, 2007). Roscovitine appears to act directly on P/Q-type calcium channels altering their deactivation kinetics, and enhancing calcium tail currents following step depolarizations in neostriatal interneurons (Yan et al. 2002). In addition, roscovitine has also been shown to slow deactivation of expressed N-, P/Q-, and R- type calcium channels (but not L-type channels), and N-type channels in bullfrog sympathetic neurons, possibly by binding to the open state of the channel (Buraei et al. 2005, 2007).

Given these apparently direct effects on calcium channel function, I have examined the possibility that roscovitine could be used as a potential tool to study transmitter release at the adult frog neuromuscular junction in the later chapters of this dissertation. Initially, however, I have examined roscovitine effects on N-type calcium channels expressed in frog motoneurons. Since the adult *Rana pipiens* frog neuromuscular junction nerve terminal is not amenable to

patch directly, the cultured *Xenopus* motoneuron-muscle co-cultures were used to record presynaptic calcium currents and characterize biophysical changes in calcium currents. *Xenopus* embryos have provided a good system to study calcium currents and neuronal differentiation (Spitzer 1979; Barish 1991), though differences in their central role and the distribution of calcium channel isoforms between soma and nerve terminal have been reported (Li et al., 2001). This preparation, derived from 1-day old *Xenopus* embryos, is a co-culture of motoneurons and muscle cells that form natural neuromuscular synapses within 1-3 days *in vitro*.

Aminopyridines, such as DAP and 4-aminopyridine, block potassium channels. DAP and 4-aminopyridine have been shown to potentiate synaptic transmission by altering the shape of presynaptic action potential in many preparations (Hue et al., 1976; Jankowska et al., 1977; Guerrero and Novakovic, 1980; Kim et al., 1980; Matsumoto and Riker, 1983; Augustine GJ, 1990; Barish et al., 1996; Seo et al., 1999; Gu et al., 2004). With respect to clinical use, DAP is well suited for treating peripheral disorders with few CNS side-effects, because it cannot cross the blood brain barrier. DAP has been studied as a treatment of neurological disorders including LEMS and amyotrophic lateral sclerosis (Murray and Newsome-Davis, 1981; Lundh et al., 1984, 1993; McEvoy et al., 1989; Bever et al., 1990; Palace et al., 1991; Aisen et al., 1995, 1996; Maddison et al., 1998; Sanders et al., 2000; Tim et al., 2000).

In my studies of roscovitine effects on cultured frog motoneuron calcium channel currents, I show that roscovitine slows the deactivation kinetics of presynaptic calcium channels and leads to an increase in total calcium entry through each open channel during an action potential stimulus. The effects of roscovitine on calcium entry are compared with the effects of DAP, an indirect manipulator of presynaptic calcium entry.

2.2 METHODS

2.2.1 Cell culture of frog motoneurons and muscle cells.

Nerve–muscle co-cultures were prepared as described previously (Yazajian et al. 1997). In short, stage 20-22 *Xenopus laevis* embryos (Nieuwkoop & Faber, 1967) were rinsed in 10% normal frog Ringer (NFR; in mM (1X): 116 NaCl, 1 NaHCO₃, 2 KCl, 1.8 CaCl₂, 1 MgCl₂, 5 HEPES, 5 glucose, pH 7.4), and the spinal cord and associated myotomes were dissected free and allowed to disaggregate in a Ca²⁺ and Mg²⁺-free Ringer saline (in mM: 125 NaCl, 2 KCl, 1.2 EDTA, and 5 HEPES, pH 7.4) for 30–60 min. Disaggregated cells were plated onto plastic tissue culture dishes and maintained at room temperature (22–24°C) for 2-3 days in a medium composed of 40% NFR and 50% L-15 (Life Technologies, Gaithersburg, MD) supplemented with 0.1 mg/ml insulin, 0.7 mg/ml sodium selenite, 0.6 mg/ml transferrin, 1 μM testosterone, and 35 ng/ml brain-derived neurotrophic factor (or 20 ml/ml fetal bovine serum).

2.2.2 Recording and analysis of currents through calcium channels.

Whole-cell currents through calcium channels were recorded from *Xenopus* motoneuron somata at 2-3 days *in vitro* as previously described (Yazajian et al. 1997). Briefly, perforated patch recordings of current through calcium channels were made with the aid of the perforating agent amphotericin-B. The pipette solution consisted of (in mM): 68 CsMeSO₄, 50 CsCl, 8 MgCl₂, 10 HEPES, pH 7.4. When calcium was used as the charge carrier, the culture was bathed in a solution consisting of (in mM): 110 TEA-Cl, 10 NaCl, 10 CaCl₂, 1 MgCl₂, 5 HEPES, 2 KCl,

3 glucose, 5 DAP, 1 μ M TTX, pH 7.4. When barium was used as the charge carrier, BaCl₂ substituted for CaCl₂ in equimolar amounts. Patch pipettes (about 2 M Ω) were filled in a two-step process: the tip was dipped in amphotericin-free pipette saline (2-5 seconds), and the rest of the pipette was filled with pipette saline plus 200-300 μ g/ml amphotericin-B. Access resistances typically ranged from 10-20 M Ω (mean \pm SEM = 15.1 \pm 1.1 M Ω ; predicted voltage error = 2.1 \pm 0.3 mV, n=30) and were compensated for by 80-85% (lag setting = 10 μ sec). I discarded recordings in which measured access resistance was greater than 30 M Ω (compensated for by at least 80%; predicted voltage error less than 3 mV), or in which there was a change in access resistance of more than 5 M Ω over the course of my recording. Capacitive currents and passive membrane responses to voltage commands were subtracted using 4 waveforms of reverse polarity, each 1/4 the size of the full waveform. Calcium currents were amplified by an Axopatch 200B amplifier, filtered at 5 KHz, and digitized at 10 KHz for subsequent analysis facilitated by pClamp 9 software (Axon Instruments, Foster City, CA).

Activation kinetics of currents were measured by fitting calcium current evoked by a square voltage-step depolarization from -60 mV to +10 mV for 10 milliseconds with a single exponential function beginning at the time that current begins to flow inward and ending at the time of maximal current (Jones & Marks, 1989). I measured current deactivation kinetics by fitting calcium current deactivation with a single exponential function beginning 100 msec after the peak of the tail current evoked at the end of a 10 msec voltage step from -60 mV to +10 mV. To prevent signal-to-noise problems from significantly complicating my measurements of the current integral evoked by a single action potential stimulus, I only used data from experiments in which peak barium currents were more than 100 pA, and in which the outward stimulus artifact preceding these currents was less than 30% of the peak current amplitude.

Action potential waveforms were recorded with the perforated patch technique as described above, except that K_2SO_4 and KCl replaced CsMeSO₄ and CsCl in the pipette solution (in mM: 60 K_2SO_4 , 45 KCl, 8 $MgCl_2$, 10 HEPES, pH 7.4) and the culture was bathed in a NFR solution. The fast current clamp mode of the Axopatch 200B was used.

To evaluate calcium current activation during an action potential, I used a previously recorded *Xenopus* motoneuron nerve terminal action potential (from Pattillo et al. 1999) as a voltage command. In some experiments, this action potential waveform was altered incrementally such that the plateau phase at the peak was of different durations. The action potential duration at half amplitude of such action potential waveforms was 0.75, 0.85 (control duration), 1, 1.2, 1.4, 1.6, 1.8, 2, 2.2, 3.2, 4.2, and 5.2 msec. The peak amplitude of calcium tail currents evoked by such a family of voltage waveforms (normalized to the peak current recorded using the broadest action potential) was plotted against the duration of the action potential at half amplitude. Using this approach, I determined the proportion of calcium current activated in response to the control action potential under different experimental conditions (see King & Meriney, 2005). Because even a prolonged strong voltage depolarization does not open all available calcium channels at any one point in time, the proportion calculated is an overestimate of the percentage of channels that open. Although this approach does not measure the percentage of channels that open, from this property of calcium channel function, I made relative comparisons for how effectively action potential stimuli activate calcium currents. All values are expressed as mean \pm SEM, and all tests of significance were performed using a Student's paired *t* test.

2.2.3 Reagents.

(R)-roscovitine and (S)-roscovitine were obtained from Dr. L. Meijer (Station Biologique de Roscoff, CNRS UPR, Roscoff cedex, Bretagne, France) or Alexis Co. (San Diego, CA, USA). Olomoucine was obtained from Alexis Co. (San Diego, CA, USA). (R)-roscovitine, (S)-roscovitine, and olomoucine were stored at -20°C as 1000X stock solutions in DMSO and all final concentrations were 100 µM. All other chemicals were obtained from Sigma (St. Louis, MO). 3,4-diaminopyridine (DAP) was made fresh daily.

2.3 RESULTS

As expected based on previous reports (Yan et al. 2002; Buraei et al. 2005), the most prominent effect of (R)-roscovitine was to strongly slow calcium current deactivation kinetics evoked by square voltage steps back to -60 mV from +10 mV ($t_{\text{control}} = 0.38 \pm 0.10$ msec; $t_{\text{roscovitine}} = 1.44 \pm 0.15$ msec; $427 \pm 176\%$ average increase when calculated within each cell [$t_{\text{roscovitine}} - t_{\text{control}} / t_{\text{control}}$]; $n = 5$; $p < 0.01$). (R)-roscovitine also significantly slowed activation kinetics by $45.2 \pm 21.9\%$ ($p < 0.05$; calculated within each cell; $t_{\text{control}} = 1.19 \pm 0.17$ msec; $t_{\text{roscovitine}} = 1.64 \pm 0.20$ msec; Figure 5A left panel; $n = 6$). In contrast, (S)-roscovitine did not significantly alter calcium current deactivation kinetics after a square voltage step ($3.9 \pm 4.1\%$ increase; Figure 5B left panel; $n = 5$) or activation kinetics ($1.6 \pm 3.4\%$ increase; Figure 5B left panel; $n = 5$). Similarly, olomoucine did not significantly alter calcium current deactivation kinetics ($2.0 \pm 3.7\%$ increase; Figure 5C left panel; $n = 5$) or activation kinetics ($5.4 \pm 1.9\%$ increase; Figure 5C left panel; $n = 5$).

L-type calcium channels carry a significant percentage of the total calcium current in *Xenopus* motoneuron somata (Yazejian et al., 1997; Thaler et al., 2001; Sand et al., 2001). After blocking L-type calcium channels with 1 μ M nitrendipine, calcium currents were significantly smaller, but (R)-roscovitine showed similar effects on calcium channel kinetics. Deactivation kinetics evoked by square voltage steps back to -60 mV from +10 mV strongly slowed ($t_{\text{control}} = 0.17 \pm 0.05$ msec; $t_{\text{roscovitine}} = 0.69 \pm 0.16$ msec; $318 \pm 22\%$ average increase when calculated within each cell; $n = 5$; $p < 0.01$). (R)-roscovitine also significantly slowed activation kinetics by $46.8 \pm 10.4\%$ (calculated within each cell; $t_{\text{control}} = 0.87 \pm 0.08$ msec; $t_{\text{roscovitine}} = 1.25 \pm 0.05$ msec; $n = 5$; $p < 0.01$). Because blocking L-type calcium channels did not significantly alter the effects of (R)-roscovitine on calcium current kinetics in this preparation, and previous studies showed that (R)-roscovitine did not affect L-type calcium channels (Yan et al., 2002; Buraei et al., 2005), the rest of experiments were performed without nitrendipine to avoid potential signal-to-noise problems associated with recording smaller calcium currents evoked by an action potential waveform.

I also measured the integral of current through the calcium channel when evoked by a single action potential stimulus because this parameter might be relevant to the magnitude of transmitter release triggered by calcium entry in the next chapter (see section 3.3.1). Because currents evoked by physiological action potential waveforms are smaller than currents evoked by square-step waveforms, for these experiments, I used a bath solution containing barium instead of calcium as the charge carrier to increase the amplitude of currents carried by the calcium channel. This made analysis of these currents less sensitive to fluctuations in noise. Using this approach, (R)-roscovitine had similar effects on deactivation kinetics during a square voltage step ($380 \pm 17.8\%$ increase, $n=5$) and this was also clearly evident in the calcium channel current

evoked by single action potential waveforms (see Figure 5A, right panel). As expected based on open-state binding of (R)-roscovitine to the calcium channel (see Buraei et al. 2005), a smaller proportion of the channels appear to demonstrate slowed deactivation when an action potential waveform is used to activate current as compared to when a square voltage step is used to activate current (compare right vs. left panel in Figure 5A). Total current entry (integral) during a single action potential was significantly increased by (R)-roscovitine ($44.2 \pm 10.4\%$; Figure 5A right panel; $n = 7$; $p < 0.05$). In contrast, (S)-roscovitine ($0.40 \pm 1.9\%$ change; Figure 5B right panel; $n = 5$) and olomoucine ($2.0 \pm 1.1\%$ change; Figure 5C right panel; $n = 4$) did not show significant effects on total current entry evoked by an action potential waveform. These effects were consistent with the results reported above using calcium as the charge carrier and square voltage steps to activate current.

To investigate the possibility that (R)-roscovitine might increase the probability that calcium channels open during an action potential stimulus, I used an indirect method to qualitatively approach this issue. I examined the proportion of calcium current activated by action potential waveforms (by measuring peak tail current amplitude) as compared with broadened waveforms as a measure of how effectively native action potentials activated calcium current in comparison with the maximal current that could be activated by a prolonged waveform (see King & Meriney, 2005). The proportion of calcium current activated by a natural motoneuron action potential was relatively low (~ 0.2) as compared with the maximal current that could be evoked, and there was little effect of (R)-roscovitine (arrow in Figure 6A). Although there was a very small decrease in the proportion of current activated by a natural nerve terminal motoneuron action potential, as the action potential was broadened, (R)-roscovitine further decreased the proportion of calcium current that was activated by these broader action potential

waveforms (Figure 6A). This would be consistent with a decrease, not an increase, in the probability that calcium channels would be activated by action potential waveforms. This might be explained by the effect of (R)-roscovitine on calcium current activation kinetics that I observed (see Figure 6B), and have also been reported at more hyperpolarized potentials by Buraei et al. (2005). In fact, using an action potential-shaped rising voltage step to +30 mV, there was a significant slowing of activation kinetics (by $11.6 \pm 4.1\%$, $n=6$; $p<0.05$). Using voltage steps as large as +30 mV, Buraei et al. (2005) did not report significant effects on activation kinetics. The small significant effect I report may be due to differences in the preparation used, or due to effects of the altered rising phase of the voltage step. The effects I report on activation kinetics may explain our results in Figure 6A, but appear to be minor in comparison with my observed effects on deactivation kinetics, which serve to increase total calcium entry (see Figure 5). In contrast to the effects of (R)-roscovitine, (S)-roscovitine and olomoucine did not significantly alter the proportion of peak calcium current activated by action potential waveforms (Figure 6C and 6D).

Finally, (R)-roscovitine effects on action potential-evoked calcium current were compared with the effects of 1 μM DAP. The concentration of DAP was determined from preliminary studies showing that 1 μM DAP had similar potency to 100 μM (R)-roscovitine when tested for the effects on evoked transmitter release (see section 3.3.1). This relatively low concentration of DAP significantly increased by $11.9 \pm 2.4\%$ ($p<0.05$; $n=5$) the amplitude of the recorded motoneuron action potential (from +30 mV to +41 mV; recorded using the fast current clamp setting of the Axopatch 200B), without significantly broadening the action potential shape (see Figure 7A). This effect on action potential peak amplitude without a change in action potential duration might be predicted because DAP, especially in very low concentrations, is a

selective blocker of transient (I_A) voltage-gated potassium channels (Thompson, 1982; Rogawski, 1988). In contrast, I did not detect any significant change in action potential shape following exposure to (R)-roscovitine ($n=6$). This lack of effect of (R)-roscovitine on action potential shape suggests that there are no significant effects of (R)-roscovitine on sodium or potassium channels in my system.

When the DAP-induced change in action potential amplitude was used to evoke calcium current, there was an $81.5 \pm 11.7\%$ increase in peak calcium current and an $89.8 \pm 14.4\%$ increase in calcium current integral ($n=9$; see Figure 7A). The significant increase in calcium current peak amplitude and integral is expected to result in the increase in transmitter release at the neuromuscular junction following exposure to $1 \mu\text{M}$ DAP in the next chapter (see section 3.3.2). Lastly, when this DAP-altered action potential waveform was used to examine the proportion of calcium current activated by an action potential waveform as compared with a broadened waveform, DAP-altered waveforms significantly increased the proportion of calcium current activated at all action potential durations examined except those broader than 4 msec (see Figure 7B; $n=8$; $p<0.05$).

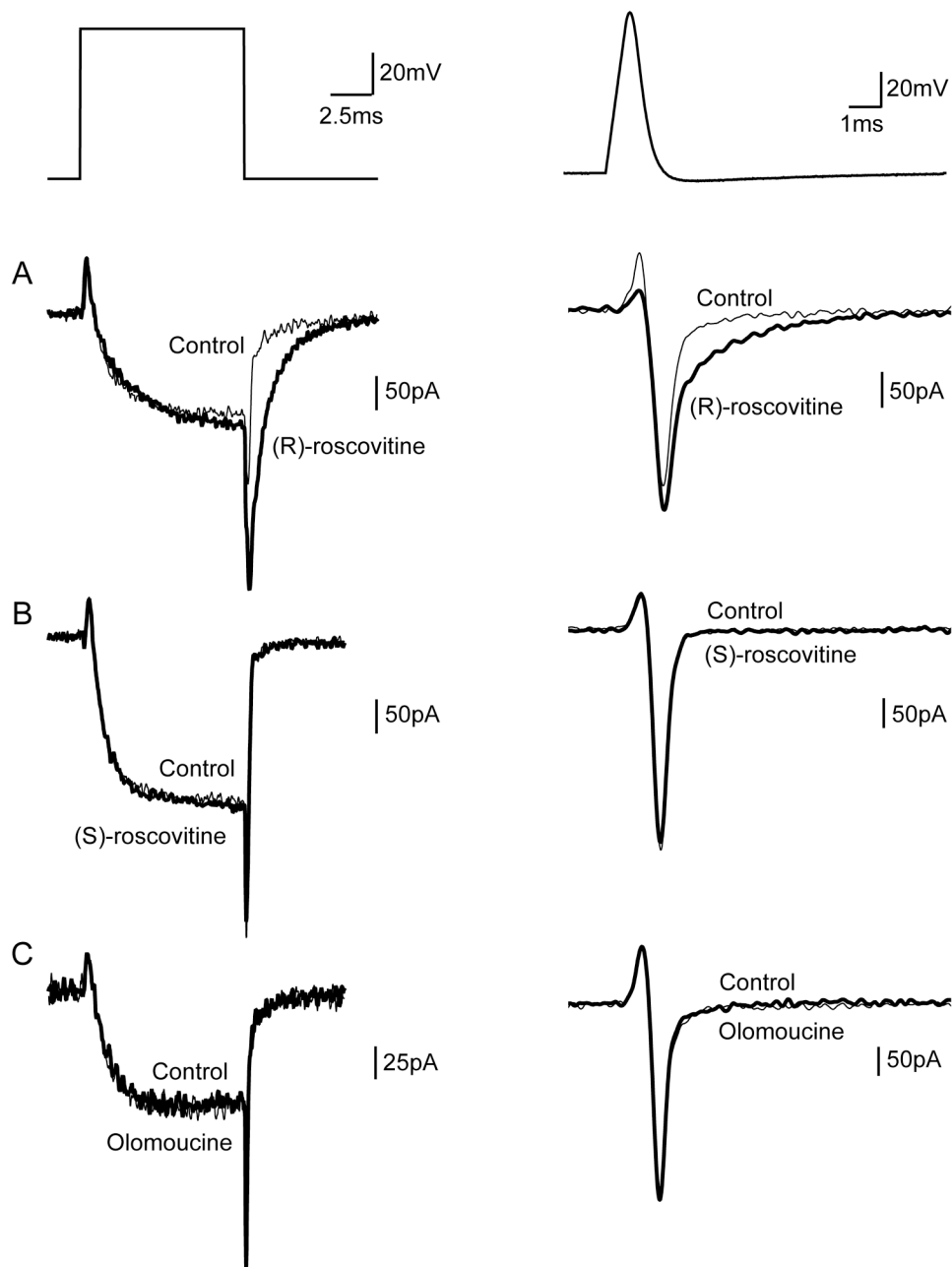


Figure 5 Effects of 100 μ M (R)-roscovitine on calcium channel current recorded from the somata of cultured frog motoneurons.

A-C. In the left column, a square-step voltage command from -60 mV to +10 mV for 10 msec was used to activate calcium currents. In the right column, a single action potential

waveform (-60 mV holding potential, peak action potential voltage of +30 mV, and a duration at half amplitude of 0.85 msec) was used to activate barium currents through calcium channels. **A.** Left : (R)-roscovitine (thick trace) significantly slowed calcium current activation kinetics (by $45.2 \pm 21.9\%$; n=6), and strongly slowed deactivation kinetics (by $427 \pm 176\%$; n=5; $p < 0.01$). Right : (R)-roscovitine (thick trace) slowed the deactivation of current activated by an action potential and significantly increased total current integral by $44.2 \pm 10.4\%$ (n=7; $p < 0.05$). These effects occurred within 10 seconds of (R)-roscovitine application. **B.** 100 μ M (S)-roscovitine did not show any significant effect on calcium channel currents. **C.** 100 μ M olomoucine did not show any significant effect on calcium channel currents.

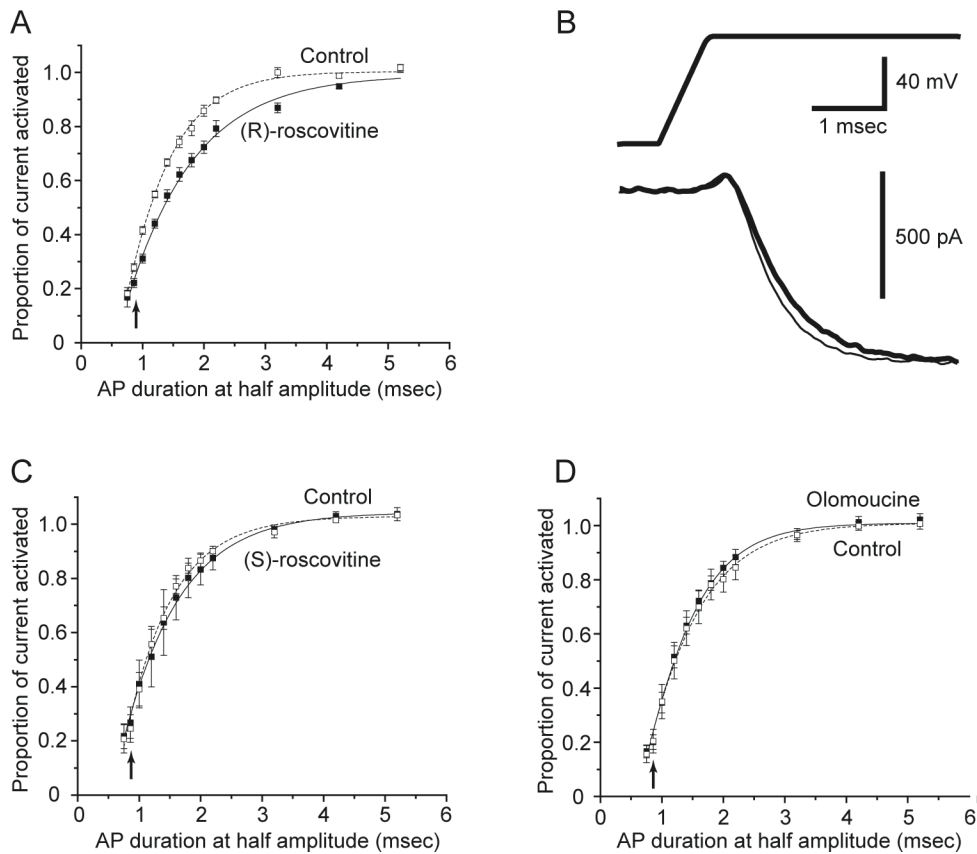


Figure 6 Changes in the proportion of calcium current activated following action potentials of various durations at half amplitude in cultured motoneurons.

Arrows at the second point in each plot indicate the use of native action potential waveforms. **A.** Effects of exposure to 100 μ M (R)-roscovitine (filled symbols, solid line; $n=8$) in comparison with control (open symbols, dashed line). Except the first and the last points, (R)-roscovitine significantly decreased the proportion of current activated during a broadened action potential stimulus ($p<0.05$, Student's paired t test). **B.** Calcium current evoked by a voltage command that had an action potential-shaped rising phase and a plateau potential of +30 mV (the longest step used in the peak tail current comparisons for panels A, C and D). Top trace: voltage command. Bottom trace: control (thin trace) and (R)-roscovitine-modulated (thick trace)

calcium currents. (R)-roscovitine slowed significantly activation of these currents by $11.9 \pm 2.4\%$ ($p < 0.05$; $n = 5$). **C.** Effects of $100 \mu\text{M}$ (S)-roscovitine (filled symbols, solid line; $n = 5$) in comparison with control (open symbols, dashed line). (S)-roscovitine did not show significant effects on the proportion of current activated during any waveform stimulus. **D.** Effects of $100 \mu\text{M}$ olomoucine (filled symbols, solid line; $n = 6$) in comparison with control (open symbols, dashed line). Olomoucine did not show significant effects on the proportion of current activated during any waveform stimulus.

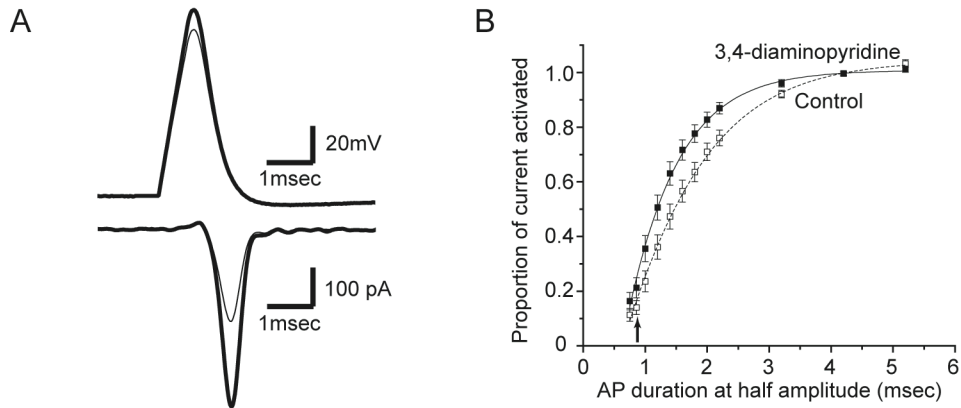


Figure 7 1 μM DAP effects on calcium influx and the proportion of calcium current activated following action potentials of various durations at half amplitude in cultured motoneurons.

A. Effects of 1 μM DAP on action potential amplitude (top traces) and evoked calcium current (bottom traces). Top traces: 1 μM DAP (thick trace) significantly increased action potential amplitude (by $11.9 \pm 2.4\%$, $n=5$), but not duration, as compared with control action potential shape (thin trace). Bottom traces: The DAP-modulated action potential waveform, when used as a voltage command, significantly increased calcium current (thick trace) peak (by $81.5 \pm 11.7\%$) and integral (by $89.8 \pm 14.4\%$) as compared with the calcium current evoked by a control action potential shape (thin trace). **B.** Effects of exposure to 1 μM DAP (filled symbols, solid line; $n=8$) in comparison with control (open symbols, dashed line). Arrows at the second point in each plot indicate the use of native action potential waveforms. DAP significantly increased the proportion of calcium current activated at all waveforms examined, except those broader than 4 msec ($p<0.05$, Student's paired t test).

2.4 DISCUSSION

Presynaptic calcium entry tightly regulates synaptic transmission and slight modifications of calcium influx have significant influences on transmitter release. At the adult frog neuromuscular junction, N-type calcium channels mediate transmitter release. My findings show that (R)-roscovitine increased total calcium entry due primarily to slowing the deactivation kinetics of presynaptic N-type calcium channels. Because I did not observe any significant effects of (S)-roscovitine or olomoucine on calcium current kinetics, I hypothesize that the effects of (R)-roscovitine are independent of cdks. Previous work has also concluded that (R)-roscovitine effects on calcium current kinetics are cdk-independent (Yan et al. 2002; Buraei et al. 2005, 2007). Along these lines, intracellular application of (R)-roscovitine has been reported not to show effects on calcium current kinetics (Yan et al. 2002; Buraei et al. 2005), and in cortical neurons deficient in p35 (a neuronal-specific activator of cdk5), (R)-roscovitine was still able to prolong deactivation of calcium currents in a manner similar to that found in wild-type neurons (Yan et al. 2002). It has been proposed that (R)-roscovitine slows deactivation of calcium channels by binding to the open state of channels (Buraei et al., 2005).

The dominant effect of (R)-roscovitine was slowing deactivation kinetics of N-type calcium current, though there was a relatively small effect on activation kinetics, and a slower effect of inhibiting currents at higher concentration in paravertebral sympathetic ganglia of adult bullfrogs (Buraei et al., 2005). For the rest of this thesis, I will focus on this dominant effect of (R)-roscovitine: slowed deactivation kinetics.

The action of (R)-roscovitine is quite similar to that of BayK 8644, a L-type calcium channel

agonist. BayK 8644 has been used successfully to elucidate the roles of L-type calcium channel in physiology and pathology (Hess et al., 1984; Bean, 1985; Nilius et al., 1985; Nowycky et al., 1985; Sturek and Hermsmeyer, 1986; Church and Stanley, 1996; Triggle, 2003; Elmslie, 2004). Single L-type calcium channels within the mix of various channel subtypes can be identified with BayK 8644, because it strongly increases the mean open time without altering the single-channel current amplitude (Hess et al., 1984; Church and Stanley, 1996; Satoh et al., 1998). Prior to the discovery of (R)-roscovitine, there had been no selective agonist for N-type calcium channels, though antagonists are available. Using (R)-roscovitine as a tool, future work may include the measurement of unitary conductances for N-type calcium channel so that characteristics of gating in normal calcium concentrations (instead of using extremely high concentrations of calcium or barium as charge carrier) can be studied.

Previous studies showed that (R)-roscovitine slowed deactivation of all Ca_v2 family channels, that is, P/Q-type ($Ca_v2.1$) and R-type ($Ca_v2.3$) as well as N-type ($Ca_v2.2$) calcium channels (Yan et al., 2002; Buraei et al., 2007). This is also similar to BayK 8644 effects on Ca_v1 L-type channels, including $Ca_v1.2$, $Ca_v1.3$, and $Ca_v1.4$ (Xu and Lipscombe, 2001; Koschak et al., 2003). As BayK 8644 is still considered as a strong tool for L-type channels, the lack of differentiation among Ca_v2 channels will not be an obstacle to use (R)-roscovitine, because there are selective blockers for each Ca_v2 channel subtype, such as ω -Agatoxin for P/Q type, ω -Conotoxin GVIA for N-type, and SNX-482 for R-type calcium channels.

One potential problem related to the use of (R)-roscovitine might be its high affinity for cdks, though the effects on calcium channels have been proven to be cdk-independent. It is possible that derivatives of (R)-roscovitine could be developed in the future, which might directly and selectively target N-type calcium channels, and not affect cdks. These would create ideal tools

for research and some of these new derivatives could have potential as treatments for neuromuscular disorders.

Very recently, Buraei et al. (2007) showed that (R)-roscovitine also affected some types of voltage-gated potassium channels in paravertebral sympathetic ganglia and in expression systems. Unfortunately, it is not exactly known what types of voltage-gated potassium channels are expressed at the frog motoneuron terminal. However, because the action potential waveform in frog motoneurons was not significantly altered by (R)-roscovitine, it seems unlikely that transmitter release effects reported in next chapter (section 3.3) are due to effects on voltage-gated potassium channels.

The data reported here lead me to hypothesize that the underlying mechanism of (R)-roscovitine effects on total calcium entry is due to the large effects on deactivation kinetics. These effects prolong presynaptic calcium channel opening with little change in the peak number or fraction of calcium channels activated by an action potential. In contrast, DAP altered the amplitude of the action potential by blocking some voltage-gated potassium channels. At very low concentration (1 μ M), DAP significantly increased the amplitude of action potential rather than broadening the width of action potential. This altered action potential waveform caused the increase in calcium influx observed. DAP is expected to increase the number of calcium channels that open with each action potential stimulus, and this is predicted to lead to an increase in calcium ion spatial distribution within the nerve terminal (Figure 13B). This difference in the mechanism by which (R)-roscovitine and DAP increase calcium entry is likely to underlie the different effects of these agents on transmitter release and short-term plasticity discussed in the later chapters of this dissertation. In that sense, these two pharmacological treatments will

function as very good contrasting tools for experimental and theoretical studies of calcium-triggered vesicle fusion.

3. ROSCOVITINE EFFECTS ON TRANSMITTER RELEASE AND SHORT-TERM PLASTICITY

In the previous chapter, the underlying mechanisms of roscovitine and DAP effects on calcium currents were characterized in cultured frog motoneurons. In this chapter, I have investigated the effects of these two pharmacological treatments on transmitter release and paired-pulse facilitation by measuring endplate potentials (EPPs) and miniature endplate potentials (mEPPs) at the adult frog neuromuscular junction. Information obtained from these physiological experiments will be also used to constrain parameters in the computational model described in next chapter, and will be interpreted using the model to extend our understanding of synaptic transmission.

3.1 INTRODUCTION

A brief, stimulus-induced calcium flux through voltage-gated calcium channels in the motor nerve terminal is known to trigger transmitter release. The frog neuromuscular junction is a synapse that transmits electrical impulses from the nerve terminal to the skeletal muscle via acetylcholine using fast and reliable communication between motoneurons and muscle cells. The N-type calcium channel is known to couple presynaptic action potential depolarization with

transmitter release at the adult frog neuromuscular junction (Kerr and Yoshikami, 1984; Robitaille et al., 1990).

In the previous chapter (section 2.3), I showed that roscovitine increased calcium influx primarily by slowing deactivation of calcium channels. In contrast, DAP increased calcium influx by altering the action potential waveform and indirectly affecting calcium channel opening (see section 2.3; Cho and Meriney, 2006). Given these apparently direct effects of roscovitine on calcium channel function, I have examined the possibility that roscovitine could be used as a potential tool to study transmitter release at the adult frog neuromuscular junction. Roscovitine had several effects on cultured frog motoneuron calcium currents (slowed deactivation kinetics, slowed activation kinetics, and decreased proportion of current activated by an action potential), but I hypothesize that transmitter release effects of roscovitine at the nerve terminal are dominated by the most prominent effect: slowing of the deactivation kinetics of presynaptic N-type calcium channels that leads to an increase in total calcium entry through each open channel during an action potential stimulus. In this chapter, I demonstrate that roscovitine increases the release of acetylcholine from the adult frog neuromuscular junction without changing paired-pulse facilitation under low calcium conditions. In contrast, DAP also increases release, but also significantly increases the paired-pulse ratio under low calcium conditions. The differential effects of these two pharmacological treatments on paired-pulse facilitation suggest that roscovitine and DAP can be used as good tools to advance our understanding of the mechanisms of short-term plasticity.

3.2 METHODS

3.2.1 Tissue preparation.

Adult frogs (*Rana pipiens*) were anesthetized by immersion in 0.6% tricaine methane sulfonate, decapitated, and double-pithed in accordance with the University of Pittsburgh's Institutional Animal Care and Use Committee. The cutaneous pectoris nerve-muscle preparation was removed bilaterally and bathed in normal frog Ringer (NFR; in mM: 116 NaCl, 1 NaHCO₃, 2 KCl, 1.8 CaCl₂, 1 MgCl₂, 5 HEPES, 5 glucose, pH 7.3).

3.2.2 Recording and analysis of transmitter release.

Intracellular recordings from the adult frog cutaneous pectoris nerve-muscle preparation were performed as described previously (Meriney & Grinnell, 1991). In brief, recordings of synaptic potentials were performed in NFR with 4-6 μ M curare to partially block postsynaptic receptors and to prevent muscle contractions, or in NFR with 4 μ M curare and 4-5 μ M μ -conotoxin PIIIA added to block selectively muscle sodium channels, or in saline containing 0.3 mM Ca²⁺ and 4 mM Mg²⁺ to prevent contractions by reducing quantal content. The cutaneous pectoris nerve was drawn into a suction electrode and stimulated with 100 μ sec pulses at five-times threshold. Intracellular recordings of membrane potential from muscle cells were obtained using glass microelectrodes (20-40 M Ω) filled with 3 M potassium acetate. Muscle cell penetrations were made under visual control with a long working distance water-immersion objective (40x; 3 mm working distance) and contrast-enhancing optics to identify individual

neuromuscular junctions. Data were acquired through a Dagan BBC 700 amplifier using Clampex 9 software (Axon Instruments, Foster City, CA) running on a pentium-based computer. Off-line data analysis was performed using Clampfit 9 software. All values are expressed as mean \pm SEM, and all tests of significance were performed using a Student's paired *t* test. All control recordings were performed with 0.1% DMSO in the bath.

3.2.3 Reagents

(R)-roscovitine and (S)-roscovitine were obtained from Dr. L. Meijer (Station Biologique de Roscoff, CNRS UPR, Roscoff cedex, Bretagne, France) or Alexis Co. (San Diego, CA, USA). Olomoucine was obtained from Alexis Co. (San Diego, CA, USA). (R)-roscovitine, (S)-roscovitine, and olomoucine were stored at -20°C as 1000X stock solutions in DMSO and all final concentrations were 100 μ M. All other chemicals were obtained from Sigma (St. Louis, MO). 3,4-diaminopyridine (DAP) was made fresh daily.

3.3 RESULTS

3.3.1 Roscovitine effects on neurotransmitter release

In order to evaluate the effects of (R)-roscovitine on neurotransmitter release at the adult frog neuromuscular junction, I measured endplate potentials (EPPs) and miniature EPPs (mEPPs) before and after the application of (R)-roscovitine. Quantal content was calculated as

the amplitude of EPPs (average of 80-100 sweeps) divided by the average amplitude of mEPPs. In 0.3 mM Ca^{2+} saline, (R)-roscovitine increased EPP amplitude by $125 \pm 21\%$ (Figure 8A and Figure 9A; $n = 39$ nerve terminals; $p < 0.01$), and increased mEPP frequency by $115 \pm 22\%$ (Figure 9B; $n = 19$ nerve terminals; $p < 0.001$). (R)-roscovitine did not significantly change mEPP amplitude (Figure 9D; $n = 19$ nerve terminals) and thus significantly increased quantal content by $149 \pm 29\%$ (Figure 9C; $n = 19$ nerve terminals; $p < 0.05$). The relationship between the increase in EPP amplitude and the increase in quantal content mediated by (R)-roscovitine was quite linear (Figure 8C; $n = 19$ nerve terminals). Furthermore, since there was no change in mEPP amplitude, these results lead to the conclusion that the effects of (R)-roscovitine on my measurements of neurotransmitter release are presynaptic. To more easily observe the time-course of (R)-roscovitine effects (as recording in low calcium saline includes a significant number of failures and quantal fluctuation), I recorded EPPs in normal frog Ringer (1.8 mM Ca^{2+}) plus 4-6 μM curare. Under these conditions, (R)-roscovitine increased transmitter release by $50.3 \pm 5.4\%$ ($n = 41$ nerve terminals; $p < 0.001$; see Figure 8B). Near maximal effects of (R)-roscovitine were often observed within the interval between pulses (2 seconds) and this was consistent with what has been reported for effects on calcium current (Yan et al. 2002; Buraei et al. 2005).

Because (R)-roscovitine is a well-known cdk inhibitor, I investigated whether the effect of (R)-roscovitine on neurotransmitter release was related to cdk activity by examining the effects of other structurally-related cdk inhibitors ((S)-roscovitine and olomoucine) on neurotransmitter release. (S)-roscovitine and olomoucine have similar structures to (R)-roscovitine, but have no reported effect on calcium current kinetics or transmitter release in other systems (Yan et al. 2002; Buraei et al. 2005). (S)-roscovitine did not significantly change EPP

amplitude (n = 23 nerve terminals), quantal content or mEPP amplitude (Figure 9; n = 19 nerve terminals). Olomoucine did not significantly change quantal content (Figure 9C; n = 15 nerve terminals), but decreased EPP amplitude (Figure 9A; n = 21 nerve terminals; $p < 0.01$) and mEPP amplitude (Figure 9D; n = 15 nerve terminals; $p < 0.01$); an apparent mild postsynaptic effect on acetylcholine receptors that was only observed with this compound. All three cdk inhibitors increased mEPP frequency significantly (Figure 9B; $p < 0.01$). The lack of similar effects of (S)-roscovitine and olomoucine on EPP amplitude or quantal content suggest that these effects of (R)-roscovitine are cdk-independent.

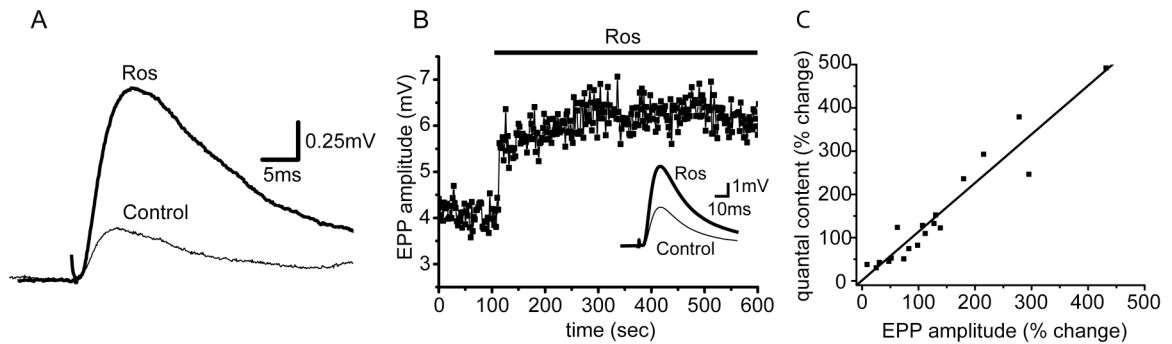


Figure 8 Effects of (R)-roscovitine on EPP amplitude at the adult frog neuromuscular junction.

- A. Representative example of averaged EPP size before (Control; thin trace) and after (Ros; thick trace) exposure to 100 μM (R)-roscovitine (recorded in 0.3 mM Ca^{2+} saline).
- B. A representative recording of EPP amplitude plotted against time as 100 μM (R)-roscovitine was perfused onto the neuromuscular junction (recorded with 5 μM curare in NFR). Inset. Representative example of averaged EPP size before (Control; thin trace) and after (Ros; thick trace) exposure to 100 μM (R)-roscovitine in NFR with 5 μM curare.
- C. The relationship between percent increase in EPP amplitude and percent increase in quantal content by (R)-roscovitine (n=19 nerve terminals).

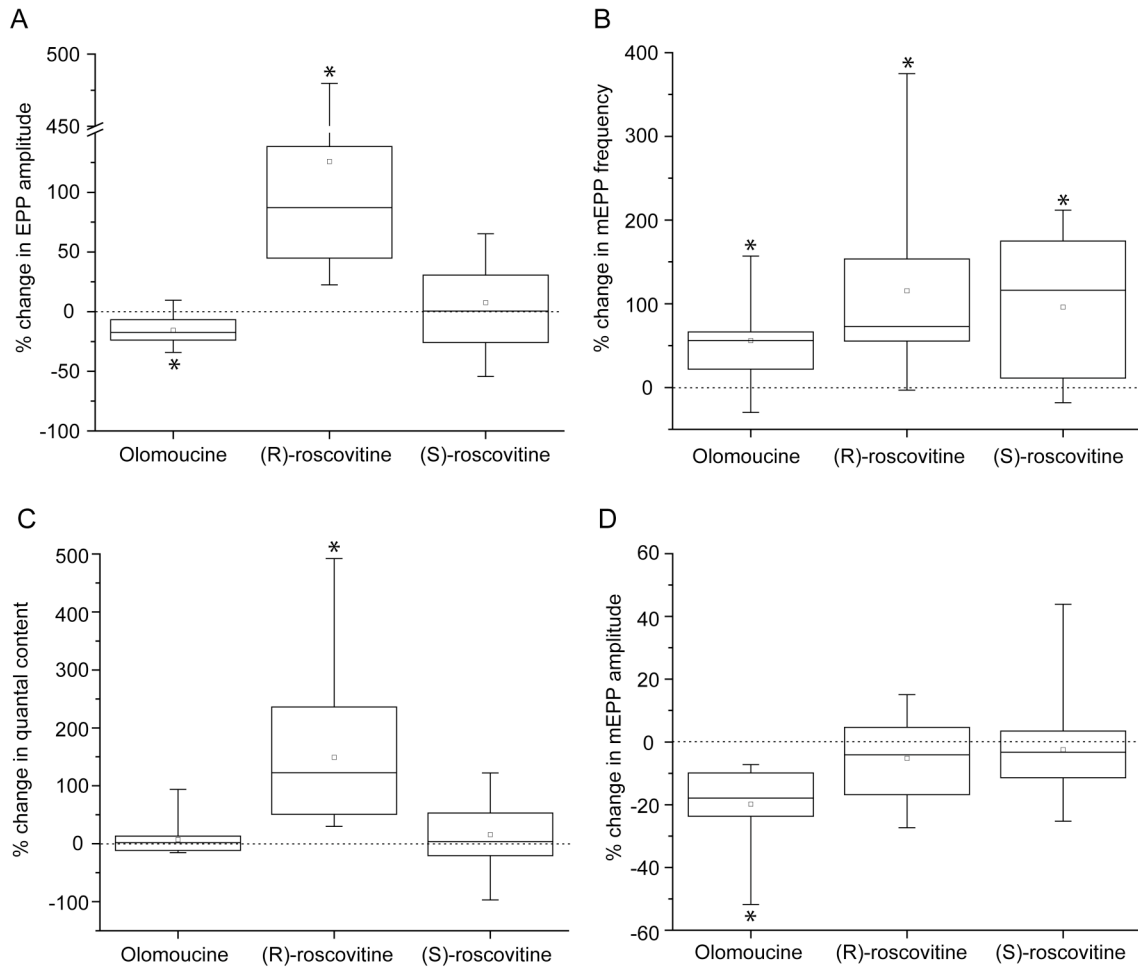


Figure 9 Comparison of the effects of (R)-roscovitine, (S)-roscovitine, and olomoucine on neurotransmitter release at the adult frog neuromuscular junction.

A. Boxplot of the changes in EPP amplitude. (R)-roscovitine significantly increased EPP amplitude by $125 \pm 21\%$ ($n=39$ nerve terminals; $*p<0.01$). Olomoucine significantly decreased EPP amplitude by $-15.6 \pm 3.3\%$ ($n=21$ nerve terminals; $*p<0.01$) and (S)-roscovitine did not have significant effects ($7.5 \pm 12.6\%$ increase; $n=23$ nerve terminals).

B. Boxplot of the changes in mEPP frequency. Olomoucine, (R)-roscovitine and (S)-roscovitine significantly increased mEPP frequency by $55 \pm 11\%$ ($n=15$ nerve terminals; $*p<0.01$), $115 \pm 22\%$ ($n=19$ nerve terminals; $*p<0.001$), and $96 \pm 19\%$ ($n=19$ nerve terminals; $*p<0.001$)

respectively.

C. Boxplot of changes in quantal content. (R)-roscovitine significantly increased quantal content by $149 \pm 29\%$ (n=19 nerve terminals; *p<0.05). Olomoucine and (S)-roscovitine did not have significant effects (increasing by $7.1 \pm 7.4\%$ (n=15) and $15.8 \pm 12.4\%$ (n=19) respectively).

D. Boxplot of the changes in mEPP amplitude. (R)-roscovitine and (S)-roscovitine did not show significant effects (changing by $-5.2 \pm 2.8\%$ (n=19) and $-2.4 \pm 3.6\%$ (n=19) respectively). Olomoucine significantly decreased mEPP amplitude by $-19.8 \pm 3.0\%$ (n=15 nerve terminals; *p<0.001). Asterisks indicate significant difference (Student's paired *t* test).

3.3.2 Roscovitine effects on short-term plasticity

Since (R)-roscovitine showed significant effects on evoked transmitter release, I examined its functional impact on short-term synaptic plasticity. Paired-pulse ratio was calculated as (the second EPP amplitude)/(the first EPP amplitude) and the second EPP amplitude was measured after correction based on the decay of the first EPP. I examined the effect of (R)-roscovitine on the magnitude of transmitter released during paired-pulse stimuli at a 30 msec interstimuli interval (ISI) in 0.3 mM Ca^{2+} saline. Under these conditions, (R)-roscovitine did not significantly alter the paired-pulse ratio ($3.3 \pm 1.6\%$ increase; Figure 10A and 10B; $n = 13$ nerve terminals). Because I hypothesize that (R)-roscovitine has a direct action on presynaptic calcium channels, I compared (R)-roscovitine effects on short-term plasticity with another modulator of transmitter release that is known to have an indirect effect on presynaptic calcium channels. For this comparison, I used DAP because this drug increases transmitter release by increasing action potential amplitude, and thus indirectly increasing calcium channel activation (see section 2.3). Exposure to 1 μM DAP produced a similar increase in EPP amplitude ($158 \pm 48\%$ increase; $n = 6$ nerve terminals) as 100 μM (R)-roscovitine. However, in contrast to (R)-roscovitine, 1 μM DAP significantly increased the paired-pulse ratio in 0.3 mM Ca^{2+} saline (by $22.6 \pm 7.8\%$; Figure 10A and 10C; $n = 6$ nerve terminals; $p < 0.05$).

I also investigated the effects of (R)-roscovitine on paired-pulse facilitation in normal calcium (1.8 mM Ca^{2+}) conditions. (R)-roscovitine significantly decreased the paired-pulse ratio at a 30 msec ISI in 1.8 mM Ca^{2+} saline (by $11.2 \pm 0.6\%$; Figure 11; $n = 12$ nerve terminals; $p < 0.01$). Under the same conditions, DAP also significantly decreased the paired-pulse ratio at a 30 msec ISI (by $9.4 \pm 1.4\%$; Figure 12; $n = 14$ nerve terminals; $p < 0.01$). Thus, with a 30 msec

ISI stimulation, the effects of (R)-roscovitine and DAP on paired-pulse ratio were not significantly different.

To examine the effects of (R)-roscovitine on paired-pulse ratio with shorter interstimulus interval, I used a 10 msec ISI. At this interval, (R)-roscovitine also significantly decreased the paired-pulse ratio in 1.8 mM Ca^{2+} saline (by $16.3 \pm 1.3\%$; Figure 11; $n = 8$ nerve terminals; $p < 0.01$). This is a significantly larger effect than observed at 30ms ISI ($p < 0.01$). Under the same conditions, DAP also significantly decreased the paired-pulse ratio (by $9.4 \pm 2.1\%$; Figure 12; $n = 10$ nerve terminals; $p < 0.01$) and this effect was not significantly different from that observed using a 30ms ISI. Thus, with a 10 msec ISI stimulation, the effects of (R)-roscovitine and DAP on paired-pulse ratio were in the same direction, but (R)-roscovitine effects were significantly larger ($p < 0.05$).

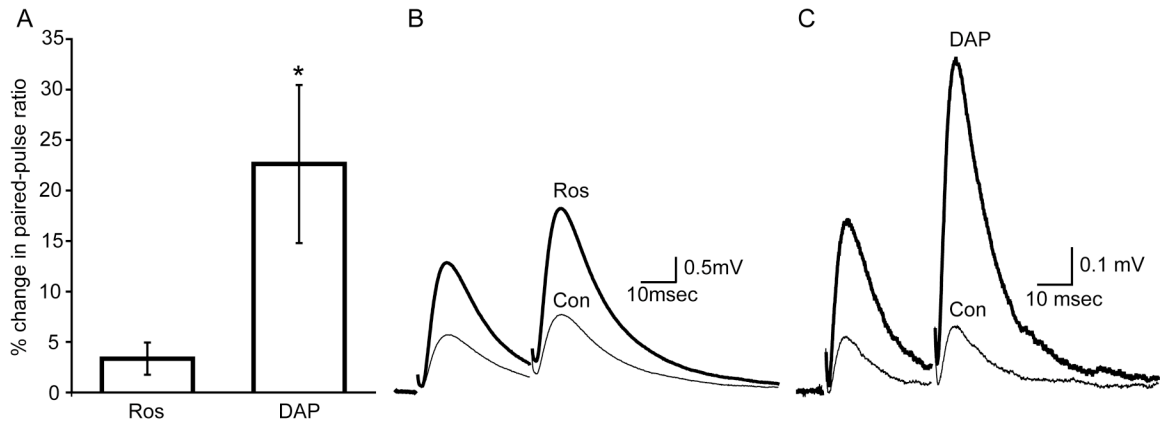


Figure 10 Effects of (R)-roscovitine and DAP on the paired-pulse ratio at the adult frog neuromuscular junction recorded in 0.3 mM Ca^{2+} .

(Interstimulus interval of 30 msec)

A. Summary of the percent changes in the paired-pulse ratio following exposure to 100 μM (R)-roscovitine or 1 μM DAP. (R)-roscovitine did not show a significant effect on the paired-pulse ratio ($3.3 \pm 1.6\%$ increase; $n=13$ nerve terminals). DAP significantly increased the paired-pulse ratio by $22.6 \pm 7.8\%$ ($n=6$ nerve terminals; $*p<0.05$).

B. A representative example of averaged EPPs during paired-pulse stimuli before (Con; thin trace) and after (Ros; thick trace) exposure to 100 μM (R)-roscovitine.

C. A representative example of averaged EPPs during paired-pulse stimuli before (Con; thin trace) and after (DAP; thick trace) exposure to 1 μM DAP. Asterisks indicate significant difference (Student's paired t test).

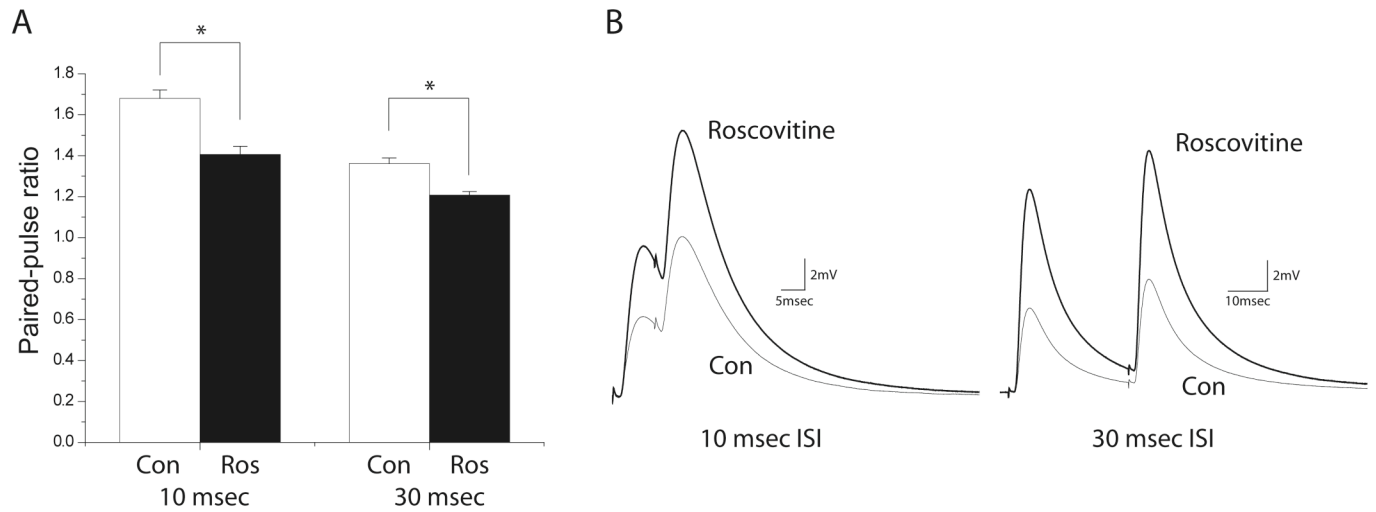


Figure 11 The effects of (R)-roscovitine on paired-pulse ratio in 1.8mM Ca²⁺

A. (R)-roscovitine significantly decreased paired-pulse facilitation by $16.3 \pm 1.3\%$ ($n=8$) with 10 msec ISI and by $11.2 \pm 0.6\%$ ($n=12$) with 30 msec ISI. Asterisks indicate significant difference (Student's paired t test; $p<0.01$).

B. A representative examples of the averaged EPPs during paired-pulse stimuli before (Con; thin trace) and after (Roscovitine; thick trace) exposure to 100 μ M (R)-roscovitine.

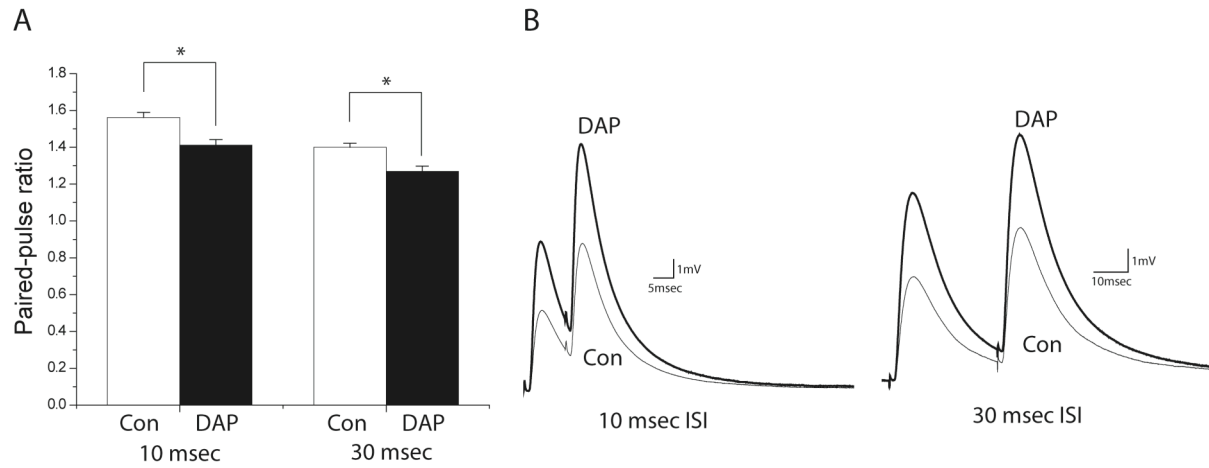


Figure 12 The effects of DAP on paired-pulse ratio in 1.8mM Ca²⁺

A. DAP significantly decreased paired-pulse facilitation by $9.4 \pm 2.1\%$ ($n=10$) with 10 msec ISI and $9.4 \pm 1.4\%$ ($n=14$) with 30 msec ISI. Asterisks indicate significant difference (Student's paired t test; $p<0.01$).

B. A representative examples of the averaged EPPs during paired-pulse stimuli before (Con; thin trace) and after (DAP; thick trace) exposure to 1 μ M DAP.

3.4 DISCUSSION

The calcium influx activated by action potentials invading the presynaptic terminal triggers transmitter release, and alterations in the gating of presynaptic voltage-gated calcium channels can result in significant changes in the magnitude of transmitter released. (R)-roscovitine increased transmitter release at the adult frog neuromuscular junction by a presynaptic mechanism that likely is mediated by an increase in total calcium entry due to slowing of the deactivation kinetics of presynaptic N-type calcium channels. Unexpectedly, although (S)-roscovitine and olomoucine did not significantly alter calcium currents or evoked release in my experiments, the frequency of mEPPs was increased by all three agents tested ((R)-roscovitine, (S)-roscovitine, and olomoucine). It is possible that this effect on mEPP frequency is mediated by an inhibition of cdks that affects spontaneous release frequency in a manner that does not alter evoked release. In this case, it appears that spontaneous and evoked release can be regulated independently of one another, as has also been observed after other experimental manipulations (see Deitcher et al. 1998; Poage et al. 1999).

The selective effects of (R)-roscovitine at the motor nerve terminal impact upon our understanding of the specific relationship between calcium entry and transmitter release at the motor synapse. Despite the fact that it has been known that transmitter release is triggered by calcium entry for more than 60 years, the specific manner in which calcium entry triggers vesicle fusion continues to be a topic of investigation, and may be different at each synapse. At the adult frog neuromuscular junction, there are many highly organized linear active zones (Heuser et al. 1979), and the fusion of vesicles is distributed along the length of the nerve terminal and appears

to occur with low probability from each active zone (D'Alonzo & Grinnell, 1985; Bennett et al. 1986). Using a high-resolution 'snapshot' imaging approach, calcium entry within adult frog neuromuscular junction active zones has been characterized during action potential invasion (Wachman et al. 2004; Luo et al. 2005). These studies have led to the conclusion that calcium enters the motor nerve terminal in spatially restricted regions of the active zone and that very few of the many calcium channels positioned in the active zone respond when an action potential invades the nerve terminal. These data are consistent with patch clamp recordings of calcium current activation in which an action potential waveform has been shown to be not very effective at gating N-type calcium channels (see Figure 6; King & Meriney, 2005). Therefore, at the frog neuromuscular junction, it appears that there is a very low probability of N-type calcium channel opening during an action potential, and each single calcium channel opening might trigger a single transmitter-containing vesicle to fuse (see Yoshikami et al. 1989). Similar conclusions have been drawn in several preparations using various experimental and modeling approaches (Llinas et al. 1981; Yoshikami et al. 1989; Augustine et al. 1991; Bertram et al. 1996; Gentile & Stanley, 2005; Pattillo et al. 2007).

The data reported here lead me to hypothesize that the underlying mechanism of (R)-roscovitine effects on transmitter release is an increase in total calcium entry at each open presynaptic calcium channel (due to slowed deactivation kinetics) with little change in the number or proportion of calcium channels that are activated in the active zone by an action potential. This (R)-roscovitine-mediated increased calcium influx may only locally increase calcium within the nano- or microdomains that are normally activated. Therefore, (R)-roscovitine may not lead to a significant change in the calcium ion spatial distribution within the nerve terminal. In this sense, the (R)-roscovitine-mediated increases in presynaptic calcium

entry might remain restricted to only a few entry sites within each active zone (Figure 13). In contrast, DAP is expected to increase the number of calcium channels that open with each action potential stimulus, and this would lead to an increase in calcium ion spatial distribution within the nerve terminal (Figure 13). This difference in the mechanism by which (R)-roscovitine and DAP increase calcium entry likely explains the different effects of these agents on paired-pulse facilitation under low calcium conditions (see Figure 10).

Because (R)-roscovitine is hypothesized not to alter the normally sparse spatial distribution of calcium entry within presynaptic active zones, I predict that (R)-roscovitine increases transmitter release by increasing the probability of vesicle fusion events from these very sparsely distributed calcium entry sites. Under these conditions, during paired-pulse stimulation, the residual calcium that exists following the first action potential invasion of the nerve terminal may not overlap significantly with calcium entry sites that are recruited during a second action potential stimulus with short inter-stimulus interval under low calcium conditions. Under normal calcium conditions, more calcium ions will enter through each open calcium channel (as compared with low calcium conditions). This will be predicted to cause increased overlap of calcium entry sites. Although (R)-roscovitine does not alter the number of calcium channel openings per stimulus, the increased flux under normal calcium conditions may explain the decrease in paired-pulse facilitation observed after (R)-roscovitine treatment. In that sense, the effects of roscovitine and DAP on paired-pulse facilitation in normal calcium condition were similar, while these two drugs showed quite contrasting effects under low calcium conditions.

Following DAP treatment, the large increase in the spatial distribution of calcium entry would lead to significant overlap in residual calcium between two action potential stimuli with short inter-stimulus interval. Under low calcium conditions, there is no vesicle depletion, so the

DAP-mediated increase in residual calcium at many release sites leads to increased paired-pulse facilitation of transmitter release. In normal levels of extracellular calcium where vesicle depletion contributes to the measured effects of paired-pulse stimuli, the effects of DAP are expected to be a balance between the effects of increased residual calcium and decreased vesicle availability. As a result, DAP leads to decreased paired-pulse facilitation under normal calcium conditions because the increased vesicle depletion dominates and overshadows the facilitation due to residual calcium. Previous studies have also reported reduced paired-pulse facilitation after DAP treatment (Thomsen & Wilson, 1983; Baker and Marion, 2002).

Lastly, the direct effects of (R)-roscovitine on presynaptic calcium channels at the motor nerve terminal may prompt future investigations into the therapeutic potential of related compounds. Treatment of neuromuscular disorders, such as Lambert-Eaton Myasthenic Syndrome might be improved by the use of a compound that has a direct agonist effect on presynaptic calcium channels. This concept will be discussed further in the general discussion (see section 5.2). It is possible that agents, which can directly and selectively target presynaptic calcium channels, and prolong deactivation kinetics, would have useful therapeutic actions with fewer side effects.

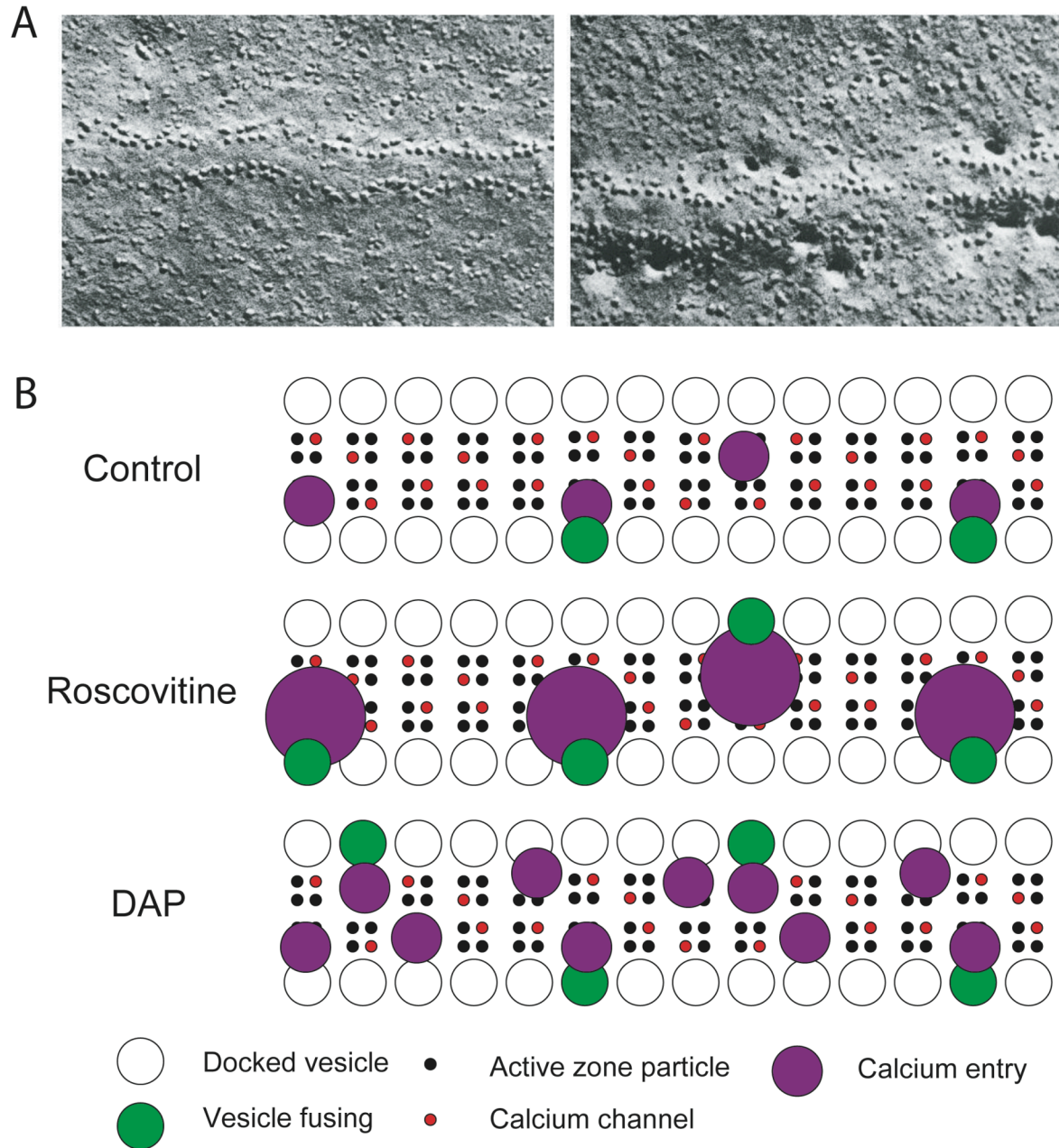


Figure 13 Schematic diagram of calcium entry and vesicle release with a single action potential before (control) and after roscovitine and DAP treatment.

A. Electron micrograph ($\times 120000$) of frog neuromuscular junction in control (left) and after treatment with 4-aminopyridine (right). From Heuser and Reese (1977).

B. Diagram of active zone comparable to electron micrograph of frog neuromuscular junction in

A. Comparison of calcium entry and vesicle fusion of control and after roscovitine and DAP treatment.

4. COMPUTATIONAL MODELING OF THE ADULT FROG NEUROMUSCULAR JUNCTION

In previous chapters, I have described the use of roscovitine and DAP as experimental agents to manipulate calcium entry and transmitter release. The goal of this work is to increase our understanding of the mechanisms that underlie calcium-triggered vesicle fusion. To aid in this endeavor, I have added the use of microphysiological computational modeling. This computer modeling approach employs three-dimensional stochastic simulations of calcium influx, diffusion, and molecular interactions using Monte Carlo methods to simulate the MCell/DReAMM microphysiological environment (Stiles and Bartol, 2000; Stiles et al., 2001; Pattillo, 2002). “MCell” (www.mcell.psc.edu) is the Monte Carlo simulator of cellular microphysiology that was used in this thesis to simulate realistic three-dimensional reactions within the active zone of the frog neuromuscular junction at a molecular level. DReAMM (Design, Render, and Animate MCell Models, www.mcell.psc.edu/DReAMM) was used for visualization of data.

4.1 INTRODUCTION

4.1.1 Overview of Monte Carlo simulation of cellular microphysiology

Computational approaches can explore synaptic transmission beyond the temporal and spatial limitations of physiological experiments. Traditionally, simulations of diffusion and interaction of molecules can be based on one of two general numerical paradigms, Continuum (e.g. finite element) or Monte Carlo methods. Continuum methods employ a set of differential equations and predict the average behavior of the model, but stochastic variability is ignored (Smart and McCammon, 1998). In contrast to the Continuum approach, Monte Carlo methods use random numbers and probabilities to predict individual molecular interactions for each molecule in the simulation. This stochastic variability is likely to be important as it may reflect the variability of biologic interactions in nature. Monte Carlo methods can be used to simulate diffusion of individual molecules with random walk movements, which approximate real Brownian motion. Reaction transitions such as ligand binding and unbinding can be simulated using random numbers that test each possibility against a corresponding Monte Carlo probability. Furthermore, diffusion and molecular reactions are simulated in three-dimensional space.

4.1.2 MCell input and output files

Simulation components, such as molecules, channels, and surfaces, are specified using the Model Description Language (MDL), a simple programming language. Input files define

simulation objects and environments, duration of each simulation time-step, and the number of time-steps. When a simulation is started, MDL input files are read, global conditions are initialized, and then time-step iterations begin. Each MCell simulation also uses a seed value for generation of random numbers. Random numbers generated by any computer are actually “pseudorandom”, because they are calculated using an algorithm that produces a deterministic set of values based on the input seed value. Different seeds produce different streams of values. In MCell, the random number generator uses a 64-bit algorithm similar to that employed for high-level computer encryption, and in practical terms can use an effectively unlimited number of seed values, and for each seed can generate an effectively unlimited number of pseudorandom values without repeating the sequence (Stiles and Bartol, 2000; Stiles et al., 2001; Pattillo, 2002). In this thesis, the averages of outputs from 1000 to 10000 different seeds for simulations are shown.

Within a MCell simulation, cellular surfaces are composed of triangulated meshes. Meshes can be characterized as “reflective”, “absorptive” or “transparent” with respect to diffusing molecules. For example, to simulate an impermeable membrane, the characteristics of individual triangles of a surface are made reflective to diffusing molecules. Molecules can diffuse and react in solution and on membranes. The distance traveled during each time step depends on the molecule’s diffusion coefficient and the time step for the simulation. Molecules on membranes cover patches of the surface area, and can be associated with reaction mechanisms to simulate events such as ligand binding and unbinding. The positions or densities of surface molecules are specified in input MDL files, and can be manually or randomly placed. On the same polygon mesh, different types of molecules can exist and function, for example, as receptors, channels or pumps. Reaction mechanisms in MDL files can specify directionality with

respect to a surface. With this feature, a molecule that binds a ligand on one side of a surface can unbind it on the other side and thus can function as a transporter. Rate constants of reaction mechanisms are also defined in input MDL files and are converted into Monte Carlo probabilities when the simulation is initialized. MCell carries out all types of transitions and interactions stochastically and thus simulates microphysiology with variability (Stiles and Bartol, 2000; Stiles et al., 2001; Pattillo, 2002).

It is possible to track each event in a simulation, because diffusion and reaction occur at a molecule-by-molecule level in a Monte Carlo simulation. Simulations can generate both reaction data output (that counts reactions and molecules, etc) and visualization data (positions and states of meshes and molecules). The desired output is specified in MDL files (Stiles and Bartol, 2000; Stiles et al., 2001; Pattillo, 2002).

4.1.3 Three dimensional model of a frog neuromuscular junction active zone

Morphological data at the electron micrograph level are required to generate realistic three-dimensional microphysiological environments. The frog neuromuscular junction has unique presynaptic active zone structure, including the regularly spaced, long linear arrays of synaptic particles in the active zone. This model synaptic system has been investigated for many years and a wealth of morphological and physiological data are available. Figure 14 shows a comparison of the structure of a frog neuromuscular junction and the MCell model. A single active zone includes two double rows of membrane proteins (some of which are calcium channels) and docked vesicles. In this dissertation, the model of a single active zone was used for all simulations. In the future, this approach using a multiple active zone model can be extended

for studying complex forms of plasticity. Figure 14B shows a model with 8 active zones. Figure 14C is a view from inside the nerve terminal and it shows some of the components of the model, including free calcium ions (yellow), buffer-bound calcium ions (purple), and docked synaptic vesicles (blue spheres).

Dimensions, topology, and the number of docked synaptic vesicles within the simulated active zone are based on averages of previous studies (Figure 14D; Heuser et al., 1979; Pumplin et al., 1981; Herrera et al., 1985; Pawson et al., 1998a, 1998b). The distance between Schwann cell finger-like intrusions, which wrap around the terminal, and the mean distance between active zones is 1.13 μm . The mean of terminal width is 1.52 μm . The mean length of the active zone is 980 nm and the width of the active zone is 60 nm. Docked vesicles are placed on either side of a shallow groove that contains presynaptic membrane particles including voltage-gated calcium channels (Figure 14E and 14F). Presynaptic membrane particles are positioned on the edges of a groove with a depth of 10 nm. The active zone model has 26 docked vesicles in double rows and each vesicle is placed 70 nm away from the center of the active zone and 5 nm above the membrane. The diameter of each vesicle is 50 nm. The average distance between a docked synaptic vesicle and voltage-gated calcium channel is ~ 40 nm.

Based on the results of calcium imaging experiments at the frog active zone, Wachman et al. (2004) hypothesized that the number of voltage-gated calcium channels is similar to the number of synaptic vesicles at the adult frog neuromuscular junction. This imaging work proposed that only a small portion of the ~ 200 synaptic particles might be voltage-gated calcium channels. Based on these conclusions, in this dissertation, a 1:1 ratio was used for voltage-gated calcium channels and synaptic vesicles.

Calcium ions and calcium buffers as well as voltage-gated calcium channels and synaptic vesicles are major components of the model. Figure 15 shows a DReAMM image view from within the synaptic cleft that depicts different states of voltage-gated calcium channels (black and white cylinders), docked synaptic vesicles (blue spheres), calcium-bound sensors on vesicles (red), unbound calcium sensors on vesicles (dark blue), free calcium ions (yellow), and buffer-bound calcium (purple). Calcium buffer sites are present throughout the space of the nerve terminal. Triangulated mesh structures of presynaptic membrane are shown in Figure 15 as wire frames.

All kinetic parameters of the model components are constrained by physiological and biochemical data. In this dissertation, simulation parameters including the calcium ion diffusion constant, calcium-binding affinity of calcium sensors on the synaptic vesicles, the duration of the simulation time-step, and the number of time-steps, were used as described in Pattillo (2002) and Pattillo et al. (2007), which showed that this model can reproduce multiple sets of experimental data from the adult frog neuromuscular junction. Synaptotagmin 1 functions as the model for the calcium sensor; its calcium binding rate was set at $1.0 \times 10^8 \text{ M}^{-1}\text{sec}^{-1}$, and its unbinding rate was set at 6000 sec^{-1} ($K_d = 60 \text{ }\mu\text{M}$; Davis et al., 1999). The total concentration of calcium buffer was set at 2 mM; this corresponds to approximately 1.1 million buffer sites within a single active zone model. The calcium-binding rate for these buffer sites was set to $1.0 \times 10^8 \text{ M}^{-1}\text{sec}^{-1}$, with a calcium-unbinding rate of $1.0 \times 10^4 \text{ sec}^{-1}$ (Winslow et al., 1994; Xu et al., 1997; Yazejian et al., 2000). The diffusion constant of calcium ions was set to $6 \times 10^{-6} \text{ cm}^2\text{sec}^{-1}$ (Hodgkin and Keynes, 1957). These initial parameters were used in most simulations performed in this dissertation, except in cases where I manipulated some kinetic parameters to test mechanistic hypotheses related to short-term synaptic plasticity.

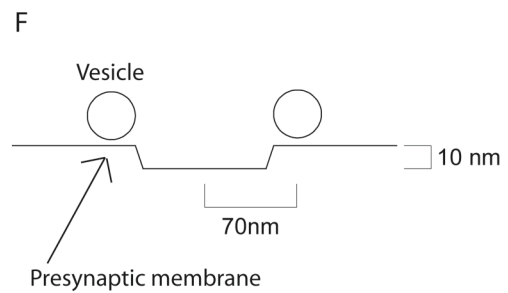
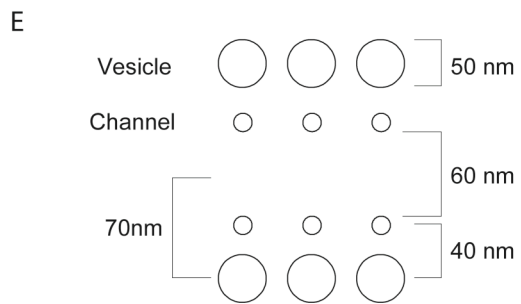
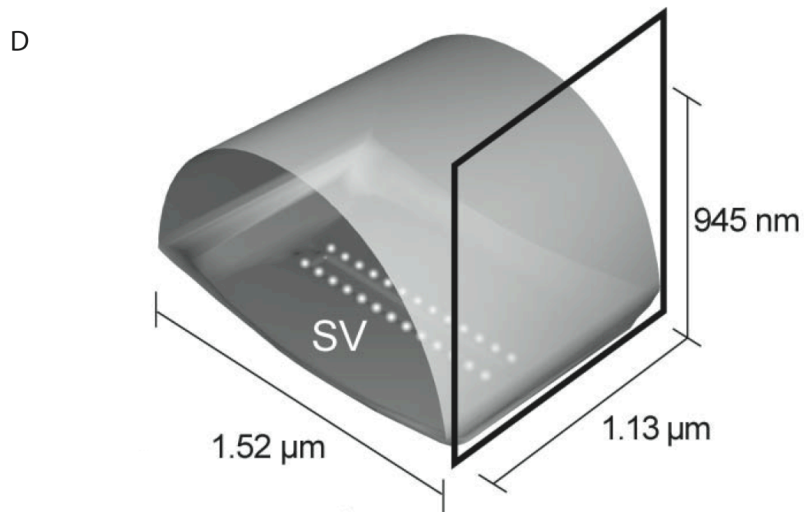
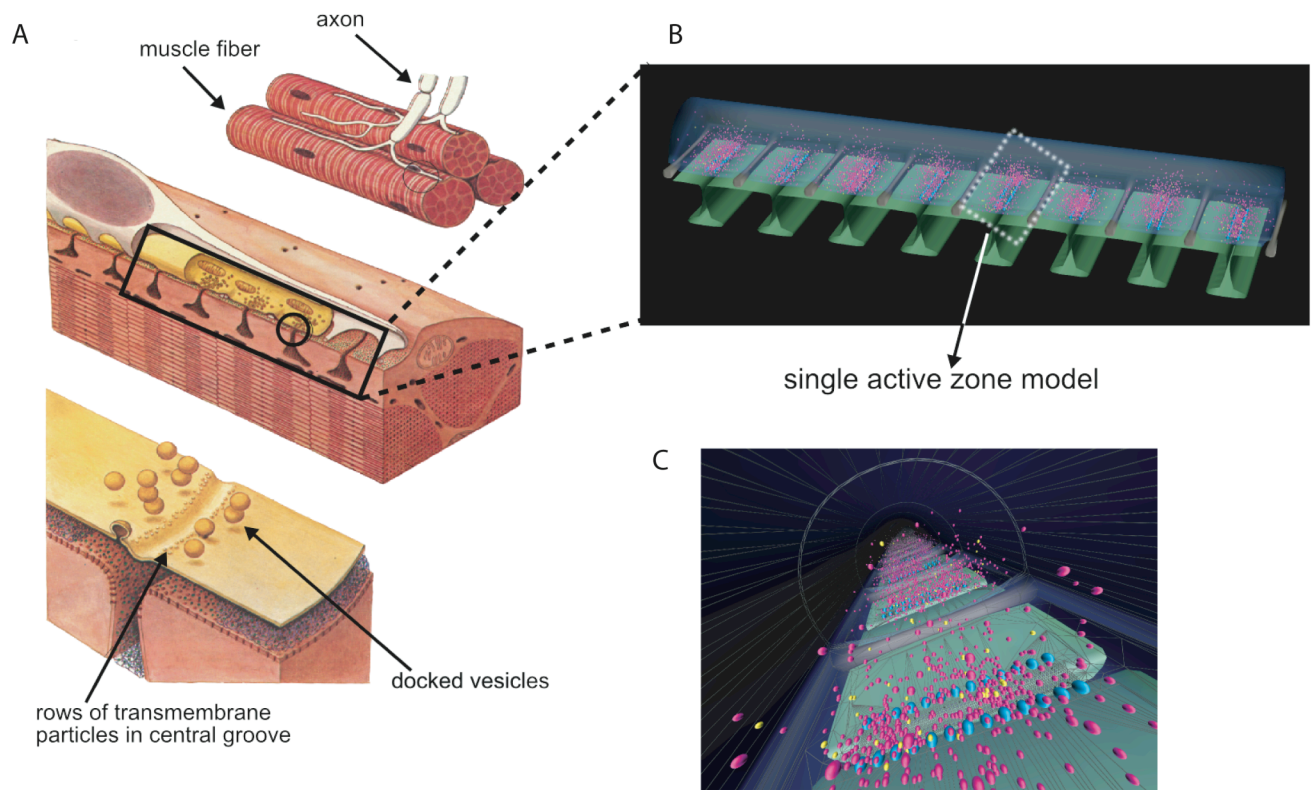


Figure 14 Multiple views of active zone model.

A. Schematic views of increasing magnification illustrating the structure of a neuromuscular junction and the active zones contained therein. **B** and **C** show two views of an *in silico* model during a simulation. The *in silico* model includes eight active zones, the opposing post-synaptic membrane, and the synaptic space. **C** depicts a view from inside the nerve terminal, and shows two rows with 13 synaptic vesicles each (blue spheres) at the edges of a central groove. These images also show free calcium ions (yellow spheres) and buffer bound calcium (purple spheres). **D.** Oblique three dimensional view of active zone model. **E.** Details of top view including vesicles and calcium channels. **F.** Side view of active zone model including vesicles and presynaptic membranes. The topology, dimensions, and number of synaptic vesicles were based on published averages. The volume of the model shown in **D** was approximately $0.9 \mu\text{m}^3$, the distance between the double rows of voltage-gated calcium channel locations was 60 nm, and the depth of the active zone groove was 10 nm. Two rows of 13 synaptic vesicles (50 nm diameter) were 70 nm from the active zone center, with 5 nm separating synaptic vesicles from terminal membrane. Panel **A** was adapted from Lester (1977).

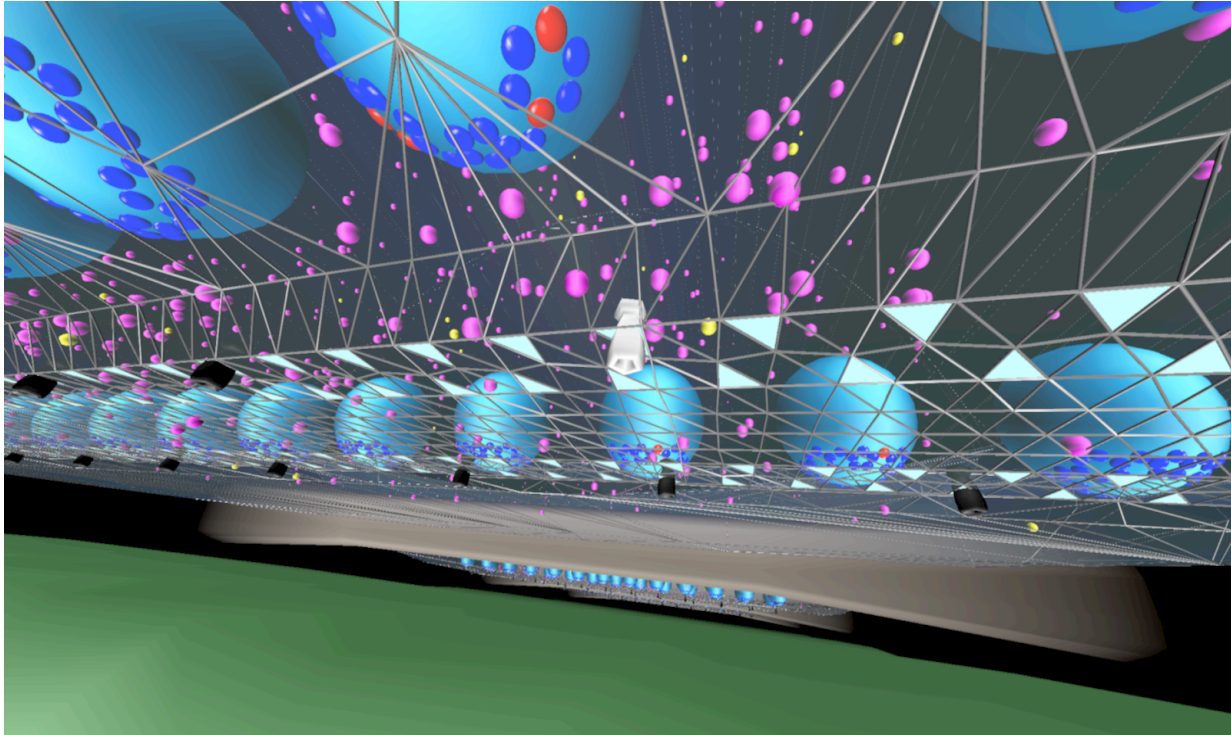


Figure 15 Close-up view from within the synaptic cleft

It showed synaptic vesicles (blue spheres), unbound calcium sensors on vesicles (dark blue), calcium-bound sensors (red), free calcium ions (yellow), and buffer-bound calcium (purple), closed calcium channels (black), and open calcium channels (white). Calcium sensors on synaptic vesicles were modeled on synaptotagmin C(2) domains. Presynaptic membranes were composed of triangular meshes.

4.1.4 Temporal and spatial resolution of the active zone model

The active zone model must encompass physiologically relevant maximal and minimal scales of time and space. Minimal spatial scales include the small distance between a docked synaptic vesicle and a voltage-gated calcium channel (~40 nm) with the corresponding diffusion time for free calcium (of order 1 μ sec). The maximum scales are defined by the length of the active zone (on the order of 1 μ m) and the synaptic delay (of order 1 msec) with the corresponding diffusion distance (of order 1 μ m). Therefore, in the simulations of the active zone model, the time scales are between μ sec and msec, and the space scales are between nm and μ m.

In MCell simulations, the Monte Carlo probabilities and the average random walk step length for diffusing molecules determine the numerical accuracy. Small time-steps in these simulations produce small step lengths and probabilities of interactions. These smaller probabilities and step lengths yield high accuracy. Therefore, in this dissertation, the time step for any simulations was set to 10 nsec to achieve high accuracy. Under these conditions, further reduction of the time step had no significant impact on simulation results.

4.1.5 Excessive number of calcium binding sites on each vesicle

As mentioned in the general introduction (section 1.2.2), the amount of transmitter released per action potential increases supralinearly, approximately as the fourth power of the extracellular calcium concentration (Jenkinson, 1957; Katz and Miledi, 1965b; Dodge and Rahamimoff, 1967; Andreu and Barrett, 1980; Barton et al., 1983). This had previously been

interpreted to reflect the presence of four calcium binding sites on each synaptic vesicle. However, Han et al. (2004) showed that each docked synaptic vesicle has up to 8 SNARE complexes. Assuming that each of these SNARE complexes is associated with a synaptotagmin molecule (the strong candidate for the calcium sensor), I hypothesized that there may be 8 synaptotagmin molecules per vesicle. Because each synaptotagmin molecule can bind 5 calcium ions (Sudhof and Rizo, 1996; Ubach et al., 1998; Earles et al., 2001; Fernandez et al., 2001; Chapman, 2002), it is possible that each synaptic vesicle has up to 40 calcium binding sites. Currently, the number of calcium binding sites and the number of calcium-bound sites required to cause vesicle fusion is still debated.

An excessive number of calcium binding sites can provide high sensitivity of vesicle release to calcium. It is possible that excessive calcium binding sites may play an important role in synaptic plasticity. Previous work (Pattillo, 2002; Pattillo et al., 2007) to develop the active zone model of the frog neuromuscular junction started with 4 calcium binding sites on synaptic vesicles, based on the experimental fourth order cooperative relationship between calcium concentration and transmitter release (Jenkinson, 1957; Katz and Miledi, 1965b; Dodge and Rahamimoff, 1967; Andreu and Barrett, 1980; Barton et al., 1983). However, simulations using 4 calcium binding sites per vesicle produced very few vesicle fusion events and could not generate the fourth order cooperative relationship between calcium concentration and transmitter release. This insensitivity was overcome by increasing calcium binding sites on synaptic vesicles. Previous work (Pattillo et al., 2007) using a model with 40 calcium binding sites per synaptic vesicle reproduced prominent experimental data, including the fourth order relationship between transmitter release and calcium concentration and the average probability of release. In those studies, simultaneous calcium binding of 6 to 8 out of 40 sites triggered

vesicle fusion. In this dissertation, 40 calcium binding sites per synaptic vesicle were used in all simulations and two sets of binding schemes (independent or cooperative binding) required to trigger vesicle fusion were applied (see details in section 4.2.4; Figure 17). The simulated number of released vesicles using these binding schemes was compared with experimentally determined number of vesicles released per action potential (see section 4.3.1).

4.2 METHODS

4.2.1 Tissue preparation.

Adult frogs (*Rana pipiens*) were anesthetized by immersion in 0.6% tricaine methane sulfonate, decapitated, and double-pithed in accordance with the University of Pittsburgh's Institutional Animal Care and Use Committee. The cutaneous pectoris nerve-muscle preparation was removed bilaterally and bathed in normal frog Ringer (NFR; in mM: 116 NaCl, 1 NaHCO₃, 2 KCl, 1.8 CaCl₂, 1 MgCl₂, 5 HEPES, 5 glucose, pH 7.3).

4.2.2 Confocal microscopy

Postsynaptic acetylcholine receptors of the cutaneous pectoris nerve-muscle preparation were stained with 2 µg/ml Alexa Fluor 594 conjugated α -bungarotoxin (BTX). The cutaneous pectoris nerve-muscle preparation was also stained with 2 mg/ml peanut agglutinin (PNA) to identify the position of the nerve terminal by staining the extracellular matrix of the Schwann cell. After

staining, the preparation was fixed with 4% paraformaldehyde. Preparations were mounted in Mowiol on glass slides. The preparations were imaged using an Olympus Fluoview FV 1000 confocal microscope with an oil immersion objective (60X). Images were taken with a 0.5 μm Z-stack through the entire neuromuscular junction and the brightest projections of all image stacks were made in order to resolve the postsynaptic receptor fold pattern and count the number of the active zones per nerve terminal.

4.2.3 Two-electrode voltage clamp experiments

Postsynaptic end-plate currents (EPCs) were recorded using the two-electrode voltage-clamp technique (Takeuchi and Takeuchi, 1959; Giniatullin et al., 1997, 2005). The resistances of intracellular electrodes were 3-5 $\text{M}\Omega$ when filled with 2.5 M KCl. EPCs and mEPCs were digitized at 5 kHz. Clamping speed was measured using a square step command (from 0 mV to -5 mV for 10 msec) and the clamp time constant (τ) was required to be less than 100 μsec . The holding potential was kept at -80 mV. In normal frog Ringer (1.8 mM Ca^{2+}), the quantal content was calculated by dividing the EPC area by the mEPC area. EPC area was corrected by considering driving force ($\text{DF} = \text{membrane potential} - E_{\text{qACh}}$) and voltage error (VE) ($\text{EPC}_{-80 \text{ mV}} = \text{EPC}_{\text{measured}} \times (\text{DF}/(\text{DF}-\text{VE}))$), because voltage clamping was determined not to be perfect due to the very large size of muscle cells and EPC events. For these calculations, equilibrium potential of the acetylcholine receptor channel (E_{qACh}) was set to 0 mV (Mallart et al., 1976; Peper et al., 1982). So, driving force was the actual membrane potential. To prevent muscle contractions, the cutaneous pectoris nerve-muscle preparation was bathed in 4-5 μM μ -conotoxin P111A (a selective, irreversible skeletal muscle sodium channel blocker) for 30 minutes and prior to

recording, and then the preparation was rinsed in NFR solution. The use of μ -conotoxin PIIIA prevents the muscle from contracting in normal calcium, while allowing the recording of spontaneous release (mEPCs).

4.2.4 Modeling of calcium channel activity and vesicle release

To simulate calcium influx, a calcium channel gating model (which reflects changes in membrane potential during an action potential) was determined (Figure 16). My model had 4 closed states and 2 open states under control and DAP conditions. To model roscovitine effects, there were 5 closed states and 4 open states. “R”states such as RO1, RO2, and RC4 were used to represent roscovitine bound states (Figure 16). This model was modified from Buraei et al. (2005), which simulated roscovitine effects on calcium currents in Bullfrog sympathetic neurons. My model was modified to fit the effects of both roscovitine and DAP on both calcium currents and vesicle release. Rate constants (k_x) were calculated from equation 1 using the rate parameters shown in Figure 16.

$$\text{equation 1: } k_x = A_x \exp((V - C_x)z_x F / RT)$$

(A_x : rate constant at the characteristic voltage (C_x); z_x : charge moved; R: gas constant; T: absolute temperature; F: Faraday’s constant)

Reversal potential for calcium was modeled at +50 mV and the single channel conductance used was 2.4 pS in 2 mM $[Ca^{2+}]_o$. Each open calcium channel emitted calcium ions according to Poisson probabilities calculated from the single channel conductance and driving

force. For example, each open state emitted an average of 800 ions/msec when the membrane potential was -60 mV (Church and Stanley, 1996).

Rate constants were determined by comparing modeling and experimental results related to calcium channel open probability, the time-course of calcium currents activated by an action potential and a step voltage command, and changes in calcium current integral after roscovitine or DAP treatments. In these studies, the calcium channel opening probability was defined as the average probability that a channel would be expected to open during a single action potential stimulation. The value used for these modeling simulations (0.14) was based on estimates derived from patch clamp and imaging results (Wachman et al., 2004; King and Meriney, 2005; Luo et al., 2005)

Vesicle release was determined by either an independent-simultaneous calcium binding scheme or a cooperative-simultaneous calcium binding scheme (Pattillo, 2002; Pattillo et al., 2007). Simultaneous binding of 8 calcium ions among any of the 40 calcium binding sites on synaptic vesicles was required for vesicle release by the independent-simultaneous calcium binding scheme (Figure 17A). Alternatively, because previous work (Earles et al., 2001) suggested that at least two sites on an individual synaptotagmin molecule needed to be occupied to trigger vesicle fusion, a cooperative scheme was tested. In my cooperative-simultaneous scheme, the 40 calcium binding sites on each synaptic vesicle were subdivided into 8 subgroups of 5 binding sites, because each synaptotagmin molecule has 5 calcium binding sites (see section 1.2.1; Sudhof and Rizo, 1996; Ubach et al, 1998; Fernandez et al., 2001). If more than 3 of the 8 subgroups bound more than 2 calcium ions, that is, more than 6 simultaneous calcium ions bound in total, those vesicles were considered “released” by the cooperative-simultaneous

calcium binding scheme (Figure 17B). The release probability of each vesicle was calculated by counting the number of released vesicles and dividing by the total number of trials.

The original calcium channel gating model (Buraei et al., 2005) was designed to model calcium current kinetics without regard for probability of vesicle release. Without modification, this original calcium channel gating model (Buraei et al., 2005) showed unreasonably high probability of vesicle release during an action potential. After modification, my calcium channel gating model (Figure 16) was able to simulate presynaptic calcium influx and vesicle release with a single action potential before and after pharmacological treatments at the adult frog neuromuscular junction (see section 4.3.2 and 4.3.3).

Figure 16 Calcium channel gating model and rate parameters.

$A(s^{-1})$ is the rate constant at the characteristic voltage (10 mV) and z is the charge moved.

The units of A for k_{46} and k_{57} are $\mu M^{-1}s^{-1}$. $[R]$ is the roscovitine concentration (μM).

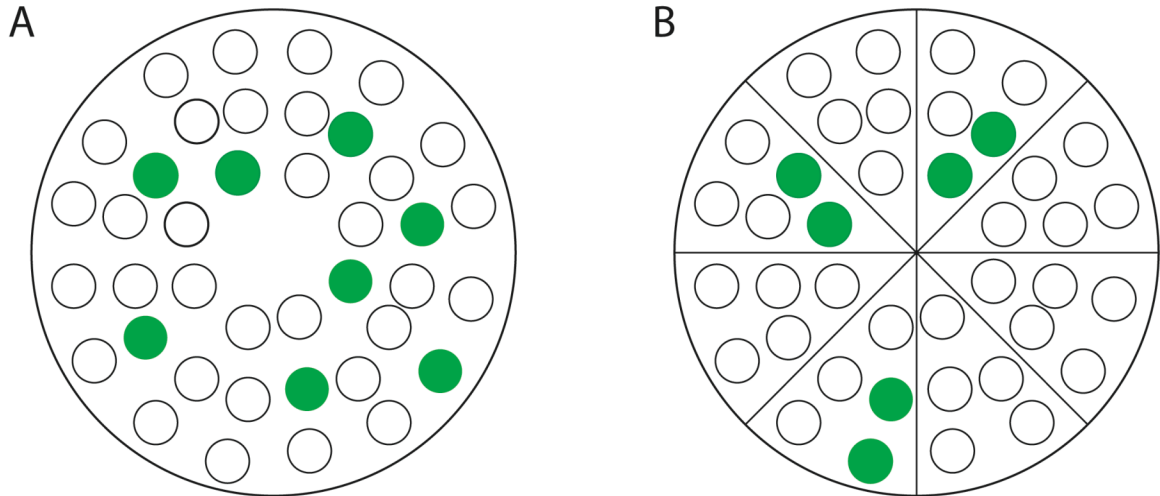


Figure 17 Vesicle release schemes.

(Green circles: calcium-bound binding sites on one synaptic vesicle; Open circles: unbound calcium binding sites)

A. The independent- simultaneous calcium binding scheme. 8 calcium bindings (green) among 40 calcium binding sites per synaptic vesicle triggers vesicle release.

B. The cooperative-simultaneous calcium binding scheme. 40 calcium binding sites on the vesicle are divided into 8 subgroups. More than 3 of the 8 subgroups with more than 2 calcium ions bound in each (in total, simultaneous binding of more than 6 calcium ions) triggers vesicle release. Using this scheme, only one calcium binding within a group of 5 binding sites will not contribute to trigger vesicle fusion.

4.2.5 Simulation and data analysis

MCell 3.0 (www.mcell.psc.edu) software was used for simulation. Individual simulations create outcomes depending on the seed value used to generate random numbers. A simulation initiated using a particular seed value is comparable to a single experimental trial. Each job ran 1000 to 10000 simulations on a single processor of a High Performance Computing platform at the Pittsburgh Supercomputing Center, jonas.psc.edu, with 128, 1.15 GHz Alpha EV7 processors and 256 Gigabytes of shared random access memory.

Approximately 1800 files were generated by each simulation and each set of simulations produced ~300 gigabytes of raw data. Data were analyzed with C-shell, PERL scripts, standard UNIX commands, python and ruby files. DReAMM (www.mcell.psc.edu/DReAMM) was used for visualization of data.

4.3 RESULTS

4.3.1 Physiology and anatomy of the adult frog neuromuscular junction

The number of active zones per nerve terminal at the adult frog neuromuscular junction was counted from confocal images (Figure 18). The average from 27 nerve terminals was 682 ± 65 (range: 181-1420; Figure 19).

To calculate how many vesicles are released by a single action potential from each active zone, I measured the quantal content in low calcium (0.3 mM Ca^{2+}) and normal calcium (1.8 mM

Ca²⁺) conditions. In 0.3 mM Ca²⁺, the quantal content was calculated by EPP amplitude/mEPP amplitude. The average EPP amplitude was 0.23±0.03 mV and the average mEPP amplitude was 0.29±0.02 mV (n=36 nerve terminals). Under these low calcium conditions, the average quantal content was 0.90±0.12 (0.1-3.4; n=36 nerve terminal). To avoid the complication of nonlinear summation when measuring very large EPPs in normal (1.8 mM) extracellular calcium, EPCs and mEPCs were measured in 1.8 mM Ca²⁺ condition using the two-electrode voltage clamp technique (Figure 20). In these experiments, the average EPC amplitude was 1.79±0.11 µA (n=35 nerve terminals) and the average mEPC amplitude was 4.49±0.22 nA (n=35 nerve terminals). The quantal content was calculated by integrating the total charge of the EPC and dividing the total charge of the mEPC. Total charge was used in these measurements in normal calcium because EPCs were very large and generated by the fusion of hundreds of vesicles that were not expected to be precisely synchronous (see Figure 23). Under these conditions measurements of total charge was expected to be more accurate than measurements of peak amplitude. The average quantal content under normal calcium conditions was 351±31 (range: 102-960; n=35 nerve terminal; Figure 21). From these data, the number of vesicles released per active zone per single action potential was calculated to be 0.0013 in 0.3 mM Ca²⁺, and 0.52 in 1.8 mM Ca²⁺. These data were used to constrain the MCell computational model output.

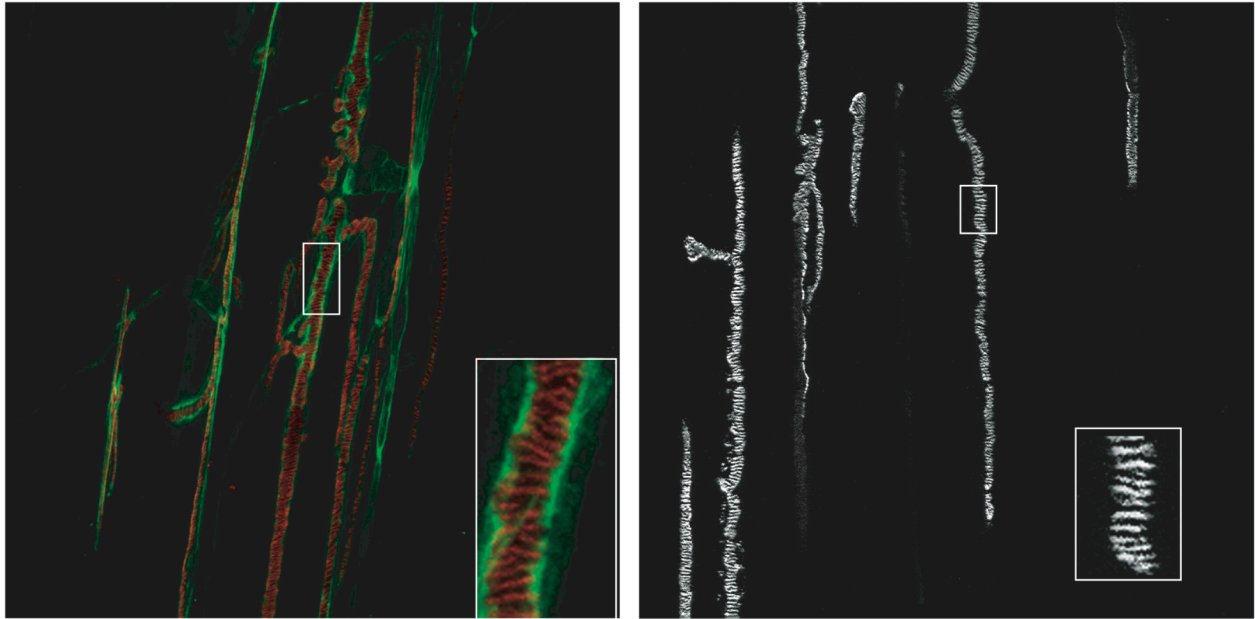


Figure 18 Projections of confocal image stacks of a frog neuromuscular junction.

Red (left) and white (right) is alexa-594- α -bungarotoxin, which labels postsynaptic nicotinic acetylcholine receptors. Green (left) is FITC-peanut agglutinin, which shows nerve terminal areas by staining the nerve terminal extracellular matrix. **Insets:** magnified images showing detail of the banding patterns characteristic of stained acetylcholine receptors.

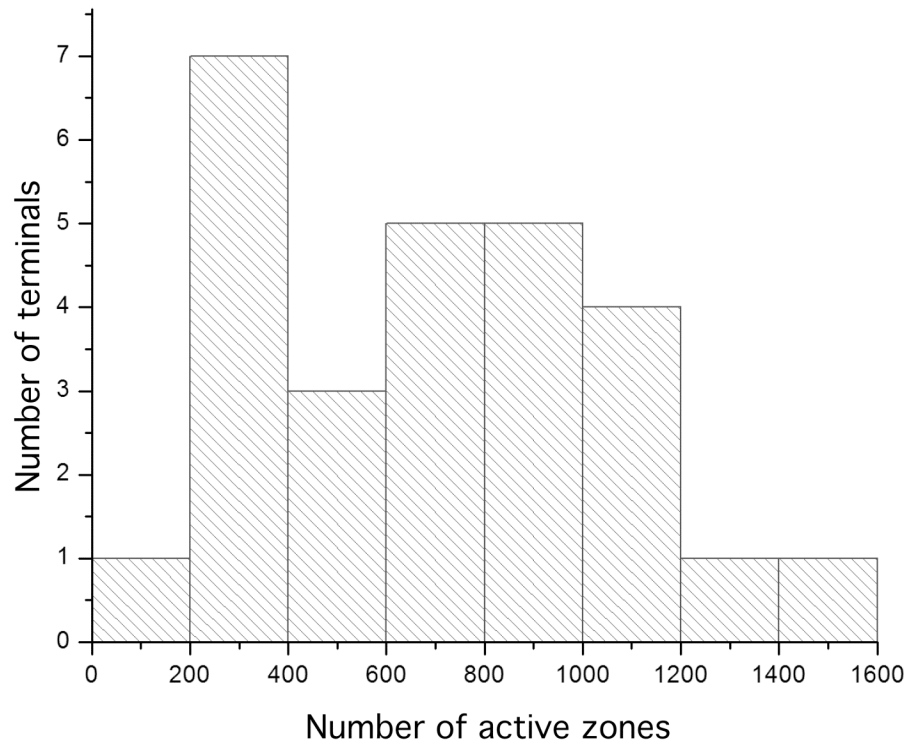


Figure 19 Frequency distribution for the number of active zones per nerve terminal.

(n=27 nerve terminals)

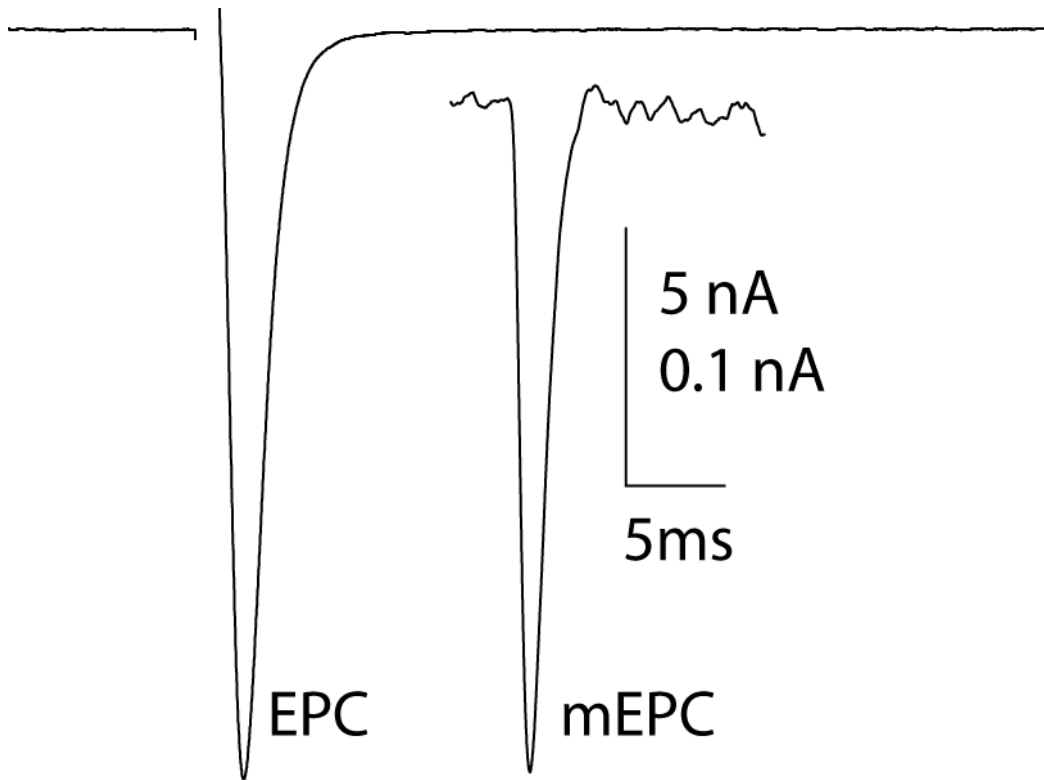


Figure 20 Two-electrode voltage clamp recordings of EPCs and mEPCs

EPCs (average of 20 responses) and mEPCs (average of more than 300 responses) at a sample neuromuscular synapse.

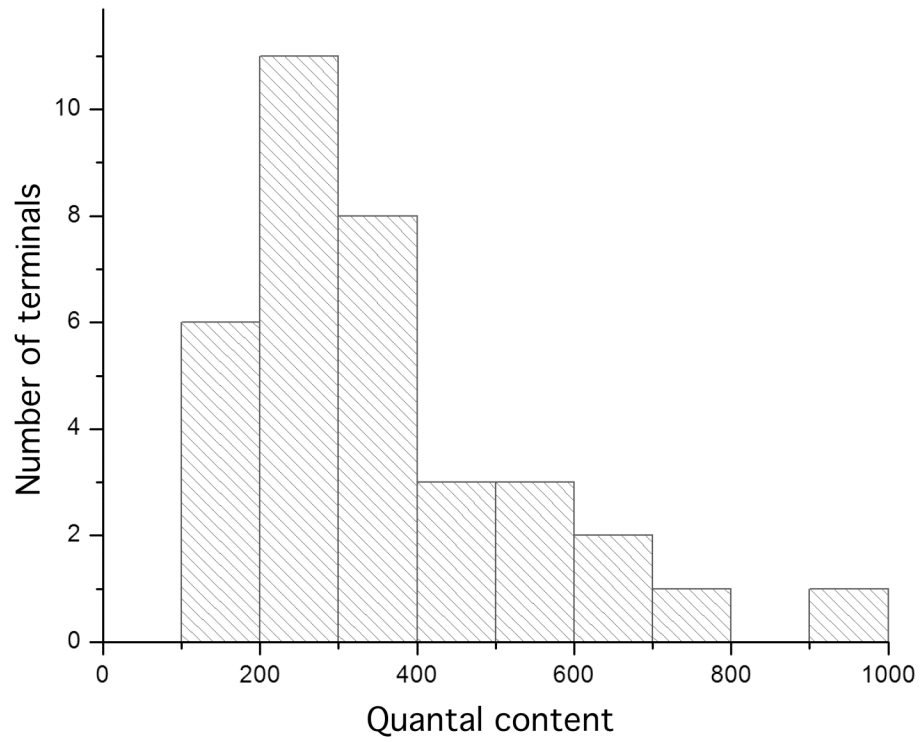


Figure 21 Frequency distribution for quantal content per nerve terminal per single action potential in 1.8 mM Ca^{2+} (n=36 nerve terminals).

4.3.2 Modeling of calcium influx

The MCell model simulated diffusion of calcium ions and binding to physiologically relevant molecules in a spatially realistic model active zone of the adult frog neuromuscular junction. Computational investigation of calcium dynamics and neurotransmitter release began with simulation of presynaptic calcium currents. Using the kinetic scheme described above (Figure 16), the MCell model reproduced physiologically recorded calcium currents (Figure 22). Simulated calcium currents with an action potential and square step voltage command (from -60 mV to +10 mV, 10 msec) showed comparable currents to the experimentally recorded calcium currents (Figure 22A). To achieve these results, the simulated opening probability of calcium channels was set to 0.14, which fits the range of experimental data (Wachman et al., 2004; King and Meriney, 2005; Luo et al., 2005). This suggests that 3 to 4 voltage-gated calcium channels per active zone may be opened by a single action potential. As expected from their underlying mechanisms, roscovitine did not alter the channel opening probability (0.14), but DAP increased channel opening probability by 57.1% to 0.22. The model also predicted the effects of roscovitine and DAP on calcium influx very well in comparison with experimental data (Figure 22D). In simulations, roscovitine increased total calcium influx by 43.9% and DAP increased total calcium influx by 58.8% (Figure 22). Simulated DAP effects on total calcium entry (58.8% increase) were smaller than experimentally measured effects (89.8% increase). This may be due to differences in the measured effects of DAP on action potentials of *Xenopus* motoneuron somata used for these simulations, as compared with effects that may be slightly different at adult *Rana pipiens* motor nerve terminals. Since we cannot record from these adult motor nerve terminals, this remains as unknown.

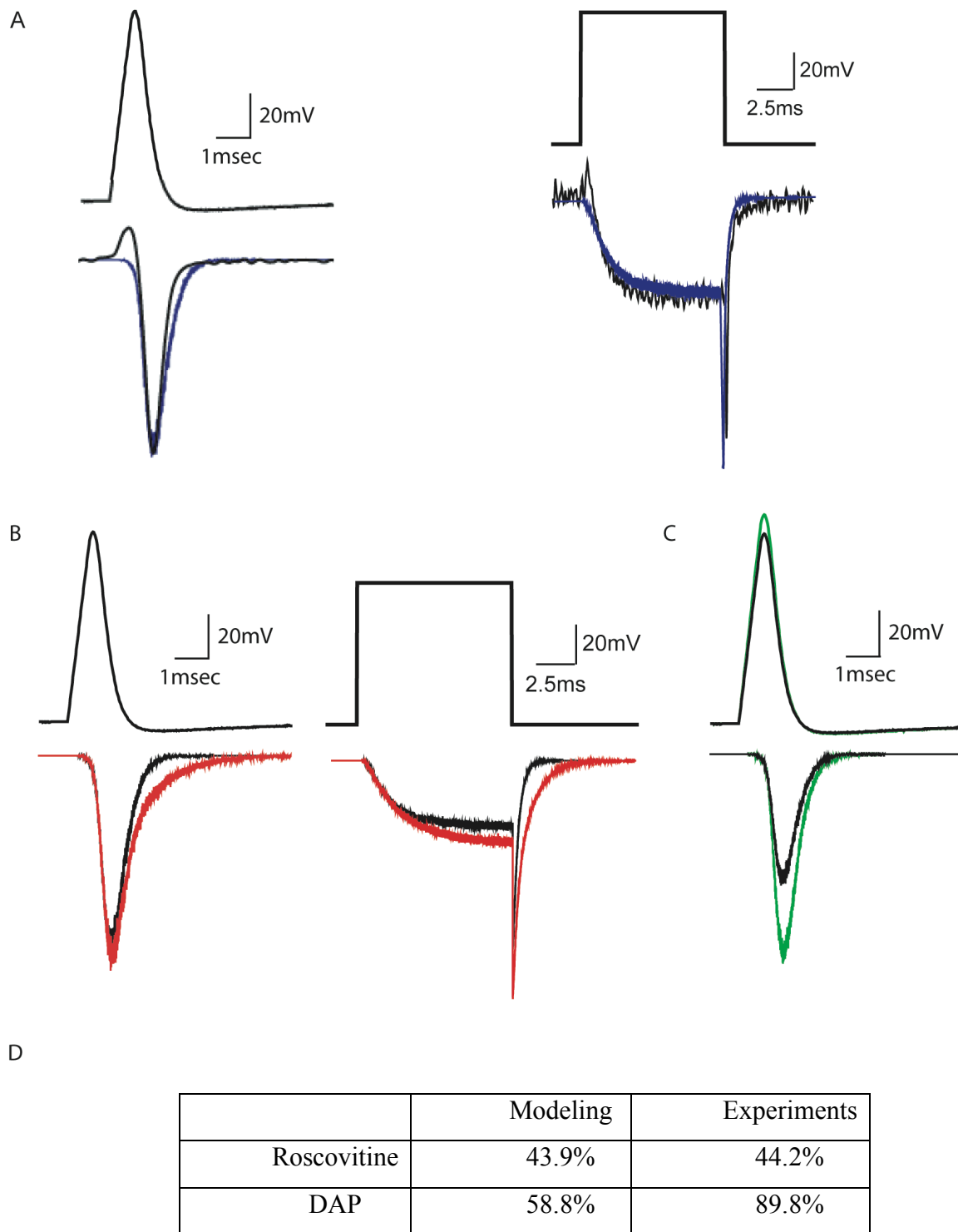


Figure 22 MCell simulated presynaptic calcium currents.

A. MCell model reproduced calcium currents under control conditions with an action potential stimulation (left) and with a step voltage command from -60 mV to +10 mV for 10 msec (right).

Experimentally recorded currents are black and simulated currents are blue.

B. MCell model simulated calcium currents using an action potential (left) and a step voltage command from -60 mV to +10 mV for 10 msec (right), before (black) and after roscovitine (red).

The simulated effects were compared with physiological effects shown in Chapter 1, Figure 5A and Figure 6E.

C. MCell model reproduced effects of DAP on calcium influx. 1 μ M DAP effects were modeled with a 10% increased amplitude of the action potential as determined experimentally in current clamp recordings from frog motoneuron somata (green; see section 2.3, Cho and Meriney, 2006).

D. Comparison of experimental and simulated drug effects on calcium influx. Each number shows the increased percentages of calcium influx after drug treatments.

4.3.3 Modeling of vesicle release during a single action potential

After fitting presynaptic calcium influx, vesicle release events were simulated. To quantify vesicle release events, two binding schemes were considered as possible vesicle fusion mechanisms (see section 4.2.4; Pattillo, 2002; Pattillo et al., 2007). Using these approaches, under control conditions, 0.62 vesicle fusion events were predicted to be released during a single action potential with the independent-simultaneous calcium binding scheme, and 0.54 vesicle fusion events were predicted to be released with the cooperative-simultaneous calcium binding scheme (1.8 mM Ca^{2+} , 3000 seeds). This simulated probability of vesicle fusion from each active zone was comparable to the value I measured physiologically (0.52) and was also similar to the probability predicted in previous studies (D'Alonzo and Grinnell, 1985; Meriney et al., 1996; Macleod et al., 1999; Poage and Meriney, 2002). In 0.3 mM Ca^{2+} , the MCell simulated probability of vesicle release was 0.0003 (10000 seeds). In comparison with my experimental value (0.0013), it seemed reasonable, though more simulations (seeds) may be necessary to determine this value more conclusively, because release rates are so low.

The effects of roscovitine and DAP on transmitter release were also reproduced with my MCell model. In 1.8 mM Ca^{2+} , roscovitine increased vesicle release by 77.9% (1.09 vesicles released per active zone per action potential) and DAP increased vesicle release by 82.6% (1.12 vesicles released per active zone per action potential) in simulations using the independent-simultaneous calcium binding scheme. Using the cooperative-simultaneous calcium binding scheme, roscovitine increased vesicle release by 67.6% (0.92 vesicles released per active zone per action potential) and DAP increased vesicle release by 74.9% (0.96 vesicles released per active zone per action potential) in normal calcium condition. Under the low calcium modeling

condition (0.3 mM Ca^{2+}), roscovitine increased release by 66.7% (0.0005 vesicles released per active zone per action potential) and DAP did not change vesicle release (0.0003 vesicles released per active zone per action potential; 10000 seeds). Again, more numbers of simulations may be necessary to determine accurately the drug effects in this low calcium condition more conclusively. Overall, the modeling data fits well experimental data, and these results are summarized in Table 2.

The temporal distribution of vesicle release events was also faithfully reproduced by my MCell model in comparison with reported data (Figure 23; Katz and Miledi, 1965a). Katz and Miledi (1965a) measured synaptic delay as the time interval between the peak of the externally recorded presynaptic spike and the beginning of the focal response at the postsynaptic membrane. Simulated synaptic delay was calculated as the peak of presynaptic action potential and the vesicle release time. The most frequent synaptic delay was 0.9 msec (Katz and Miledi, 1965a). The average of simulated synaptic delay was around 1 msec.

After confirming that my model could reproduce physiological data triggered by a single action potential, several questions that cannot be addressed by physiological experiments were investigated in the model environment. Figure 24 shows how many voltage-gated calcium channels contribute calcium ions to each vesicle fusion event. Under control conditions, most vesicle fusion events were triggered by the calcium ions originating from one (44.0%) or two (39.1%) channels. Sometimes, calcium ions from three channels (12.8%) triggered vesicle fusion and a small fraction of events were triggered by calcium from four or more calcium channels (4 channels: 3.69%; 5 channels: 0.37%). In summary, the average number of calcium channels that contributed calcium ions to each vesicle fusion event was 1.77 ± 0.02 under control conditions. In comparison with this control condition, roscovitine did not significantly alter the calcium

channel contribution to vesicle fusion. After roscovitine treatment, one (44.1%) or two calcium channels (39.4%) still triggered most vesicle fusion events. 12.9% of vesicle fusion events were triggered by calcium ions from three calcium channels and a small fraction (4 channels: 3.27%; 5 channels: 0.33%) were triggered by calcium ions coming from four or more calcium channels. After treatment with roscovitine, the average number of calcium channels that contributed calcium ions to each vesicle fusion event was 1.76 ± 0.03 .

In contrast, DAP showed quite a different pattern of calcium channel contribution to vesicle fusion. The average number of calcium channels that contributed calcium ions to each vesicle fusion event was significantly increased to 2.10 ± 0.03 after DAP treatment ($p < 0.001$). Fewer vesicle fusion events were triggered by one calcium channel opening (28.6%), and two calcium channels showed a similar contribution (42.4%). However, many more events were triggered by three calcium channel openings after DAP treatment (20.9%). Furthermore, there was an increase in the number of events triggered by 4 or more channel openings (8.09%). This is more than twofold the percentage under control or roscovitine conditions.

The next question I addressed using the MCell model was how far calcium ions traveled from voltage-gated calcium channels to trigger vesicle fusion. Figure 25 shows the average percentage of vesicle bound calcium ions that originate from each calcium channel in the active zone. As expected, calcium channels closest to a particular vesicle (~40 nm apart) most frequently contributed ions for the fusion of that vesicle (Ves) under all conditions (control: 77.6%; roscovitine: 74.9%; DAP: 73.1%). Neighboring calcium channels showed minor contributions (Figure 25; Group 1), and those calcium channels farther away rarely contributed (Figure 25; Group 2). Results are summarized in the table at the bottom of Figure 25. This suggests that the closest calcium channel to the vesicle contributes most strongly to the each

fusion event, though neighboring channels can also contribute. In comparison with control, roscovitine and DAP showed similar effects, although the two drugs slightly decreased the contribution of the closest calcium channel, and increased the contribution from channels other than the closest channel (Figure 25; Groups 1 and 2).

		Modeling	Experiments
Control vesicle release per active zone per single action potential	1.8 mM Ca ²⁺	0.54	0.52
	0.3 mM Ca ²⁺	0.0003	0.0013
Drug effects on neurotransmitter release in 1.8 mM Ca ²⁺ (% increases)	Roscovitine	67.6%	60.1%
	DAP	74.9%	79.8%

Table 2 MCell simulation reproduced transmitter release by single action potential.

The average number of vesicle fusion events was predicted with cooperative-simultaneous calcium binding scheme.

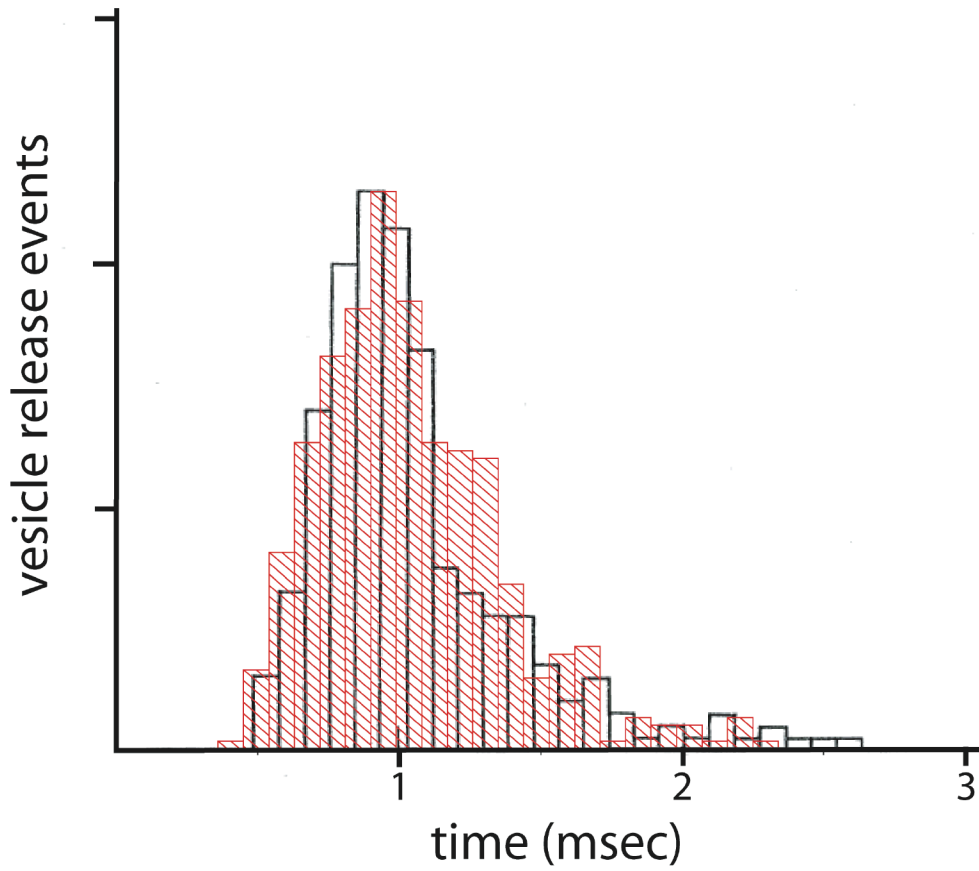


Figure 23 Comparison of MCell simulated variability in control synaptic delay with experimental measurements.

Simulated data (1628 fusion events; Red filled columns) and experimental data (open bins) from Katz and Miledi (1965a) are vertically scaled to match amplitudes.

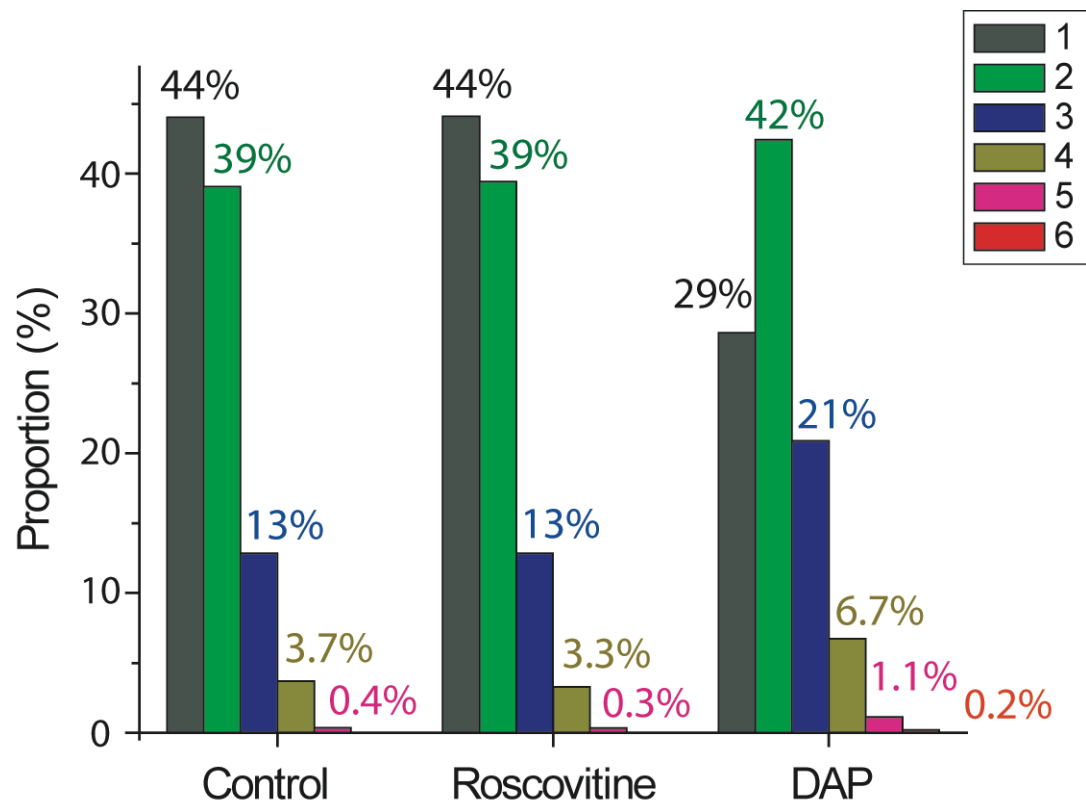
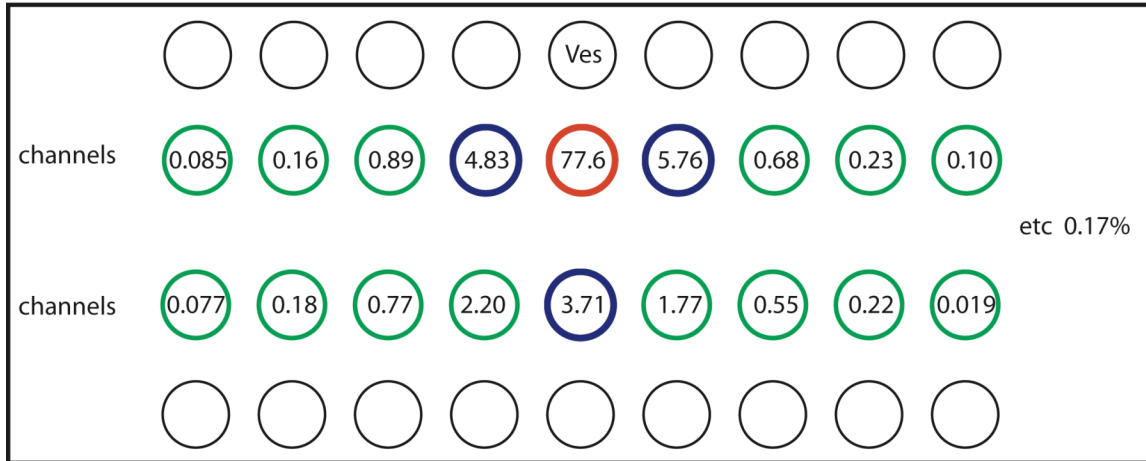


Figure 24 The percentage of vesicle fusion events triggered by calcium ions originating from the indicated numbers of calcium channels in the active zone.

1 calcium channel (grey), 2 (green), 3(dark blue), 4 (dark yellow), 5 (pink) or 6 (red) calcium channels contributed to release events under control, roscovitine and DAP conditions.

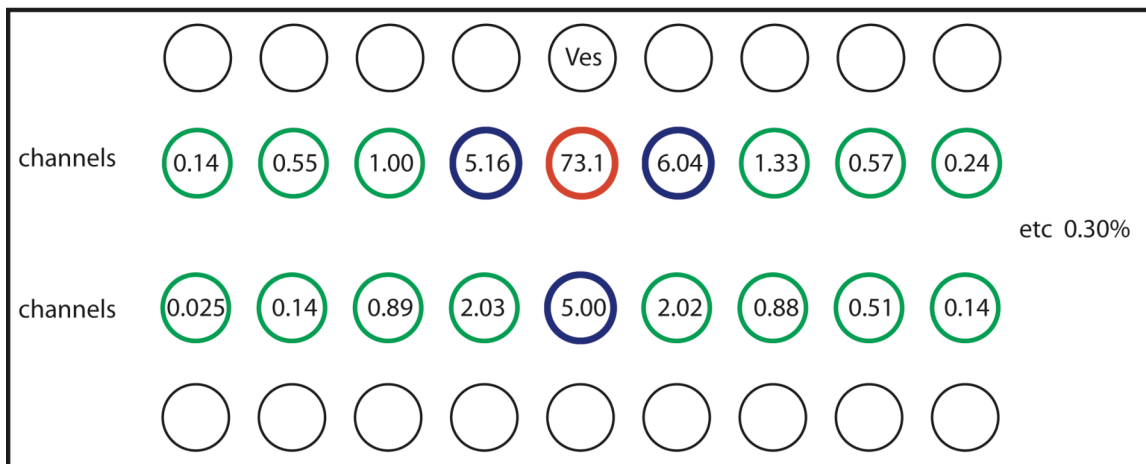
Control



Roscovitine



DAP



	control	roscovitine	DAP
Closest channel	77.6%	74.9%	73.1%
Group 1 (blue)	14.3%	15.6%	16.2%
Group 2 (green)	8.1%	9.5%	10.7%

Figure 25 Relative location of calcium channel contribution to vesicle release.

Black circles show the locations of synaptic vesicles and red, blue and green circles indicate voltage-gated calcium channels. “Ves” indicates specific fused vesicle and the number in each circle shows the fraction of trials for which calcium channel in the active zone contributed calcium ions that bound to the indicated vesicle (“Ves” vesicle) to trigger vesicle fusion. “Etc” indicates the calcium channels located farther in the same active zone than channels showing in the charts. Relative contributions are summarized in the table. Neighboring calcium channels (except the closest one) of “Ves” vesicle are group 1 (blue) and calcium channels other than the closest and neighboring calcium channels are group 2 (green).

4.3.4 MCell simulation of paired-pulse stimulation at the frog neuromuscular junction

Next, I used MCell simulations to address effects of paired-pulse facilitation. To avoid confusion and to see the effects of adjustments more clearly, the paired-pulse ratio using the cooperative-simultaneous calcium binding scheme will be described here. With respect to these paired-pulse ratio manipulations, the independent-simultaneous calcium binding scheme showed similar results to the cooperative-simultaneous scheme. In all cases, the paired-pulse ratio is defined as (the number of vesicles released by the second action potential)/(the number of vesicle released by the first action potential).

Without any modification, the basic MCell model used to simulate single action potential evoked release resulted in a paired-pulse ratio (10 msec interstimulus interval) of 1.0 under normal calcium condition (1.8 mM Ca^{2+}). In other words, the MCell model did not show any difference in the magnitude of released transmitter between the two stimuli. This is in contrast to experimental data that showed a paired-pulse ratio of 1.6, which meant that the second response was enhanced by 60% (see section 3.3.2). Furthermore, using my basic model conditions, roscovitine decreased the paired-pulse ratio by 7% and DAP decreased the paired-pulse ratio by 4%. Though control model did not show facilitation, the modeled effects of the two drugs on paired-pulse ratio demonstrated a decrease, similar to experimental data (roscovitine: $16.3 \pm 1.3\%$ decrease; DAP: $9.4 \pm 2.1\%$ decrease).

Thus, modification of some parameters in the model was done in an attempt to investigate their influence on paired-pulse facilitation, and in an attempt to fit experimental data more closely. This included changing the calcium buffer capacity, the calcium ion diffusion rate, more realistic and sophisticated changes in active zone geometry, alterations in the second action

potential waveform, reducing the effective volume of the nerve terminal by adding a storage pool of vesicles, altering calcium ion binding affinity to calcium sensors on synaptic vesicles, and considering possible conformational changes in SNARE complexes that might result from calcium binding. Though these modifications were not necessary for my model to fit the experimental data during a single action potential, the possibility that such sophisticated adjustments in the model might be required to simulate paired-pulse results was investigated. These modifications, and the resulting paired-pulse ratio using a 10 msec interstimulus interval, are summarized in Table 3. Furthermore, a description of the effects of each manipulation is given below.

Calcium buffer

First, the calcium buffering conditions were altered. In an attempt to increase paired-pulse facilitation, I wanted to increase free calcium ion concentration. Therefore, the only manipulations that I performed were those hypothesized to attain this goal. Though decreasing buffer concentration increased facilitation slightly, it did not show strong effects on the paired-pulse ratio (from 1.0 into 1.03 with 25% decrease in buffer concentration; from 1.0 into 1.07 with 50% decrease in buffer concentration). The effects of changing calcium unbinding rates from the buffer were also investigated. Increasing this unbinding rate also increased facilitation slightly (from 1.0 into 1.06 with 50% increase of unbinding rate). Furthermore, alterations in buffer concentration and calcium unbinding rates did not show synergistic effects.

Calcium diffusion

The effect of altering the modeled calcium diffusion coefficient was investigated.

Vesicle release was quite sensitive to changes in the calcium diffusion coefficient, but the first and the second responses were similarly affected with no significant change in the paired-pulse ratio.

Active zone geometry

The effects of changing the geometry of the active zone and nerve terminal were tested. First, the effect of different calcium channel distributions was examined. Originally, all of the channels were distributed evenly, one to one with docked vesicles. Clustering of the channels near some vesicles, and not others (total 32 channels), increased both the first and the second responses without increasing facilitation.

Next, a pool of storage vesicles was added inside the nerve terminal to limit calcium diffusion space. Previously, the terminal was empty except for the vesicles docked to the active zone. These storage vesicles were modeled to fill much of the nerve terminal space. Their surfaces were modeled to reflect calcium ions, and they could not be triggered to fuse. These extra vesicles increased paired-pulse ratio from 1.0 into 1.16.

Calcium affinity of sensors for release

I also examined whether changes in the calcium affinity for binding to sensors that trigger vesicle release would have effects on paired-pulse facilitation. For this initial test, I changed all of the modeled vesicle sensors uniformly using many values derived from published reports. Higher affinity sensors strongly increased release during the first pulse, but did not enhance paired-pulse facilitation. Along this line, in future work a model in which some of the sensors are changed to high affinity, while others maintain a low affinity for calcium binding will be tested.

Changes in action potential shape

According to previous studies, the shape of the action potentials can be altered during repetitive stimulation (Jackson et al., 1991; Borst et al., 1995; Borst and Sakmann, 1996, 1999; Geiger and Jonas, 2000; Poage and Zengel, 2002). To address this, I modified the falling phase of the second action potential in the pair by broadening its width at half-peak amplitude. Figure 26 shows the action potential waveforms used for the action potential broadening manipulations. Increasing the second action potential width by 10% (from 0.84 msec to 0.924 msec) increased the paired-pulse ratio to 1.32. A 20% broadening in width (from 0.84 msec to 1.008 msec) increased the paired-pulse ratio to 1.39, and 30% broadening in width (from 0.84 msec to 1.092 msec) increased the paired-pulse ratio to 1.44. I also tested the effects of broadening the action potential width by extending the falling phase at a time point after the half-amplitude time point, but this was not as effective as broadening at half-peak amplitude.

Combined effects of action potential broadening and the addition of a storage pool of vesicles

When I increased action potential duration by 10% in the presence of a storage pool of vesicles, paired-pulse ratio increased to 1.39. When a 20% broadening of action potential duration was added to the storage pool of vesicles, the paired-pulse ratio increased to 1.48. Lastly, when a 30% broadening of action potential duration was added to the storage pool of vesicles, the paired-pulse ratio increased to 1.63. Although this matched closely the expected physiological measurement of paired pulse facilitation, a 30% broadening of the action potential duration seemed rather extreme. Therefore, in an attempt to avoid extreme broadening of the

action potential, a combination that included mild broadening of the action potential, decreasing buffer concentration, and a storage pool of vesicles was tested. In comparison with action potential broadening plus a storage vesicle pool, the additional manipulation of decreasing buffer concentration did not show any additive effects. It increased the first response similarly to the second response.

To examine the effects of roscovitine and DAP again under these modified model conditions, I tested drug effects using the combination of action potential broadening with a storage pool of vesicles. With a 10% broadening of action potential duration and the storage pool of vesicles, the paired-pulse ratio after roscovitine was decreased by 7.9%, and the paired-pulse ratio after DAP was decreased by 18.7%. After roscovitine, the paired-pulse ratio with 20% broadened action potential plus a storage pool of vesicles was decreased by 5.4% and with 30% broadened action potential was decreased by 8.0%. In the case of DAP, the paired-pulse ratio with 20% broadened action potential plus a storage pool of vesicles was decreased by 14.9% and with 30% broadened action potential was decreased by 16.7%. Thus, after modifying modeling conditions so that the control paired-pulse ratio could be observed, both drugs continued to show qualitatively accurate effects.

Conformational changes of SNARE complex

When calcium ions bind vesicles, this can trigger vesicle fusion, or fusion may not occur and these calcium ions can unbind from the vesicle in the model. Once calcium ions unbind from the vesicle, the unbound calcium binding sites on the vesicle go back to the states that existed before calcium binding. However, a recent study (Martens et al., 2007) showed that synaptotagmin-1 triggered vesicle fusion by buckling of the plasma membrane together with the

zippering of SNARE complexes. Therefore, it is possible that the first action potential may trigger calcium entry that imparts some conformational changes in vesicle release machinery that may be maintained even after calcium ions unbind from vesicle binding sites.

This possibility has been investigated in my MCell model. Because vesicle release may require calcium binding of at least two sites on an individual synaptotagmin molecule (Earles et al., 2001), two (scheme 1) or four (scheme 2) simultaneous calcium bindings in the same subgroup of 5 calcium binding sites on the vesicle during the first action potential was considered to be a SNARE complex in which conformation was altered and maintained until the next action potential in the pair (Figure 27). With this altered SNARE complex, fewer calcium-binding events were required during the second action potential to trigger vesicle release. Under both of these modified conditions (scheme 1 and scheme 2), 6 simultaneously cooperative calcium bindings in total were required to trigger vesicle release.

In scheme 1, when two simultaneous calcium bindings occurred in one subgroup during the first action potential, four additional simultaneous calcium bindings in two subgroups during the second action potential were required to trigger vesicle fusion (Figure 27). Using scheme 1 in my model, the paired-pulse ratio was 1.53. In scheme 2, when four simultaneous calcium bindings in two subgroups occurred during the first action potential, only two additional calcium bindings in one subgroup during the second action potential were required to trigger vesicle fusion (Figure 27). Using scheme 2 in my model, the paired-pulse ratio was 1.64. Therefore, both schemes produced comparable paired-pulse facilitation to my experimental data. This is intriguing and future work can investigate this manipulation further.

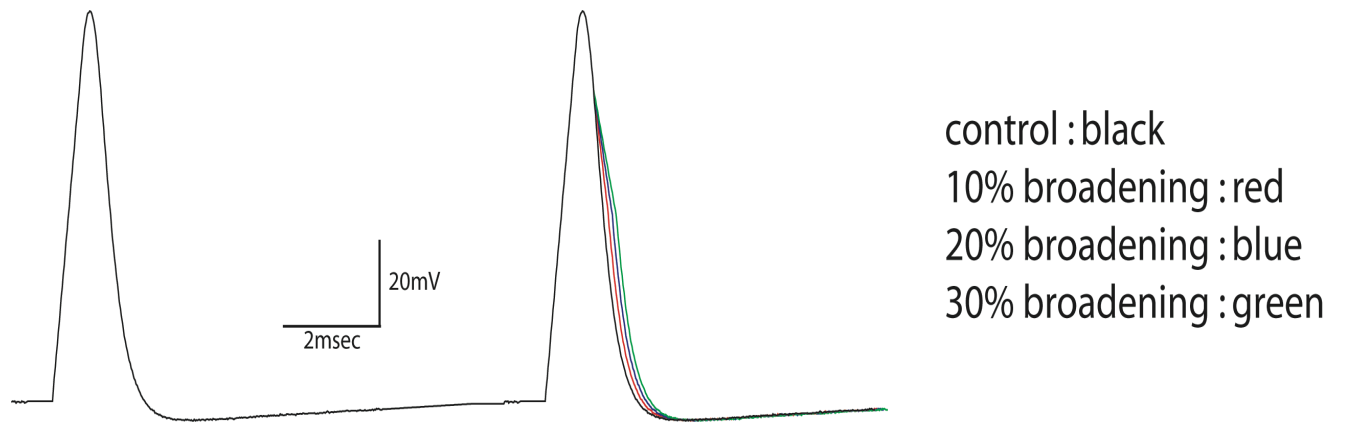


Figure 26 The action potential waveforms used for the action potential broadening manipulations.

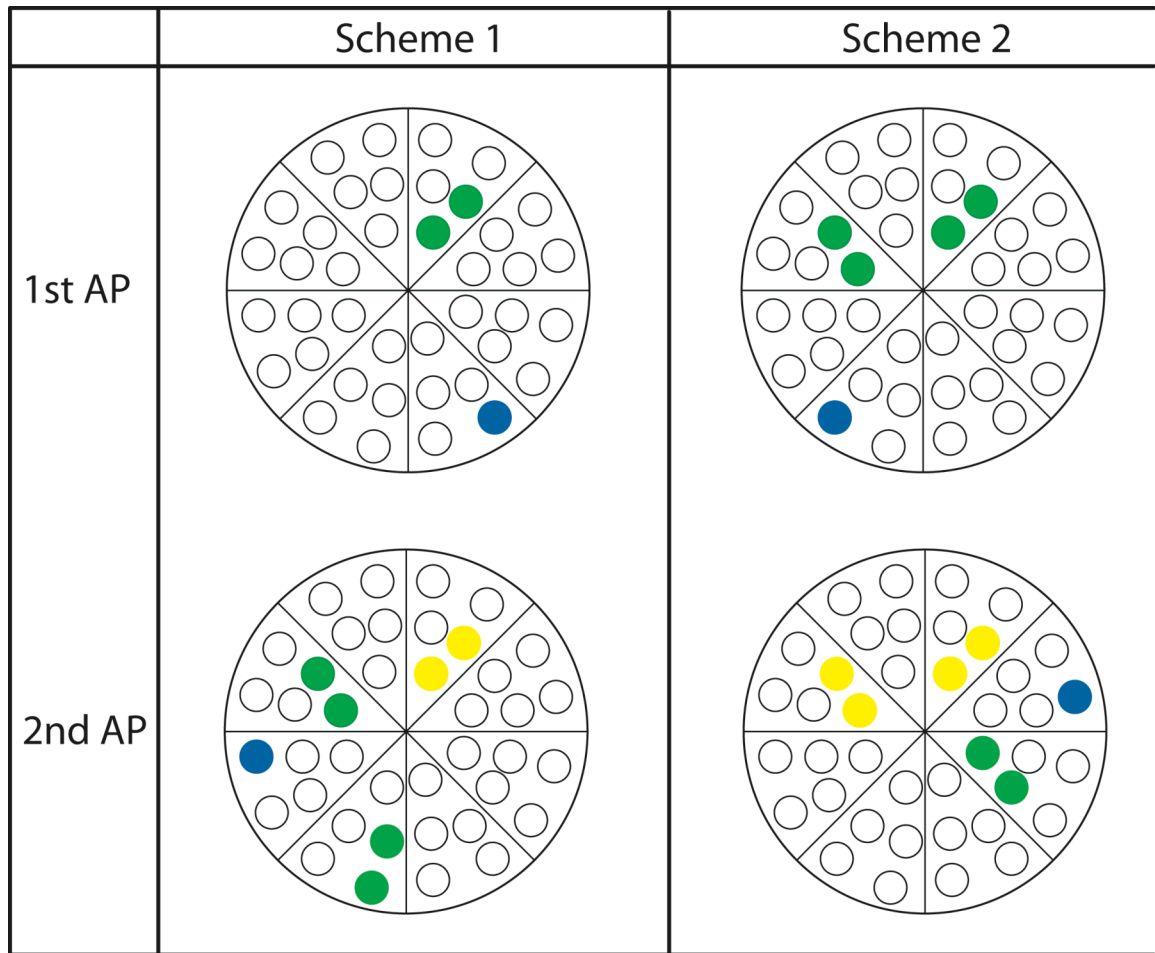


Figure 27 Vesicle release schemes for persistent conformational change of SNARE complexes.

Scheme 1: 2 calcium bindings (within one group of 5) during the first action potential result in a persistent conformational change of these SNARE complexes, and this change is maintained for the second action potential. During the second action potential, 4 additional calcium bindings (within 2 groups of 5) are required to trigger vesicle fusion.

Scheme 2: 4 calcium bindings (within 2 groups of 5) during the first action potential result in a persistent conformational change of these SNARE complexes and during the second action potential, 2 additional calcium bindings (within a group of 5) are required to vesicle fusion.

(**Green**: calcium-occupied binding sites in the same subgroup; **Yellow**: calcium binding sites that calcium ions used to be bound to during the first action potential which have altered the conformation of the SNARE complex; **Blue**: one bound calcium (within a subgroup of 5 binding sites) which cannot evoke a conformational change, and cannot affect vesicle fusion during the second action potential)

Manipulations	Paired-pulse ratio
Basic Model	1.0
Decreasing buffer concentration (25%)	1.03
Increasing buffer off-rate (50%)	1.06
Decreasing buffer off-rate (10%)	0.99
Decreasing buffer conc. + increasing off-rate	0.93
Channel cluster (6 calcium channels more)	0.97
Decreasing calcium diffusion constant (1/3)	0.98
Adding storage pool of vesicles	1.16
10% broadening of action potential	1.32
20% broadening of action potential	1.39
30% broadening of action potential	1.44
10% broadening of action potential + a storage pool of vesicles	1.39
20% broadening of action potential + a storage pool of vesicles	1.48
30% broadening of action potential + a storage pool of vesicles	1.62
Persistent Ca-dependent changes in SNARE (scheme 1)	1.53
Persistent Ca-dependent changes in SNARE (scheme 2)	1.64

Table 3 Manipulations of active zone parameters and their resulting paired-pulse ratio.

(with 10 msec interstimulus interval in normal calcium condition (1.8 mM Ca²⁺))

4.4 DISCUSSION

The molecular events that underlie synaptic transmission are very complex. As computer hardware and software advancements have been made, quantitative modeling of highly realistic reconstructed synapses has become possible, and this approach is expected to yield profound insights into our understanding of the nervous system. While simple equation-based approaches predict directly the average behavior of the system under one condition, Monte Carlo methods can provide realistic three-dimensional simulation with stochastic variability and dynamics that reflect small numbers of reactants in small spaces; a property critical to nervous system function. The availability of physiological and morphological data is a prerequisite for realistic reconstruction and modeling of the synapse. In that sense, the adult frog neuromuscular junction is ideally suited for this type of computer modeling.

Though the past literature of the frog neuromuscular junction provides a wealth of background information, I needed more precise physiological and anatomical information related to transmitter release per active zone during a single action potential in order to simulate more accurately spatially realistic microphysiology at this synapse. Although there were incidental reports that turned out to be similar to my data, their approaches were quite different from my experimental conditions, and it was not always possible to determine experimental details. Therefore, I counted the number of active zones per nerve terminal and measured quantal content per active zone during a single action potential at the adult frog neuromuscular junction. Previous measurements of quantal content were performed in different muscle preparations, or using cut-muscle methods to prevent muscle contractions at various holding potentials (Katz and Miledi, 1979; Giniatullin et al., 1997, 2005). Here, I measured quantal content from the cutaneous-pectoris nerve-muscle preparation in normal calcium (1.8 mM Ca^{2+}), in attempt to

obtain accurate estimates for my experimental conditions. Surprisingly, my measured quantal content (average = 351, range 102-960, n=35) was quite similar to Katz and Miledi's estimate. Their average quantal content at 19-20 °C was 390 (n=18 fibers; range: 80 and 900), though they used the frog sartorius muscle with focal stimulation at a preterminal node of Ranvier, and their clamping methods were not explained (Katz and Miledi, 1979).

In contrast to previous modeling studies (Bennett et al., 2000a, 2000b; Glavinovic and Rabie, 2001; Shahrezaei and Delaney 2004, Shahrezaei et al., 2006), the active zone model in this study used a spatially realistic active zone ultrastructure and stochastic methods to simulate action potential-dependent calcium channel gating, calcium ion permeation, and calcium binding and unbinding from buffer molecules and synaptic vesicles. The fourth-order relationship between extracellular calcium concentration and transmitter release (Jenkinson, 1957; Katz and Miledi, 1965b; Dodge and Rahamimoff, 1967; Andreu and Barrett, 1980; Barton et al., 1983) had led to the hypothesis that approximately four calcium binding sites per synaptic vesicle may exist. From this prevailing conceptual view, earlier models of transmitter release used four or five binding sites per synaptic vesicle (Bennett et al., 2000a, 2000b; Glavinovic and Rabie, 2001; Meinrenken et al., 2002; Shahrezaei and Delaney 2004). These modeling studies were also distinct from my work in that they performed various combinations of deterministic or mixed deterministic-Monte Carlo methods, simplified calcium current waveforms and/or a small value for free calcium mobility. To accurately predict calcium dynamics using a very small absolute number of calcium ions in a temporally and spatially restricted environment such as an active zone, full Monte Carlo simulation algorithms and stochastic calcium influx using spatially realistic active zone structure is critical (Pattillo et al., 2007). In a previous study using this approach (Pattillo et al., 2007), simulations with 4-6 calcium binding sites per synaptic vesicle

showed very low calcium sensitivity and could not reproduce basic experimental observations (in particular, the 4th order relationship between calcium concentration and transmitter release, and physiological levels of vesicle fusion). Using only 4-6 calcium binding sites per vesicle, calcium sensitivity could be increased by extreme changes in model parameters (such as 4-fold increase of the numbers of voltage-gated calcium channels in the active zone, or a 20-fold decrease in the calcium diffusion constant), but these conflicted with experimental constraints (Pattillo et al., 2007). An alternative method to increase calcium sensitivity was to use more calcium binding sites per synaptic vesicle. Using an approach with 40 calcium binding sites per vesicle, Pattillo et al. (2007) could reproduce basic experimental data including the fourth order relationship between calcium and vesicle release, the temporal distribution of vesicle release events evoked by single action potentials, and the average probability of release under normal physiological conditions. Previously published experimental data supported the presence of excess calcium binding sites per vesicle, because each vesicle has been shown to have up to 8 synaptotagmin-associated SNARE complexes (Han et al., 2004), and each synaptotagmin molecule can bind up to 5 calcium ions (Sudhof and Rizo, 1996; Ubach et al., 1998; Earles et al., 2001; Fernandez et al., 2001; Chapman, 2002). Vesicle fusion schemes, such as independent-simultaneous or cooperative-simultaneous calcium binding schemes (see section 4.2.4) were evaluated by determining whether the model showed proper calcium sensitivity and was able to reproduce physiological levels of transmitter release.

As mentioned in the introduction (see section 4.1), the dimensions and geometry of the active zone, the initial parameters of model components, and the vesicle fusion schemes in this study were adapted from previous work (Pattillo et al., 2007), though they used a different calcium channel gating model. In this study, under normal calcium conditions, simulated data,

including calcium current during a single action potential, roscovitine and DAP effects on calcium influx, the average number of released synaptic vesicles, roscovitine and DAP effects on vesicle release, and synaptic delay were quite comparable with physiological data. Under low calcium conditions, control vesicle release appeared to be modeled faithfully, though the effects of roscovitine and DAP could not be reliably determined.

How many voltage-gated calcium channels contribute calcium ions to the release of a synaptic vesicle after a single action potential?

The number of calcium channels contributing calcium ions to vesicle fusion is still debated. Different types of synapses have shown different cooperativity and even the same synapse shows changes during development. For example, channel cooperativity at the calyx of Held synapse is diminished during development (Borst and Sakmann, 1996; Fedchyshyn and Wang, 2005). My model suggested that calcium ions originating from 1 or 2 (average = 1.77) voltage-gated calcium channels triggered the release of most vesicles by an action potential under control conditions at the frog neuromuscular junction. This is consistent with previous studies suggesting that calcium influx through single calcium channels (Stanley, 1993) or a few channels triggers fusion of each synaptic vesicle (Llinas et al., 1981; Yoshikami et al., 1989; Quastel et al., 1992; Bertram et al., 1996; Augustine, 2001; Mulligan et al., 2001; Wachman et al., 2004; Sharezaei et al., 2006) and contrasts with other studies concluding that multiple calcium channels need to open to trigger a single vesicle fusion event (Zucker and Fogelson, 1986; Borst and Sakmann, 1996; Meinrenken et al., 2002).

It is hard to examine the calcium channel contribution to vesicle fusion directly in physiological experiments because of the temporal and spatial limitations of these measurements.

However, indirect tests to measure the relationship between imaged calcium entry and measured effects on transmitter release at the adult frog neuromuscular junction, as calcium channels are gradually blocked (using varying concentrations of ω -conotoxin GVIA), have provided supportive evidence (Luo, King and Meriney, unpublished observations). This approach has revealed a slope in the relationship between changes in calcium entry and transmitter release of 1.72. If a slope of 1.0 had been observed, these data would lead to the conclusion that only one calcium channel opened for each vesicle fusion event. At the other extreme, if a slope of 4.0 had been observed, one could conclude that a large number of calcium channels opened to trigger each vesicle fusion event. In this case, the 4th order dependence of transmitter release on calcium is observed. In contrast, these data (a slope of 1.72) suggest that only a few calcium channels contribute to each vesicle fusion event. These physiological observations are in good agreement with my modeling results.

While roscovitine did not alter the number of calcium channels that trigger fusion, there were changes after DAP treatment (Figure10). This likely results from differences in the underlying mechanisms of these two pharmacological treatments. Roscovitine slows deactivation kinetics of open calcium channels without changing opening probability. In contrast, 1 μ M DAP alters action potential amplitude by blocking potassium channels and thereby increases the number of calcium channel openings during the altered action potential. Under these conditions, more vesicles were triggered for fusion by calcium ions originating from multiple calcium channels in the active zone after DAP treatment.

How far do calcium ions travel to trigger the fusion of a synaptic vesicle?

This question is hard to address with physiological experiments. In contrast, MCell modeling is well suited to address this issue. My modeling data conclude that the closest calcium channel predominately (77.6% in control) contributes to the fusion of each vesicle, though other neighboring calcium channels still show mild (22.4% in control) contributions (Figure 25). It appears that calcium ions bind buffers instead of diffusing long distances to bind distant vesicles. Furthermore, because my simulated opening probability for the calcium channel was set at 0.14 (and this is consistent with low probabilities (10-30%) from previous studies (Bertram et al., 1996; Poage and Meriney, 2002; Wachman et al., 2004; King and Meriney, 2005), it is unlikely that too many neighboring channels would open anyway. In this sense, when a calcium channel does open, it strongly contributes to potential fusion of the closest vesicle.

Paired-pulse facilitation

My MCell model reproduced faithfully single action potential evoked release and the effects of roscovitine and DAP on calcium influx and transmitter release. However, my basic model required more sophisticated modifications to simulate paired-pulse facilitation accurately. The process of adjusting the model to reproduce paired-pulse facilitation provided insights into the potential sub-active zone mechanisms that may underlie these measured effects. Along these lines, most of the tested modifications affected basal synaptic transmission directly, but did not alter paired-pulse facilitation much because they altered both the first and the second responses similarly.

To explain facilitation, the residual calcium hypothesis has been widely accepted at the majority of synapses (Katz and Miledi, 1968; Magleby and Zengel, 1982). In this view, calcium

ions remain within the nerve terminal after the first action potential and enhance transmitter release during the second action potential. Numerous studies have supported this hypothesis. Presynaptic calcium concentrations have been shown to be elevated during facilitation at many central and peripheral synapses (Charlton et al., 1982; Delaney and Tank, 1994; Regehr et al., 1994; Brain and Bennett, 1995, 1997; Atluri and Regehr, 1996; Feller et al., 1996; Lin et al., 1998; Kreitzer and Regehr, 2000). Experimentally, the activation of a caged calcium chelator has been shown to rapidly eliminate synaptic facilitation (Kamiya and Zucker, 1994). Conversely, intracellular calcium release by photolysis of a presynaptic caged calcium chelator can cause facilitation at the crayfish neuromuscular junction (Kamiya and Zucker, 1994). Synaptic facilitation has also been reduced by presynaptic loading of exogenous calcium buffers such as EGTA and BAPTA (Hochner et al., 1991; Tanabe and Kijima, 1992; Van der Kloot and Molgo, 1993; Regehr et al., 1994; Atluri and Regehr, 1996; Feller et al., 1996; Rozov et al., 2001) or by presynaptic injection of calcium buffers into the terminal (Swandulla et al., 1991; Jiang and Abrams, 1998; Tang et al., 2000). All of these observations have supported the concept that residual calcium following the first action potential in a pair leads to measured facilitation in transmitter release.

Despite wide support for the residual calcium hypothesis, there are other possible mechanisms of facilitation, such as broadening of presynaptic action potentials or changes in presynaptic calcium entry, though various preparations have shown different results. During trains of stimuli, facilitation of the voltage-gated calcium channel has been observed at the calyx of Held (however, this mechanism did not dominate the overall plasticity because synaptic depression was observed; Borst and Sakmann, 1998; Cuttle et al., 1998). In hippocampal neurons, G-protein mediated calcium channel inhibition can be relieved by action potential trains

resulting in increased calcium influx through P/Q-type calcium channels, and this can cause facilitation (Brody and Yue, 2000a). Alternatively, at the crayfish neuromuscular junction (Wright et al., 1996) and at the parallel fiber synapses in the cerebellum (Silver et al., 1998; Kreitzer and Regehr, 2000), changes in presynaptic calcium currents were shown not to be important for facilitation.

The shape of the presynaptic action potential plays a critical role in determining timing and strength of synaptic transmission (Augustine, 1990; Sabatini and Regehr, 1999). Previous studies demonstrated short-term broadening of the presynaptic action potential during repetitive stimulation (Jackson et al., 1991; Borst et al., 1995; Borst and Sakmann, 1996, 1999; Geiger and Jonas, 2000; Poage and Zengel, 2002). In particular, Poage and Zengel (2002) measured the shapes of presynaptic action potentials in the chick ciliary ganglion using paired-pulse stimuli with a 50 msec interstimulus interval. They observed that the second action potential was identical in the rising phase, peak and early falling phase, followed by a slightly slower repolarization as compared with the first action potential waveform. This altered second action potential waveform significantly increased total calcium influx ($5.0 \pm 1.3\%$). Conversely, at some synapses, decreases in presynaptic action potential amplitudes or durations have been shown to contribute to synaptic depression (Parker, 1995; Brody and Yue, 2000b). In contrast, modulation of the presynaptic action potential waveform was shown not to contribute to facilitation at the crayfish neuromuscular junction. Even when the second action potential was of shorter duration than the first action potential, facilitation at the crayfish neuromuscular junction was still observed (Vyshedskiy et al., 2000). Therefore, although there are some reports of additional mechanisms that may contribute to short-term plasticity, there is some disagreement between preparations.

The manipulations that increased paired-pulse ratio in my model included reduction in terminal volume by addition of a storage pool of vesicles, broadening the second action potential in the pair, and considering potential long-lasting conformational changes in the calcium-trigger for release.

The reduction in terminal volume by addition of a storage pool of vesicles is expected to confine calcium ions to the area around a docked vesicle by filling intraterminal space. Previous studies showed that only 1-2% of all vesicles are docked in the so called “readily releasable pool”, while most vesicles reside in the recycling pool (10-20%) or reserve pool (80-90%). These vesicles are scattered in the terminal spatially (Rizzoli and Betz, 2004, 2005). In that sense, adding a storage pool of vesicles makes the model more realistic. Under these conditions, when the second action potential invades the nerve terminal, residual calcium may be more prominent in the local active zone area.

My simulations with broadened second action potential waveforms can show similar paired-pulse facilitation to the measured experimental value, but this required a 30% broadening of the action potential duration which I consider to be rather extreme. Though direct recordings of presynaptic action potentials at the adult frog neuromuscular junction are not amenable, extracellular recordings might be useful to investigate whether the first and the second action potential waveforms are different during paired stimulation. In an attempt to avoid extreme action potential broadening in my model, other factors and combinations of adjustments need to be investigated.

One possibility that also reproduced physiological observations was a model for persistent conformational changes in SNARE complexes after calcium binding during the first action potential. This is related to a very recent study (Martens et al., 2007) suggesting that membrane

curvature is induced by calcium binding to synaptotagmin-1. My preliminary simulations showed this modification could reproduce experimental paired-pulse facilitation. This preliminary test did not include time-dependent decay of conformational changes, but this should be considered in future evaluations of this manipulation. Along this line, a model in which some of the sensors are high affinity, and others are low affinity, should also be tested. An averaged calcium binding affinity for all calcium sensors on vesicles is used currently in my model, and this matches with the known biochemical characteristics of synaptotagmin (Ubach et al., 1998; Davis et al., 1999; Fernandez et al., 2001). However, it is possible that using both high and low affinity calcium sensors may help to simulate paired-pulse facilitation more accurately, though I have shown that it is not necessary for the simulation of release triggered by a single action potential.

Another factor to be considered is intracellular calcium storage. One possible storage site that may affect short-term plasticity could be mitochondria. Previous studies have shown that calcium release from mitochondria can affect posttetanic potentiation and long-term synaptic plasticity. Mitochondrial influences on paired-pulse facilitation were not studied, and the time scale of calcium uptake and release from mitochondria might be rather slow to be relevant to paired-pulse facilitation (Magnus and Keizer, 1997; Levy et al., 2003; Talbot et al., 2003; Tong, 2007).

In this dissertation, simulations with paired-pulse stimuli were performed using a single active zone. Though a previous study showed that reflected calcium ions from the lateral walls of a single active zone model did not significantly contribute to release (Shahrezaei et al., 2006), and alteration from absorptive endcaps into reflective endcaps in my model did not affect vesicle release by a single action potential, it is possible that calcium ions traveling from neighboring

active zones may play a role in building up residual calcium during long interstimulus intervals. In my simulations, calcium ions that are reflected from the boundaries, called ‘endcaps’, are modeled as calcium ions entering from a neighboring active zone. However, a future model with multiple active zones may help to elucidate possible complex mechanisms that regulate short-term synaptic plasticity.

In summary, my present MCell model simulated synchronous calcium-triggered vesicle release during a single action potential very accurately. Using this model, I was able to predict calcium channel stoichiometric interactions with vesicles, and effects of two drugs that alter calcium influx. These studies increased our understanding of calcium-triggered vesicle fusion. My simulation of paired-pulse facilitation using this model needed more adjustments to predict accurately paired-pulse facilitation experimental observations. In the process of adjusting my present model, various aspects of short-term synaptic plasticity were explored. More investigations are required using this model to evaluate the effects of roscovitine and DAP on paired-pulse facilitation. A combination of multiple factors may be necessary to explain physiological observations.

5. GENERAL DISCUSSION

Synaptic transmission at the neuromuscular junction is tightly regulated by calcium influx through voltage-gated calcium channels. The frog neuromuscular junction is a very useful model system to study synaptic transmission in general and neuromuscular transmission specifically. In this dissertation, I have used roscovitine as a tool to study presynaptic function. The effects of roscovitine and DAP, a comparison drug, on presynaptic calcium influx and transmitter release were characterized at the frog neuromuscular junction. Results of experimental and computational studies provided a deeper understanding of calcium-triggered transmitter release and paired-pulse facilitation.

5.1 ROSCOVITINE, AS A NOVEL TOOL TO STUDY PRESYNAPTIC CALCIUM CHANNELS AND SYNAPTIC TRANSMISSION

Roscovitine increased presynaptic calcium influx by prolonging deactivation kinetics of N-type calcium currents, and as a result increased transmitter release at the adult frog neuromuscular junction. The action of roscovitine on N-type calcium channels is similar to the effect of BayK 8644 on L-type calcium channels. BayK 8644 has played an important role in studying the function, gating properties and permeation of L-type calcium channels (Nilius et al.,

1985; Nowycky et al., 1985; Sturek and Hermsmeyer, 1986; Elmslie, 2004). Because no specific agonist is available for N-type calcium channels, roscovitine will provide an opportunity to investigate N-type calcium channels and synaptic function further. In this dissertation, whole-cell patch clamp recordings were used to study effects of roscovitine, but a complete characterization of roscovitine effects at the single channel level will be necessary in the future.

To function as a more valuable research tool targeting N-type calcium channels selectively, roscovitine needs to be improved. First, roscovitine currently also functions as a cyclin dependent kinase (cdk) inhibitor, though the effects of roscovitine on calcium channels are direct and cdk-independent (Yan et al., 2002; Buraei et al., 2005, Cho and Meriney, 2006). Unexpectedly, my data showed that all tested cdk inhibitors (olomoucine, (S)-roscovitine, and (R)-roscovitine) increased mEPP frequency significantly (see section 3.3.1; Cho and Meriney, 2006). This suggests that the observed increases in mEPP frequency may not be mediated by changes in calcium channel function. Therefore, the possibility that inhibition of cdks in a presynaptic nerve terminal may cause changes in mEPP frequency cannot be completely ruled out. This non-specific effect on mEPP frequency did not impede my investigation described in this dissertation because the effects on calcium channel activity and evoked transmitter release were controlled for using other related cdk inhibitors. However, it would be ideal to identify a derivative of roscovitine that only has effects on calcium channels without influencing cdks. In fact, these studies are under way in our laboratory in collaboration with Dr. Meijer (Station Biologique de Roscoff, CNRS UPR, Roscoff cedex, Bretagne, France).

Second, roscovitine can affect all types of Ca_v2 channels (N-, P/Q- and R-type channels). Because specific blockers of each Ca_v2 channel subtype are available, one can still study effects of roscovitine on selective Ca_v2 subtypes. Furthermore, in a recent study, Buraei et al. (2007)

showed that some types of potassium channels were also affected by roscovitine. In that sense, a roscovitine derivative that has selectivity for subtypes of calcium channels would be desirable.

5.2 ROSCOVITINE EFFECTS ON CA_v2 CHANNELS ARE REMINISCENT OF BAYK 8644 EFFECTS ON CA_v1 CHANNELS.

With respect to dihydropyridine (DHP), including BayK 8644, binding to L-type channels, the specific amino acid sequence important in binding in the α 1 subunit has been mapped. Site directed mutation has revealed not only the essential amino acid binding sequence, but substitutions have conferred DHP binding to Ca_v2 type channels (Hockerman et al., 1997; Peterson et al., 1997; Sinnegger et al., 1997; Yamaguchi et al., 2000, 2003). In a similar way, the roscovitine binding site on Ca_v2 calcium channel subtypes should be identified in future. Using experiments that focus on the structure-activity relationship, derivatives of roscovitine targeting only certain type of calcium channels can be developed.

If, and when, a crystal structure can be solved for Ca_v1 and Ca_v2 channels, as has recently been published for some types of potassium channels (Cabral et al., 1998; Doyle et al., 1998; Jiang et al., 2002, 2003; Long et al., 2005), one will be able to use molecular modeling approaches to investigate the mechanisms that lead to DHP action as antagonists ((R)-(+)-BayK 8644) or agonists ((S)-(-)-BayK 8644). Using this wealth of information on BayK 8644 action on Ca_v1 channels, contrasting effects of roscovitine enantiomers ((R)- and (S)-roscovitine) on Ca_v2 channels can be explored further. I hypothesize that this study might reveal the subtle differences that exist to create agonist vs antagonist effects and to generate calcium channel subtype specificity. This information is predicted to be of value in future drug development.

5.3 CLINICAL ASPECTS REGARDING NEUROMUSCULAR WEAKNESS

The generation of highly selective roscovitine derivatives will also be essential in the evaluation of these chemicals as treatments for neuromuscular disease, as the current non-selective drugs have some side effects. Lambert-Eaton Myasthenic Syndrome (LEMS) is an autoimmune disorder that is characterized by a decrease in the number of presynaptic calcium channels (Lambert et al., 1956; Elmqvist et al., 1968; O'Neill et al., 1988; Vincent et al., 1989). Currently, potassium channel blockers, such as guanidine hydrochloride, 4-aminopyridine, and DAP, are recommended as treatments. They increase the magnitude of transmitter released with each action potential, but they also lead to a variety of clinical side effects (Oh and Kim 1973; Matthews and Wickelgren, 1977; Anderson and Harvey, 1988; Silbert et al., 1990; Sanders, 1995; Molgo and Guglielmi, 1996; Oh et al., 1997; Sanders et al., 2000). This may result from the significant reduction in paired-pulse facilitation caused by large increases in basal transmission at the nerve terminal (Thomsen and Wilson, 1983), and/or the effects on axonal potassium channels that limit the frequencies at which nerves can conduct (Miralles and Solsona, 1998).

Instead of indirectly increasing calcium influx by potassium channel blockers, drugs that directly target calcium channel might become better treatments for LEMS with fewer side effects. In most clinical trials for LEMS, 10-20 mg of DAP is administered 3 times per day, which leads to serum levels that have been measured as about 1 μ M (Aisen et al., 1995). Therefore, using DAP 1 μ M as a comparison drug in this dissertation was also clinically relevant.

5.4 GLYCEROTOXIN

Although not part of my thesis work, I did perform some experiments examining the effects of another novel calcium channel modulator: glycerotoxin. Glycerotoxin is a 320 kD protein, isolated as a fraction from the venom of a marine worm (*Glycera convoluta*). Glycerotoxin was known to enhance spontaneous release of transmitter and increase quantal content of evoked transmitter release, possibly by increasing the open probability of N-type calcium channels (Meunier et al., 2002). I performed patch clamp recordings of calcium current in cultured *Xenopus* motoneurons and showed that 1 $\mu\text{g/ml}$ glycerotoxin increased peak amplitude of calcium current evoked by an action potential by 41% (n=2) without altering deactivation kinetics of calcium currents. Total calcium entry increased by 37% (n=2; Figure 28). Though glycerotoxin has not been well characterized and it is not commercially available, it might be interesting to compare the effects of roscovitine and glycerotoxin as both of these agents appear to directly target presynaptic calcium channels, increasing calcium entry and transmitter release by apparently different mechanisms.

Considering potential treatment strategies for the disease LEMS, it is important to study these novel agents that directly alter presynaptic calcium influx and transmitter release with the hope that they might reverse neuromuscular weakness while maintaining aspects of short-term synaptic plasticity that are important for normal synaptic function. In frogs, a partial blockade of transmitter release at the neuromuscular junction using ω -conotoxin GVIA, a specific and irreversible N-type calcium channel blocker, mimics the LEMS condition by the functional removal of a subset of presynaptic calcium channels. In mice, one could use passive transfer of the disease by injecting immunoglobulin from LEMS patients, and evaluate effects of novel

drugs. Using these models, the ability of roscovitine, DAP and glycerotoxin to reverse muscle weakness can be evaluated.

5.5 COMPLEMENTARY EXPERIMENTAL AND COMPUTATIONAL STUDIES OF THE SYNAPSE

I have investigated presynaptic calcium influx, calcium-triggered transmitter release and short-term plasticity at the frog neuromuscular junction using both physiological experiments and computational modeling in a complementary way. First, I characterized the underlying mechanisms of pharmacological tools by recording effects on calcium currents and presynaptic action potentials (section 2). Next I examined effects of two pharmacological agents on transmitter release using single action potentials and paired-pulse stimuli (section 3). These physiological data provided important constraints for my computational model. Using these approaches, I interpreted physiological data and tested hypotheses related to the sub-active zone mechanisms that control vesicle fusion (section 4). This is the first modeling approach to simulate the effects of pharmacological tools on calcium currents and vesicle release using a spatially realistic three dimensional active zone model.

For comparison with modeling data, calcium currents and action potential waveforms were recorded from *Xenopus* motoneuron somata, since the adult *Rana pipiens* frog motor nerve terminal is not amenable to direct patch clamp study. Though the use of recordings from the somata of cultured frog motoneurons provided a good preparation with which to characterize underlying mechanisms of drugs, it is also possible to record directly from cultured motor nerve terminals in this preparation. The use of these *Xenopus* presynaptic varicosities, instead of

somata, might be useful for future work as they might provide a more appropriate synaptic model preparation. This cultured synaptic preparation, derived from 1-day old *Xenopus* embryos, is a natural neuromuscular synapse that forms within 1-3 days *in vitro*. Cultured synapses exhibit physiological and morphological properties that parallel closely their developing counterparts *in vivo* (Kullberg et al., 1977; Weldon and Cohen, 1979). Within hours of contact, synapses exhibit spontaneous and evoked acetylcholine release, membrane ‘thickenings’, clouds of presynaptic vesicles, and a postsynaptic aggregation of acetylcholine receptors (Anderson et al., 1977; Weldon and Cohen, 1979; Nakajima et al., 1980; Cohen and Weldon, 1980; Kidokoro et al., 1980; Kidokoro and Yeh, 1982; Takahashi et al., 1987; Buchanan et al., 1989; Evers et al., 1989). While I believe that my use of the soma was effective, it is possible that there are differences that may exist if studied at the *Xenopus* cultured varicosity. These could be investigated in future work.

Because roscovitine did not significantly alter the shape of the action potential at the frog motoneuron somata, I considered that the recently reported roscovitine effects on potassium channels (Buraei et al., 2007) would not impair my investigations described in this dissertation. However, it might be useful to confirm whether roscovitine alters action potential shape using recordings of action potentials at cultured *Xenopus* neuromuscular varicosities, or at the adult frog neuromuscular junction by extracellular recordings.

The present model does not include vesicle recycling because the timing of endocytosis and refilling is too slow to affect vesicle release by a single action potential, or by paired-pulse stimuli of 10 to 30 msec interstimulus interval (Gundelfinger et al., 2003; Sudhof, 2004). At the Calyx of Held, kiss and run endocytosis time constants for a single spontaneous vesicle release event was ~60 msec, and was even longer (110 msec) after single action potential, or following

low-frequency stimulation (Sun et al., 2002). In general, the time constant for vesicle recycling gradually increased as the frequency of stimulation became higher (Sun et al., 2002). At the ribbon synapses of retinal bipolar cells (von Gersdorff and Matthews, 1994; Neves and Lagnado, 1999; Neves et al., 2001) or inner ear hair cells (Beutner et al., 2001), rapid endocytosis has been reported to have a ~ 1 sec time constant.

Overall, under normal calcium conditions, my model predicted presynaptic calcium influx and transmitter release by a single action potential very well. However, it was hard to evaluate experimental effects under low calcium conditions even running simulations using 10000 seeds. These simulations did not appear to run enough seeds to observe reliable model results because the probability of a vesicle fusion event was so low that often less than 5 occurred in 10000 runs. Furthermore, as discussed in section 4, more sophisticated adjustments will be necessary to simulate paired-pulse facilitation.

Regarding short-term synaptic plasticity, every synapse experiences a combination of facilitation and depression influences with repetitive stimulation. Facilitation results from buffered residual calcium lingering for ~ 100 msec after a nerve stimulation. Vesicle depletion at release sites is thought to be the most prominent cause of depression. My model incorporates both features, though in its present state it did not demonstrate physiological levels of facilitation. With regard to depression, my model predicted that the control probability of vesicle release by the first action potential in a pair was 0.54, and about 2% of the vesicle release events predicted to occur during the second action potential would be prevented because of vesicle depletion. In other words, in 1000 simulations, 540 vesicles were released by the first action potential and during the second action potential, 11 vesicles could not be released because those sites were used during the first stimulation. With only vesicle depletion, the paired-pulse ratio

using a 10 msec interstimulus interval should be 0.98 $((540-11)/540)$. However, my model predicted a paired-pulse ratio of 1.0. This suggests that residual calcium-mediated facilitation must have provided equal and opposite compensation so that the paired-pulse ratio increased from 0.98 to 1.0. However, in my simulations the residual calcium has not been measured directly.

As expected, differential adjustments affecting only the response during the second action potential in a pair, such as action potential broadening and possible conformational changes of SNARE complex, were more effective at eliciting significant facilitation than changes in global model conditions, which generally affected both responses (such as changes in kinetic parameters or active zone geometry). If I adapted other differential manipulations including the presence of local buffer saturation, as used in previous modeling studies (Klingauf and Neher, 1997; Neher, 1998; Matveev et al., 2004), I could demonstrate enormous facilitation. Thus, one can generate very large facilitation effects with selective adjustments either between stimuli, or during only the second action potential in a pair. In this dissertation, I focused on testing adjustments based on published physiological or biochemical data to evaluate a potential effect on facilitation. However, using this approach, it was not easy to demonstrate facilitation at experimentally determined levels. My modeling approach of paired-pulse facilitation in this dissertation is novel because it is the first to evaluate short-term plasticity with a spatially realistic active zone model, in contrast with previous models using numerical equations. Though my basic model requires more adjustments to accurately predict physiological levels of facilitation, I expect it could simulate experimental paired-pulse facilitation with the inclusion of additional factors, and testing combinational manipulations. For these further adjustments, the

tested manipulations and resulting effects shown in this dissertation will provide a framework and fundamental information.

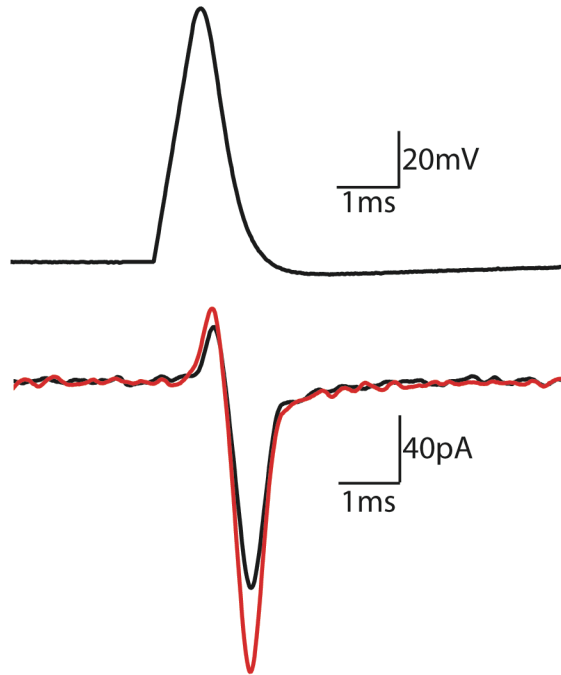


Figure 28 Effect of 1 $\mu\text{g/ml}$ glycerotoxin on calcium currents.

Glycerotoxin (red) increased peak current amplitude by 41% and increased total calcium entry by 37% without altering deactivation of calcium current in cultured *Xenopus* motoneurons.

BIBLIOGRAPHY

Adler EM, Augustine GJ, Duffy SD and Charlton MP (1991) Alien intracellular calcium chelators attenuate neurotransmitter release at the squid giant synapse. *J Neurosci*, **11**, 1496-1507.

Adolfson B, Saraswati S, Yoshihara M and Littleton JT (2004) Synaptotagmins are trafficked to distinct subcellular domains including the postsynaptic compartments. *J Cell Biol*, **166**, 249-260.

Aisen ML, Sevilla D, Gibson G, Kutt H, Blau A, Edelstein L, Hatch J and Blass J (1995) 3,4-Diaminopyridine as a treatment for amyotrophic lateral sclerosis. *J Neurol Sci*, **129**, 21-24.

Aisen ML, Sevilla D, Edelstein L and Blass J (1996) A double-blind placebo-controlled study of 3,4-diaminopyridine in amyotrophic lateral sclerosis patients on a rehabilitation unit. *J Neurol Sci*, **138**, 93-96.

Atluri PP and Regehr WG (1996) Determinants of the time course of facilitation at the granule cell to Purkinje cell synapse. *J Neurosci*, **16**, 5661-5671.

Anderson AJ, Cohen MW and Zorychta E (1977) Effects of innervation on the distribution of acetylcholine receptors on cultured muscle cells. *J Physiol*, **268**, 731-756.

Anderson AJ and Harvey AL (1988) Effects of the facilitatory compounds catechol, guanidine, noradrenaline and phencyclidine on presynaptic currents of mouse motor nerve terminals. *Naunyn-Schmiedeberg's Arch Pharmacol*, **338**, 133-137.

Andreu R and Barrett EF (1980) Calcium dependence of evoked transmitter release at very low quantal contents at the frog neuromuscular junction. *J Physiol*, **308**, 79-97.

Augustine GJ, Charlton MP and Smith SJ (1985) Calcium entry and transmitter release at voltage-clamped nerve terminals of squid. *J Physiol*. **367**, 163-181.

Augustine GJ, Charlton MP and Smith SJ (1987) Calcium action in synaptic transmitter release. *Annu Rev Neurosci*, **10**, 633-693.

Augustine GJ (1990) Regulation of transmitter release at the squid giant synapse by presynaptic delayed rectifier potassium current. *J Physiol*, **431**, 343-364.

Augustine GJ, Adler EM and Charlton MP (1991) The calcium signal for transmitter secretion from presynaptic nerve terminals. *Ann NY Acad Sci*, **635**, 365-381.

Augustine GJ (2001) How does calcium trigger neurotransmitter release? *Curr Opin Neurobiol*, **11**, 320-326.

Bajjalieh SM (1999) Synaptic vesicle docking and fusion. *Curr Opin Neurobiol*, **9**, 321-328.

Baker B and Marion B (2002) A presynaptic K⁺ channel-independent neurotransmitter release mechanism caused by serotonin may exist in crayfish. *Pioneering Neuroscience*, **4**, 7-11.

Bargas J, Howe A, Eberwine J, Cao Y and Surmeier DJ (1994) Cellular and molecular characterization of Ca²⁺ currents in acutely isolated, adult rat neostriatal neurons. *J Neurosci*, **14**, 6667-6686.

Barish ME (1991) Voltage-gated calcium currents in cultured embryonic *Xenopus* spinal neurons. *J Physiol*, **444**, 523-543.

Barish ME, Ichikawa M, Tominaga T, Matsumoto G, and Toshio Iijima (1996) Enhanced fast synaptic transmission and a delayed depolarization induced by transient potassium current blockade in rat hippocampal slice as studied by optical recording. *J Neurosci*, **16**, 5672-5687.

Barnes-Davis M and Forsythe ID (1995) Pre- and postsynaptic glutamate receptors at a giant excitatory synapse in rat auditory brainstem slices. *J Physiol*, **488**, 387-406.

Barton SB, Cohen IS, and Van der Kloot W (1983) The calcium dependence of spontaneous and evoked quantal release at the frog neuromuscular junction. *J Physiol*, **337**, 735-751.

Bean BP (1985) Two kinds of calcium channels in canine atrial cells. Differences in kinetics, selectivity, and pharmacology. *J Gen Physiol*, **86**, 1-30.

Bennett MR, Jones P and Lavidis NA (1986) The probability of quantal secretion along visualized terminal branches at amphibian (*Bufo marinus*) neuromuscular synapses. *J Physiol (Lond)*, **379**, 257-274.

Bertram R, Sherman A and Stanley EF (1996) Single-domain/bound calcium hypothesis of transmitter release and facilitation. *J Neurophysiol*, **75**, 1919-1931.

Bertram R, Smith GD and Sherman A (1999) Modeling study of the effects of overlapping Ca^{2+} microdomains on neurotransmitter release. *Biophys J*, **76**, 735-750.

Bennett MR, Farnell L and Gibson WG (2000a) The probability of quantal secretion near a single calcium channel of an active zone. *Biophys J*, **78**, 2201-2221.

Bennett MR, Farnell L and Gibson WG (2000b) The probability of quantal secretion within an array of calcium channels of an active zone. *Biophys J*, **78**, 2222-2240.

Betz WJ (1970) Depression of transmitter release at the neuromuscular junction of the frog. *J Physiol*, **206**, 629-644.

Beutner D, Voets T, Neher E and Moser T (2001) Calcium dependence of exocytosis and endocytosis at the cochlear inner hair cell afferent synapse. *Neuron*, **29**, 681-690.

Bever CT, Leslie J, Camenga DC, Panitch HS and Johnson KP (1990) Preliminary trial of 3,4-diaminopyridine in patients with multiple sclerosis. *Ann. Neurol*, **27**, 421-427.

Bollmann JH, Sakmann B and Borst JG (2000) Calcium sensitivity of glutamate release in a calyx-type terminal. *Science*, **289**, 953-957.

Borst JG, Helmchen F and Sakmann B (1995) Pre- and postsynaptic whole-cell recordings in the medial nucleus of the trapezoid body of the rat. *J Physiol (Lond)*, **489**, 825-840.

Borst JG and Sakmann B (1996) Calcium influx and transmitter release in a fast CNS synapse. *Nature*, **383**, 431-434.

Borst JG and Sakmann B (1998) Facilitation of presynaptic calcium currents in the rat brainstem. *J Physiol (Lond)*, **513**, 149-155.

Borst JG and Sakmann B (1999) Effect of changes in action potential shape on calcium currents and transmitter release in a calyx-type synapse of the rat auditory brainstem. *Phil Trans R Soc Lond B*, **354**, 347-355.

Brain KL and Bennett MR (1995) Calcium in the nerve terminals of chick ciliary ganglia during facilitation, augmentation and potentiation. *J Physiol*, **489**, 637-648.

Brain KL and Bennett MR (1997) Calcium in sympathetic varicosities of mouse vas deferens during facilitation, augmentation and autoinhibition. *J Physiol*, **502**, 521-536.

Brody DL and Yue DT (2000a) Relief of G-protein inhibition of calcium channels and short-term synaptic facilitation in cultured hippocampal neurons. *J Neurosci*, **20**, 889-898.

Brody DL and Yue DT (2000b) Release-independent short-term synaptic depression in cultured hippocampal neurons. *J Neurosci*, **20**, 2480-2494.

Brose N, Petrenko AG, Sudhof TC and Jahn R (1992) Synaptotagmins: a calcium sensor on the synaptic vesicle surface. *Science*, **256**, 1021-1025.

Brown AM, Kunze DL and Yatani A (1984) The agonist effect of dihydropyridines on Ca channels. *Nature*, **311**, 570-572.

Buchanan J, Sun YA and Poo MM (1989) Studies of nerve-muscle interactions in *Xenopus* cell culture: fine structure of early functional contacts. *J Neurosci*, **9**, 1540-1554.

Buraei Z, Anghelescu M and Elmslie KS (2005) Slowed N-type calcium channel (Cav2.2) deactivation by the cyclin-dependent kinase inhibitor Roscovitine. *Biophys J*, **89**, 1681-1691.

Buraei Z, Schofield G and Elmslie KS (2007) Roscovitine differentially affects CaV2 and Kv channels by binding to the open state. *Neuropharmacology*, **52**, 883-894.

Cabral JHM, Lee A, Cohen SL, Chait BT, Li M and Mackinnon R (1998) Crystal structure and functional analysis of the HERG potassium channel N terminus: a eukaryotic PAS domain. *Cell*, **95**, 649-655.

Catterall WA (2000) Structure and regulation of voltage-gated Ca²⁺ channels. *Annu Rev Cell Dev Biol*, **16**, 521-555.

Chapman ER, Hanson PI, An S, and Jahn R (1995) Ca²⁺ regulates the interaction between synaptotagmin and syntaxin-1. *J Biol Chem*, **270**, 23667-23671.

Chapman ER, Desai RC, Davis AF, and Tornehl CK (1998) Delineation of the oligomerization, AP-2 binding, and synprint binding region of the C2B domain of synaptotagmin. *J Biol Chem*, **273**, 32966-32972.

Chapman ER (2002) Synaptotagmin: A Ca²⁺ sensor that triggers exocytosis? *Nat Rev Mol cell Biol*, **3**, 498-508.

Charlton MP, Smith SJ and Zucker RS (1982) Role of presynaptic calcium ions and channels in synaptic facilitation and depression at the squid giant synapse. *J Physiol*, **323**, 173-193.

Cheng K and Ip NY (2003) Cdk5: a new player at synapses. *Neurosignals*, **12**, 180-190.

Cho S and Meriney SD (2006) The effects of presynaptic calcium channel modulation by roscovitine on transmitter release at the adult frog neuromuscular junction. *Eur J Neurosci*, **23**, 3200-3208.

Church PJ and Stanley EF (1996) Single L-type calcium channel conductance with physiological levels of calcium in chick ciliary ganglion neurons. *J Physiol*, **496**, 59-68.

Cohen MW and Weldon PR (1980) Localization of acetylcholine receptors and synaptic ultrastructure at nerve- muscle contacts in culture: dependence on nerve type. *J Cell Biol*, **86**(2), 388-401.

Cohen MW, Jones OT and Angelides KJ (1991) Distribution of Ca²⁺ channels on frog motor nerve terminals revealed by fluorescent omega-conotoxin. *J Neurosci*, **11**, 1032-1039.

Craxton M (2004) Synaptotagmin gene content of the sequenced genomes. *BMC Genomics*, **5**, 43.

Cuttle MF, Tsujimoto T, Forsythe ID, and Takahashi T (1998) Facilitation of the presynaptic calcium current at an auditory synapse in rat brainstem. *J Physiol (Lond)*, **512**, 723-729.

D'Alonzo AJ and Grinnell AD (1985) Profiles of evoked release along the length of frog motor nerve terminals. *J Physiol (Lond)*, **359**, 235-258.

Davis AF, Bai J, Fasshauer D, Wolowick MJ, Lewis JL, and Chapman ER (1999) Kinetics of synaptotagmin responses to Ca^{2+} and assembly with the core SNARE complex onto membranes. *Neuron*, **24**, 363-376.

Davletov B and Sudhof TC (1993) A single C2-domain from synaptotagmin I is sufficient for high affinity Ca^{2+} /phospholipids-binding. *J Biol Chem*, **268**, 26386-26390.

Deitcher DL, Ueda A, Stewart BA, Burgess RW, Kidokoro Y and Schwarz TL (1998) Distinct requirements for evoked and spontaneous release of neurotransmitter are revealed by mutations in the *Drosophila* gene neuronal-synaptobrevin. *J Neurosci*, **18**(6), 2028-2039.

Delaney KR and Tank DW (1994) A quantitative measurement of the dependence of short-term synaptic enhancement on presynaptic residual calcium. *J Neurosci*, **14**, 5885-5902.

Delgado R, Maureira C, Oliva C, Kidokoro Y and Labarca P (2000) Size of vesicle pools, rates of mobilization, and recycling at neuromuscular synapses of a *Drosophila* mutant, *shibire*. *Neuron*, **28**, 941-953.

DeWaard M, Gurnett CA and Campbell KP (1996) Structural and functional diversity of voltage-activated calcium channels. In *Ion Channels*, Volume 4, ed. Narahashi T, pp41-87, Plenum Press.

Dhavan R and Tsai LH (2001) A decade of CDK5. *Nat Rev Mol Cell Biol*, **2**(10), 749-759.

Dodge FA Jr. and Rahamimoff R (1967) Co-operative action of calcium ions in transmitter release at the neuromuscular junction. *J Physiol*, **193**, 419-432.

Doyle DA, Cabral JM, Pfuetzner RA, Kuo A, Gulbis JM, Cohen SL, Chait BT and MacKinnon R (1998) The structure of the potassium channel: Molecular basis of K⁺ conduction and selectivity. *Science*, **280**, 69-77.

Dudel J (1981) The effect of reduced calcium on quantal unit current and release at the crayfish neuromuscular junction. *Pflugers Archiv – Eur J Physiol*, **391**, 35-40.

Earles CA, Bai J, Wang P, and Chapman ER (2001) The tandem C2 domains of synaptotagmin contain redundant Ca²⁺ binding sites that cooperate to engage t-SNAREs and trigger exocytosis. *J Cell Biol*, **154**, 1117-1123.

Elmqvist D and Lambert EH (1968) Detailed analysis of neuromuscular transmission in a patient with the myasthenic syndrome sometimes associated with bronchogenic carcinoma. *Mayo Clin Proc*, **43**, 689-713.

Elmslie KS (2004) Calcium channel blockers in the treatment of disease. *J Neurosci Res*, **75**, 733-741.

Ertel EA, Campbell KP, Harpold MM, Hofmann F, Mori Y, Perez-Reyes E, Schwartz A, Snutch TP, Tanabe T, Birnbaumer L, Tsien RW and Catterall WA (2000) Nomenclature of voltage-gated calcium channels. *Neuron*, **25**, 533-535.

Evers J, Laser M, Sun YA, Xie ZP and Poo MM (1989) Studies of nerve-muscle interactions in *Xenopus* cell culture: analysis of early synaptic currents. *J Neurosci*, **9**, 1523-1539.

Fedchyshyn MJ and Wang LY (2005) Developmental transformation of the release modality at the calyx of Held synapse. *J Neurosci*, **25**, 4131-4140.

Feller MB, Delaney KR and Tank DW (1996) Presynaptic calcium dynamics at the frog retinotectal synapse. *J Neurosci*, **76**, 381-400.

Fernandez I, Arac D, Ubach J, Gerber SH, Shin O, Gao Y, Anderson RGW, Sudhof TC, and Rizo J (2001) Three-dimensional structure of the synaptotagmin 1 C2B-domain: synaptotagmin 1 as a phospholipid-binding module. *Neuron*, **32**, 1057-1069.

Fernandez-Chacon R, Konigstorfer A, Gerber SH, Garcia J, Matos MF, Stevens CF, Brose N, Rizo J, Rosenmund C, and Sudhof TC (2001) Synaptotagmin I functions as a calcium regulator of release probability. *Nature*, **410**, 41-49.

Flink MT and Atchison WD (2002) Passive transfer of Lambert-Eaton syndrome to mice induces dihydropyridine sensitivity of neuromuscular transmission. *J Physiol*, **543**, 567-576.

Forsythe ID, Tsujimoto T, Barnes-Davies M, Cuttle MF, and Takahashi T (1998) Inactivation of presynaptic calcium current contributes to synaptic depression at a fast central synapse. *Neuron*, **20**, 797-807.

Fox AP, Nowycky MC and Tsien TW (1987) Single-channel recordings of three types of calcium channels in chick sensory neurons. *J Physiol*, **394**, 173-200.

Fukunaga H, Engel AG, Osame M and Lambert H (1982) Paucity and disorganization of presynaptic active zones in the Lambert-Eaton myasthenic syndrome. *Muscle Nerve*, **5**, 686-697.

Fukunaga H, Engel AG, Lang B, Newsom-Davis J and Vincent A (1983) Passive transfer of Lambert-Eaton myasthenic syndrome with IgG from man to mouse depletes the presynaptic membrane active zones. *PNAS*, **80**, 7636-7640.

Geiger JR and Jonas P (2000) Dynamic control of presynaptic Ca^{2+} inflow by fast-inactivating K^+ channels in hippocampal mossy fiber boutons. *Neuron*, **28**, 927-939.

Gentile L and Stanley EF (2005) A unified model of presynaptic release site gating by calcium channel domains. *Eur J Neurosci*, **21**(1), 278-282.

Geppert M, Archer BT III, and Sudhof TC (1991) Synaptotamin II: a novel differentially distributed form of synaptotagmin. *J Biol Chem*, **266**, 13548-13552.

Gerber SH, Garcia J, Rizo J and Sudhof TC (2001) An unusual C2-domain in the active-zone protein piccolo: implications for Ca^{2+} regulation of neurotransmitter release. *EMBO J*, **20**, 1605-1619.

Gerber SH, Josep R and Sudhof TC (2002) Role of electrostatic and hydrophobic interactions in Ca^{2+} -dependent phospholipids binding by the C2A-domain from synaptotagmin I. *Diabetes*, **51**, S12-S18.

Giniatullin RA, Talantova M and Vyskocil F (1997) Desensitization shortens the high-quantal-content endplate current time course in frog muscle with intact cholinesterase. *J Physiol*, **502.3**, 641-648.

Giniatullin AR, Grishin SN, Sharifullina ER, Petrov AM, Zefirov AL and Giniatullin RA (2005) Reactive oxygen species contribute to the presynaptic action of extracellular ATP at the frog neuromuscular junction. *J Physiol*, **565.1**, 229-242.

Glavinovic MI and Narahashi T (1988) Depression, recovery and facilitation of neuromuscular transmission during prolonged titanic stimulation. *Neuroscience*, **25**, 271-281.

Glavinovic MI and Rabie HR (2001) Monte Carlo evaluation of quantal analysis in the light of Ca^{2+} dynamics and the geometry of secretion. *Pflugers Arch*, **443**, 132-145.

Gu Y, Ge SY and Ruan DY (2004) Effect of 4-aminopyridine on synaptic transmission in rat hippocampal slices. *Brain Res*, **1006**, 225-232.

Guerrero S and Novakovic L (1980) Effects of 4-aminopyridine on pacemaker activity of frog sinus venosus. *Eur J Pharmacol*, **62**, 335-340.

Gundelfinger ED, Kessels MM and Qualmann B (2003) Temporal and spatial coordination of exocytosis and endocytosis. *Nat Rev Mol Cell Biol*, **4**, 127-139.

Guy HR and Conti F (1990) Pursuing the structure and function of voltage-gated channels. *Trends Neurosci*, **13**, 201-206.

Hagiwara S, Ozawa S and Sand O (1975) Voltage clamp analysis of two inward current mechanisms in the egg cell membrane of a starfish. *J Gen Physiol*, **65**, 617-644.

Han X, Wang CT, Bai J, Chapman ER and Jackson MB (2004) Transmembrane segments of syntaxin line the fusion pore of Ca²⁺-triggered exocytosis. *Science*, **304**, 289-292.

Harlow ML, Ress D, Stoschek A, Marshall RM and McMahan UJ (2001) The architecture of active zone material at the frog's neuromuscular junction. *Nature*, **409**, 479-484.

Heidelberger R, Heinemann C, Neher E and Matthews G (1994) Calcium dependence of the rate of exocytosis in a synaptic terminal. *Nature*, **371**, 513-515.

Heinemann SH, Terlau H, Stuhmer W, Imoto K and Numa S (1992) Calcium channel characteristics conferred on the sodium channel by single mutations. *Nature*, **356**, 441-443.

Herrera AA, Grinnell AD and Wolowske B (1985) Ultrastructural correlates of naturally occurring differences in transmitter release efficacy in frog motor nerve terminals. *J Neurocytol*, **14**, 193-202.

Hess P, Lansman JB and Tsien RW (1984) Different modes of Ca channel gating behaviour favoured by dihydropyridine Ca agonists and antagonists. *Nature*, **311**, 538-544.

Heuser JE, Reese TS and Landis DM (1974) Functional changes in frog neuromuscular junctions studied with freeze-fracture. *J Neurocytol*, **3**(1), 109-131.

Heuser JE and Reese TS (1977) Structure of the synapse. In Kandel ER (ed.), *Handbook of Physiology. The Nervous System. Cellular Biology of Neurons*. Bethesda: American Physiology Society, 1977, Sect. 1, Vol. I, 261-294.

Heuser JE, Reese TS, Dennis MJ, Jan Y, Jan L and Evans L (1979) Synaptic vesicle exocytosis captured by quick freezing and correlated with quantal transmitter release. *J Cell Biol*, **81**, 275-300.

Hilfiker S, Schweizer FE, Kao HT, Czernik AJ, Greengard P and Augustine GJ (1998) Two sites of action for synapsin domain E in regulating neurotransmitter release. *Nat Neurosci*, **1**, 29-35.

Hochner B, Parnas H and Parnas I (1991) Effects of intra-axonal injection of Ca²⁺ buffers on evoked release and on facilitation in the crayfish neuromuscular junction. *Neurosci Lett*, **125**, 215-218.

Hockerman GH, Peterson BZ, Sharp E, Tanada TN, Scheuer T and Catterall WA (1997) Construction of a high-affinity receptor site for dihydropyridine agonists and antagonists by single amino acid substitutions in a non-L-type Ca²⁺ channel. *PNAS*, **94**, 14906-14911.

Hodgkin AL and Keynes RD (1957) Movement of labeled calcium in squid giant axons. *J Physiol*, **138**, 253-281.

Hofmann F, Lacinova L and Klugbauer N (1999) Voltage-dependent calcium channels: from structure to function. *Rev Physiol Biochem Pharmacol*, **139**, 33-87.

Hue B, Pelahate M, Callec JJ and Chanelet J (1976) Synaptic transmission in the sixth ganglion of the cockroach: Action of 4-aminopyridine. *J Exp Biol*, **65**, 517-527.

Hui E, Bai J, Wang P, Sugimori M, Llinas RR, and Chapman ER (2005) Three distinct kinetic groupings of the synaptotagmin family: Candidate sensors for rapid and delayed exocytosis. *PNAS*, **102**(14), 5210-5214.

Jackson MB, Konnerth A, and Augustine GJ (1991) Action potential broadening and frequency-dependent facilitation of calcium signals in pituitary nerve terminals. *PNAS*, **88**, 380-384.

Jankowska E, Lundberg A, Rudomin P and Sykova E (1977) Effects of aminopyridine on transmission in excitatory and inhibitory synapses in spinal cord. *Brain Res*, **136**, 387-392.

Jenkinson DH (1957) The nature of the antagonism between calcium and magnesium ions at the neuromuscular junction. *J Physiol*, **138**, 434-444.

Jiang XY and Abrams TW (1998) Use-dependent decline of paired-pulse facilitation at *Aplysia* sensory neuron synapses suggests a distinct vesicle pool or release mechanism. *J Neurosci*, **18**, 10310-10319.

Jiang Y, Lee A, Chen J, Cadene M, Chait BT and MacKinnon R (2002) Crystal structure and mechanism of a calcium-gated potassium channel. *Nature*, **417**, 515-522.

Jiang Y, Lee A, Chen J, Ruta V, Cadene M, Chait B and MacKinnon R (2003) X-ray structure of a voltage-dependent K⁺ channel. *Nature*, **423**, 33-41.

Jones SW and Jacobs LS (1990) Dihydropyridine actions on calcium currents of frog sympathetic neurons. *J Neurosci*, **10**, 2261-2267.

Jones SW and Marks TN (1989) Calcium currents in bullfrog sympathetic neurons. I. Activation kinetics and pharmacology. *J Gen Physiol*, **94**(1), 151-167.

Kamiya H and Zucker RS (1994) Residual Ca²⁺ and short-term synaptic plasticity. *Nature*, **371**, 603-606.

Katz B and Thesleff S (1957) A study of the “desensitization” produced by acetylcholine at the motor end plate. *J Physiol*, **138**, 63-80.

Katz B and Miledi R (1965a) The measurement of synaptic delay, and the time course of acetylcholine release at the neuromuscular junction. *Proceedings of the Royal Society of London, Series B, Biological Sciences*, **161**, 483-495.

Katz B and Miledi R (1965b) The effect of calcium on acetylcholine release from motor nerve terminals. *Proceedings of the Royal Society of London, Series B, Biological Sciences*, **161**, 496-503.

Katz B and Miledi R (1968) The role of calcium in neuromuscular facilitation. *J Physiol*, **195**, 481-492.

Katz B and Miledi R (1970) Further study on the role of calcium in synaptic transmission. *J Physiol*, **207**, 789-801.

Katz B and Miledi R (1979) Estimates of quantal content during chemical potentiation of transmitter release. *Proceedings of the Royal Society of London, Series B, Biological Sciences*, **205**, 369-378.

Kee Y and Scheller RH (1996) Localization of synaptotagmin-binding domains on syntaxin. *J Neurosci*, **16**, 1975-1981.

Kerr LM and Yoshikami D (1984) A venom peptide with a novel presynaptic blocking action. *Nature*, **308**, 282-284.

Kidokoro Y, Anderson MJ and Gruener R (1980) Changes in synaptic potential properties during acetylcholine receptor accumulation and neurospecific interactions in *Xenopus* nerve-muscle cell culture. *Dev Biol*, **78**, 464-483.

Kidokoro Y and Yeh E (1982) Initial synaptic transmission at the growth cone in *Xenopus* nerve-muscle culture. *PNAS*, **79**, 6727-6731.

Kim YI, Goldner MM and Sanders DB (1980) Facilitatory effects of aminopyridine on normal neuromuscular transmission. *Muscle and Nerve*, **3**, 105-111.

Kim YI and Neher E (1988) IgG from patients with Lambert-Eaton syndrome blocks voltage-dependent calcium channels. *Science*, **239**, 405-408.

King JD and Meriney SD (2005) Proportion of N-type calcium current activated by action potential stimuli. *J Neurophysiol*, **94**, 3762-3770.

Klingauf J and Neher E (1997) Modeling buffered Ca^{2+} diffusion near the membrane: implications for secretion in neuroendocrine cells. *Biophys J*, **72**, 674-690.

Kokubun S and Reuter H (1984) Dihydropyridine derivatives prolong the open state of Ca channels in cultured cardiac cells. *PNAS*, **81**, 4824-4827.

Koschak A, Reimer D, Walter D, Hoda JC, Heinzle T, Grabner M and Striessnig J (2003) Cav1.4 $\alpha 1$ subunits can form slowly inactivating dihydropyridine-sensitive L-type calcium channels lacking Ca^{2+} -dependent inactivation. *J Neurosci*, **23**, 6041-6049.

Kreitzer AC and Regehr WG (2000) Modulation of transmission during trains at a cerebellar synapse. *J Neurosci*, **20**, 1348-1357.

Kullberg RW, Lentz TL and Cohen MW (1977) Development of the myotomal neuromuscular junction in *Xenopus laevis*: an electrophysiological and fine-structural study. *Dev Biol*, **60**(1), 101-129.

Lacinova L (2005) Voltage-dependent calcium channels. *Gen Physiol Biophys*, **24**, Suppl 1, 1-78.

Lambert EH, Eaton LM and Rooke ED (1956) Defect of neuromuscular conduction associated with malignant neoplasm. *Amer J Physiol*, **187**, 612-613.

Lambert EH and Lennon VA (1988) Selected IgG rapidly induces Lambert-Eaton myasthenic syndrome in mice: complement independence and EMG abnormalities. *Muscle Nerve*, **11**, 1133-1145.

Lennon VA, Kryzer TJ, Griesmann GE, O'Suilleabhain PE, Windebank AJ, Woppmann A, Miljanich GP and Lambert EH (1995) Calcium-channel antibodies in the Lambert-Eaton syndrome and other paraneoplastic syndromes. *N Engl J Med*, **332**(22), 1467-1474.

Lester HA (1970) Transmitter release by presynaptic impulses in the squid stellate ganglion. *Nature*, **227**, 493-496.

Lester HA (1977) The response to acetylcholine. *Scientific American*, **236**(2), 106-116, 118.

Levy M, Faas GC, Saggau P, Craigen WJ and Sweatt JD (2003) Mitochondrial regulation of synaptic plasticity in the hippocampus. *J Biol Chem*, **278**(20), 17727-17734.

Li C, Ullrich B, Zhang JZ, Anderson RGW, Brose N, and Sudhof TC (1995) Ca²⁺-dependent and -independent activities of neural and non-neural synaptotagmins. *Nature*, **375**, 594-599.

Li L and Chin LS (2003) The molecular machinery of synaptic vesicle exocytosis. *Cellular and Molecular Life Sciences*, **60**, 823-1025.

Li W, Thaler C and Brehem P (2001) Calcium channels in *Xenopus* spinal neurons differ in somas and presynaptic terminals. *J Neurophysiol*, **86**, 269-279.

Lin YQ, Brain KL and Bennett MR (1998) Calcium in sympathetic boutons of rat superior cervical ganglion during facilitation, augmentation and potentiation. *J Auton Nerv Syst*, **73**, 26-37.

Llinas R, Steinberg IZ and Walton K (1981) Relationship between presynaptic calcium current and postsynaptic potential in squid giant synapse. *Biophys J*, **33**, 323-351.

Llinas R and Yarom Y (1981) Electrophysiology of mammalian inferior olivary neurons *in vitro*. Different types of voltage-dependent ionic conductances. *J Physiol*, **315**, 569-584.

Llinas R and Moreno H (1998) Local calcium signaling in neurons. *Cell Calcium*, **24**(5-6), 359-366.

Long SB, Campbell EB and MacKinnon R (2005) Crystal structure of a mammalian voltage-dependent *Shaker* family K⁺ channel. *Science*, **309**, 897-903.

Lundh H, Nilsson O and Rosen I (1984) Treatment of Lambert Eaton Syndrome: 3,4-diaminopyridine and pyridostigmine. *Neurology*, **34**, 1324-1330.

Lundh H, Nilsson O, Rosen I and Johansson S (1993) Practical aspects of 3,4-diaminopyridine treatment of the Lambert-Eaton myasthenic syndrome. *Acta Neurol Scand*, **88**, 136-140.

Luo F, Stiles JR and Meriney SD (2005) Variance analysis of action potential-evoked calcium influx reveals low-opening probability of presynaptic calcium channels at the frog neuromuscular junction. *Society for Neuroscience abstract*, 963.16.

Macleod GT, Gan JB and Bennett MR (1999) Vesicle-associated proteins and quantal release at single active zones of amphibian (*Bufo marinus*) motor-nerve terminals. *J Neurophysiol*, **82**, 1133-1146.

Maddison P, Newsom-Davis J and Mills KR (1998) Effect of 3,4-diaminopyridine on the time course of decay of compound muscle action potential augmentation in the Lambert-Eaton myasthenic syndrome. *Muscle and Nerve*, **21**, 1196-1198.

Magnus G and Keizer J (1997) Minimal model of β -cell mitochondrial Ca^{2+} handling. *Am J Physiol Cell Physiol*, **273**, C717-C733.

Magleby KL and Zengel JE (1982) A quantitative description of stimulation-induced changes in transmitter release at the frog neuromuscular junction. *J Gen Physiol*, **80**, 613-638.

Mallart A, Dreyer F and Peper K (1976) Current-voltage relation and reversal potential at junctional and extrajunctional ACh-receptors of the frog neuromuscular junction. *Pfluger Arch – Eur J Physiol*, **362**, 43-47.

Martens S, Kozlov M and McMahon HT (2007) How synaptotagmin promotes membrane fusion. *Science*, **316**, 1205-1208.

Matveev V, Zucker RS and Sherman A (2004) Facilitation through buffer saturation: Constraints on endogenous buffering properties. *Biophys J*, **86**, 2691-2709.

Matsumoto M and Riker WK (1983) Synaptic transmission in low extracellular calcium is preserved by 3,4-Diaminopyridine. *J Pharmacol Exp Ther*, **227**, 16-21.

Matthews G and Wickelgren WO (1977) Effects of guanidine on transmitter release and neuronal excitability. *J Physiol (Lond)*, **266**, 69-89.

McEvoy KM, Windebank AJ, Daube JR and Low P (1989) 3,4-Diaminopyridine in the treatment of Lambert-Eaton myasthenic syndrome. *N Engl J Med*, **321**, 1567-1571.

Meinrenken CJ, Borst JG and Sakmann B (2002) Calcium secretion coupling at calyx of held governed by nonuniform channel-vesicle topography. *J Neurosci*, **22**, 1648-1667.

Mennerick S and Matthews G (1996) Ultrafast exocytosis elicited by calcium current in synaptic terminals of retinal bipolar neurons. *Neuron*, **17**, 1241-1249.

Mennerick S and Zorumski CF (1996) Postsynaptic modulation of NMDA synaptic currents in rat hippocampal microcultures by paired-pulse stimulation. *J Physiol*, **490**, 405-417.

Meriney SD and Grinnell AD (1991) Endogenous adenosine modulates stimulation-induced depression at the frog neuromuscular junction. *J Physiol (Lond)*, **443**, 441-455.

Meriney SD, Hulsizer SC, Lennon VA and Grinnell AD (1996) Lambert-Eaton myasthenic syndrome IgG removes multiple types of calcium channels from a human small cell lung cancer cell line. *Annals of Neurology*, **40**, 739-749.

Meunier FA, Feng ZP, Molgo J, Zamponi G and Schiavo G (2002) Glycerotoxin from *Glycera convoluta* stimulates neurosecretion by targeting N-type Ca^{2+} channels $Ca_v 2.2$. *EMBO J*, **21**, 6733-6743.

Miralles F and Solsona C (1998) 3,4-diaminopyridine-induced impairment in frog motor nerve terminal response to high frequency stimulation. *Brain Res*, **789**, 239-244.

Molgo J and Guglielmi JM (1996) 3,4-diaminopyridine, an orphan drug, in the symptomatic treatment of Lambert-Eaton myasthenic syndrome. *Pflugers Archiv – Eur J Physiol*, **431**, R295-R296.

Mulholand J, Wesp A, Riezman H, and Botstein D (1997) Yeast actin cytoskeleton mutants accumulate a new class of Golgi-derived secretory vesicle. *Mol Biol Cell*, **8**, 1481-1499.

Mulligan SJ, Davison I, and Delaney KR (2001) Mitral cell presynaptic Ca^{2+} influx and synaptic transmission in frog amygdala. *Neuroscience*, **104**, 137-151.

Murray NB and Newsom-Davis J (1981) Treatment with oral 4-aminopyridine in disorders of neuromuscular transmission. *Neurology*, **31**, 265-271.

Murray AW (2004) Recycling the cell cycle: cyclins revisited. *Cell*, **116**, 221-234.

Nakajima Y, Kidokoro Y and Klier FG (1980) The development of functional neuromuscular junctions *in vitro*: An ultrastructural and physiological study. *Dev Biol*, **77**, 52-72.

Neher E (1998) Usefulness and limitations of linear approximations to the understanding of Ca^{2+} signals. *Cell Calcium*, **24**, 345-357.

Neves G and Lagnado L (1999) The kinetics of exocytosis and endocytosis in the synaptic terminal of goldfish retinal bipolar cells. *J Physiol*, **515**, 181-202.

Neves G, Gorris A and Lagnado L (2001) Calcium influx selects the fast mode of endocytosis in the synaptic terminal of retinal bipolar cells. *PNAS*, **98**, 15282-15287.

Nieuwkoop PD and Faber J (1967) *Normal Table of Xenopus laevis* (Daudin) N-Holland, Amsterdam.

Nilius B, Hess P, Lansman JB and Tsien RW (1985) A novel type of cardiac calcium channel in ventricular cells. *Nature*, **316**, 443-446.

Nowycky MC, Fox AP, Tsien RW (1985) Long-opening mode of gating of neuronal calcium channels and its promotion by the dihydropyridine calcium agonist BayK 8644. *PNAS*, **82**, 2178-2182.

O'Conner V and Lee AG (2002) Synaptic vesicle fusion and synaptotagmin: 2b or not 2b? *Nat Neurosci*, **5**, 823-824.

Oh SJ and Kim KW (1973) Guanidine hydrochloride in the Eaton-Lambert syndrome: Electrophysiologic improvement. *Neurology*, **23**, 1084-1090.

Oh SJ, Kim DS, Head TC and Claussen GC (1997) Low-dose guanidine and pyridostigmine: relatively safe and effective long-term symptomatic therapy in Lambert-Eaton myasthenic syndrome. *Muscle and Nerve*, **20**, 1146-1152.

Oleskevich S, Clements J and Walmsley B (2000) Release probability modulates short-term plasticity at a rat giant terminal. *J Physiol*, **524**, 513-523.

O'Neill JH, Murray NMF and Newsom-Davis J (1988) The Lambert-Eaton myasthenic syndrome: a review of 50 cases. *Brain*, **111**, 577-596.

Otis T, Zhang S and Trussell LO (1996) Direct measurement of AMPA receptor desensitization induced by glutamatergic synaptic transmission. *J Neurosci*, **16**, 7496-7504.

Palace J, Wiles CM and Newsom-Davis J (1991) 3,4-Diaminopyridine in the treatment of congenital (hereditary) myasthenia. *J Neurol Neurosurg Psychiatry*, **54**, 1069-1072.

Parker D (1995) Depression of synaptic connections between identified motor neurons in the locust. *J Neurophysiol*, **74**, 529-538.

Parnas H, Dudel J and Parnas I (1982) Neurotransmitter release and its facilitation in crayfish. I. Saturation kinetics of release, and of entry and removal of calcium. *Pflugers Archiv – Eur J Physiol*, **393**, 1-14.

Patil PG, Brody DL, and Yue DT (1998) Preferential closed-state inactivation of neuronal calcium channels. *Neuron*, **20**, 1027-1038.

Pattillo JM, Artim DE, Simples JE, and Meriney SD (1999) Variations in onset of action potential broadening: effects on calcium current studied in chick ciliary ganglion neurons. *J Physiol (Lond)*, **514**, 719-728.

Pattillo JM (2002) The relationship between calcium influx and neurotransmitter release: The role of active zone organization studied with Monte Carlo simulations. Ph.D. dissertation, University of Pittsburgh.

Pattillo JM, Meriney SD and Stiles JR (2007) Design principles of neurotransmitter exocytosis predicted by spatially realistic Monte Carlo simulations. (submitted)

Pawson PA, Grinnell AD and Wolowske B (1998a) Quantitative freeze fracture analysis of the frog neuromuscular junction synapse – I. Naturally occurring variability in active zone structure. *J Neurocytol*, **2**, 361-377.

Pawson PA, Grinnell AD and Wolowske B (1998b) Quantitative freeze fracture analysis of the frog neuromuscular junction synapse – II. Proximal-distal measurements. *J Neurocytol*, **2**, 361-377.

Peers C, Johnston I, Lang B and Wray D (1993) Cross-linking of presynaptic calcium channels: a mechanism of action for Lambert-Eaton myasthenic syndrome antibodies at the mouse neuromuscular junction. *Neurosci Lett*, **153**(1), 45-48.

Peper K, Bradley RJ and Dreyer F (1982) The acetylcholine receptor at the neuromuscular junction. *Physiol Rev*, **62**, 1271-1340.

Perin MS, Fried VA, Mignery GA, Jahn R, and Sudhof TC (1990) Phospholipid binding by a synaptic vesicle protein homologous to the regulatory region of protein kinase C. *Nature*, **345**, 260-263.

Peterson BZ, Johnson BD, Hockerman GH, Acheson M, Scheuer T and Catterall WA (1997) Analysis of the dihydropyridine receptor site of L-type calcium channels by alanine-scanning mutagenesis. *J Biol Chem*, **272**(30), 18752-18758.

Pieribone VA, Shupliakov O, Brodin L, Hilfiker-Rothenfluh S, Czernik AJ and Greengard P (1995) Distinct pools of synaptic vesicles in neurotransmitter release. *Nature*, **375**, 493-497.

Pinto A, Iwasa K, Newland C, Newsom-Davis J and Lang B (2002) The action of Lambert-Eaton myasthenic syndrome immunoglobulin G on cloned human voltage-gated calcium channels. *Muscle Nerve*, **25**(5), 715-724.

Poage RE, Meriney SD, Gundersen CB, and Umbach JA (1999) Antibodies against cysteine string proteins inhibit evoked neurotransmitter release at *Xenopus* neuromuscular junctions. *J Neurophysiol*, **82**, 50-59.

Poage RE and Meriney SD (2002) Presynaptic calcium influx, neurotransmitter release, and neuromuscular disease. *Physiology and Behavior*, **77**(4-5), 507-512.

Poage RE and Zengel JE (2002) Repolarization of the presynaptic action potential and short-term synaptic plasticity in the chick ciliary ganglion. *Synapse*, **46**, 189-198.

Prekeris R and Terrian DM (1997) Brain myosin V is a synaptic vesicle-associated motor protein: evidence for a calcium-dependent interaction with the synaptobrevin-synaptophysin complex. *J Cell Biol*, **137**, 1589-1601.

Pumplin DW, Reese TS and Llinas R (1981) Are the presynaptic membrane particles the calcium channels? *PNAS*, **78**, 7210-7213.

Quastel DM, Guan YY, and Saint DA (1992) The relation between transmitter release and Ca^{2+} entry at the mouse motor nerve terminal: role of stochastic factors causing heterogeneity. *Neuroscience*, **51**, 657-671.

Regehr WG, Delaney KR and Tank DW (1994) The role of presynaptic calcium in short-term enhancement at the hippocampal mossy fiber synapse. *J Neurosci*, **14**, 523-537.

Rettig J and Neher E (2002) Emerging roles of presynaptic proteins in Ca^{2+} -triggered exocytosis. *Science*, **298**, 781-785.

Richards DA, Guatimosim C and Betz WJ (2000) Two endocytic recycling routes selectively fill two vesicle pools in frog motor nerve terminals. *Neuron*, **27**, 551-559.

Richards DA, Guatimosim C, Rizzoli SO and Betz WJ (2003) Synaptic vesicle pools at the frog neuromuscular junction. *Neuron*, **39**, 529-541.

Rivosecchi R, Pongs O, Theil T and Mallart A (1994) Implication of frequenin in the facilitation of transmitter release in *Drosophila*. *J Physiol*, **474**, 223-232.

Rizzoli SO and Betz WJ (2004) The structural organization of the readily releasable pool of synaptic vesicles. *Science*, **303**, 2037-2039.

Rizzoli SO and Betz WJ (2005) Synaptic vesicle pools. *Nat Rev Neurosci*, **6**, 57-69.

Robitaille R, Adler EM and Charlton MP (1990) Strategic location of calcium channels at transmitter release sites of frog neuromuscular synapses. *Neuron*, **5**, 773-779.

Robitaille R, Garcia ML, Kaczorowski GJ and Charlton MP (1993) Functional colocalization of calcium and calcium-gated potassium channels in control transmitter release. *Neuron*, **11**, 645-655.

Rogawski MA (1988) Transient outward current (I_A) in cloned anterior pituitary cells: blockade by aminopyridine analogs. *Naunyn-Schiedeberg's Arch Pharmacol*, **338**, 125-132.

Rosahl TW, Spillane D, Missler M, Herz J, Selig DK, Wolff JR, Hammer RE, Malenka RC and Sudhof TC (1995) Essential functions of synapsins I and II in synaptic vesicle regulation. *Nature*, **375**, 488-493.

Rozov A, Burnashev N, Sakmann B and Neher E (2001) Transmitter release modulation by intracellular Ca²⁺ buffers in facilitating and depressing nerve terminals of pyramidal cells in layer 2/3 of the rat neocortex indicates a target cell-specific difference in presynaptic calcium dynamics. *J Physiol*, **531**, 807-826.

Ryan TA, Reuter H, Wendland B, Schweizer FE, Tsien RW, and Smith SJ (1993) The kinetics of synaptic vesicle recycling measured at single presynaptic boutons. *Neuron*, **11**, 713-724.

Ryan TA and Smith SJ (1995) Vesicle pool mobilization during action potential firing at hippocampal synapses. *Neuron*, **14**, 983-989.

Ryan TA, Li L, Chin LS, Greengard P and Smith SJ (1996) Synaptic vesicle recycling in synapsin I knock-out mice. *J Cell Biol*, **134**(5), 1219-1227.

Ryan TA (1999) Inhibitors of myosin light chain kinase block synaptic vesicle pool mobilization during action potential firing. *J Neurosci*, **19**(4), 1317-1323.

Sabatini BL and Regehr WG (1996) Timing of neurotransmission at fast synapses in the mammalian brain. *Nature*, **384**, 170-172.

Sabatini BL and Regehr WG (1999) Timing of synaptic transmission. *Annu Rev Physiol*, **61**, 521-542.

Sand O, Chen BM and Grinnell AD (2001) Contribution of L-type Ca²⁺ channels to evoked transmitter release in cultured *Xenopus* nerve-muscle synapses. *J Physiol*, **536.1**, 21-33.

Sanders DB (1995) Lambert-Eaton myasthenic syndrome: Clinical diagnosis, immune-mediated mechanisms, and update of therapies. *Annals of Neurology*, **35**, (supplement 5S) 63S-73S.

Sanders DB, Massey JM, Sanders LL and Edwards LJ (2000) A randomized trial of 3,4-diaminopyridine in Lambert-Eaton myasthenic syndrome. *Neurology*, **54**, 603-607.

Sanguinetti MC, Krafte DS and Kass RS (1986) Voltage-dependent modulation of Ca channel current in heart cells by BayK 8644. *J Gen Physiol*, **88**, 369-392.

Satoh H, Katoh H, Velez P, Fill M and Bers DM (1998) Bay K 8644 increases resting Ca²⁺ spark frequency in ferret ventricular myocytes independent of Ca influx. *Circulation Res*, **83**, 1192-1204.

Sausville EA (2002) Complexities in the development of cyclin-dependent kinase inhibitor drugs. *Trends Mol Med*, **8**(4 Suppl), S32-37.

Scanziani M, Salin PA, Vogt KE, Malenka RC, and Nicoll RA (1997) Use-dependent increases in glutamate concentration activate presynaptic metabotropic glutamate receptors. *Nature*, **385**, 630-634.

Schiavo G, Stenbeck G, Rothman JE and Sollner TH (1997) Binding of the synaptic vesicle v-snare, synaptotagmin, to the plasma membrane t-snare, snap-25, can explain docked vesicles at neurotoxin-treated synapse. *PNAS*, **94**, 997-1001.

Schneggenburger R, Meyer AC and Neher E (1999) Released fraction and total size of a pool of immediately available transmitter quanta at a calyx synapse. *Neuron*, **23**, 399-409.

Schneggenburger R and Neher E (2000) Intracellular calcium dependence of transmitter release rates at a fast central synapse. *Nature*, **406**, 889-893.

Schneggenburger R and Neher E (2005) Presynaptic calcium and control of vesicle fusion. *Curr Opin Neurobiol*, **15**, 266-274.

Seo WS, Shin JH and Suh CK (1999) 4-aminopyridine (4-AP) augments Ca^{2+} -dependent action potential and changes oscillatory firing patterns in rat cerebellar Purkinje cells. *Yonsei Med J*, **40**, 112-117.

Shahrezaei V and Delaney KR (2004) Consequences of molecular-level Ca^{2+} channel and synaptic vesicle colocalization for the Ca^{2+} microdomain and neurotransmitter exocytosis: a Monte Carlo study. *Biophys J*, **87**, 2352-2364.

Shahrezaei V, Cao A and Delaney KR (2006) Ca^{2+} from one or two channels controls fusion of a single vesicle at the frog neuromuscular junction. *J Neurosci*, **26** (51), 13240-13249.

Shelton SB and Johnson GV (2004) Cyclin-dependent kinase-5 in neurodegeneration. *J Neurochem*, **88**, 1313-1326.

Silbert PL, Hankey GJ and Barr AL (1990) Successful alternate day guanidine therapy following guanidine-induced neutropenia in Lambert-Eaton myasthenic syndrome. *Muscle and Nerve* **13**, 360-361.

Silver RA, Momiyama A, Cull-Candy SG (1998) Locus of frequency-dependent depression identified with multiple-probability fluctuation analysis at rat climbing fibre-Purkinje cell synapses. *J Physiol*, **510**, 881-902.

Sinnegger MJ, Wang Z, Grabner M, Hering S, Striessnig J, Glossmann H and Mitterdorfer J (1997) Nine L-type amino acid residues confer full 1,4-Dihydropyridine sensitivity to the neuronal calcium channel α 1A subunit. *J Biol Chem*, **272**(44), 27686-27693.

Smart JL and McCammon JA (1998) Analysis of synaptic transmission in the neuromuscular junction using a continuum finite element model. *Biophys J*, **75**, 1679-1688.

Smith D (2003) Cdk5 in neuroskeletal dynamics. *Neurosignals*, **12**, 239-251.

Smith DO, Conklin MW, Jensen PJ and Atchison WD (1995) Decreased calcium currents in motor nerve terminals of mice with Lambert-Eaton myasthenic syndrome. *J Physiol*, **487**, 115-123.

Smith SJ, Augustine GJ and Charlton MP (1985) Transmission at voltage-clamped giant synapse of the squid: Evidence for cooperativity of presynaptic calcium action. *PNAS*, **82**, 622-625.

Spafford JD and Zamponi GW (2003) Functional interactions between presynaptic calcium channels and the neurotransmitter release machinery. *Curr Opin Neurobiol*, **13**, 308-314.

Spitzer NC (1979) Ion channels in development. *Ann Rev Neurosci*, **2**, 363-395.

Stanley EF (1986) Decline in calcium cooperativity as the basis of facilitation at the squid giant synapse. *J Neurosci*, **6**, 782-789.

Stanley EF (1993) Single calcium channels and acetylcholine release at a presynaptic nerve terminal. *Neuron*, **11**, 1007-1011.

Stanley EF (1997) The calcium channel and the organization of the presynaptic transmitter release face. *TINS*, **20**, 404-409.

Stefani A, Pisani A, Mercuri NB, Calabresi P (1996) The modulation of calcium currents by the activation of mGluRs: functional implications. *Mol Neurobiol*, **13**, 81-95.

Stevens CF and Wesseling JF (1999) Augmentation is a potentiation of the exocytotic process. *Neuron*, **22**, 139-146.

Stewart BA, Mohtashami M, Trimble WS, and Boulianne GL (2000) SNARE proteins contribute to calcium cooperativity of synaptic transmission. *PNAS*, **97**, 13955-13960.

Stiles JR and Bartol TM (2000) Monte Carlo methods for simulating realistic synaptic microphysiology using MCell. In *Computational neuroscience: Realistic modeling for experimentalists*, ed. DeSchutter E, pp.87-127, CRC Press.

Stiles JR, Bartol TM, Salpeter MM, Salpeter EE and Sejnowski TJ (2001) Synaptic variability: New insights from reconstructions and Monte Carlo simulations with MCell. In *Synapses*, ed. Cowan WM, Sudhof TC and Stevens CF, pp.681-731, The Johns Hopkins University Press.

Sturek M and Hermsmeyer K (1986) Calcium and sodium channels in spontaneously contracting vascular muscle cells. *Science*, **233**, 475-478.

Sudhof TC and Rizo J (1996) Synaptotagmins: C2-domain proteins that regulate membrane traffic, *Neuron*, **17**, 379-388.

Sudhof TC (2004) The synaptic vesicle cycle. *Annu Rev Neurosci*, **27**, 509-547.

Sugita S, Shin OH, Han W, Lao Y, and Sudhof TC (2002) Synaptotagmins form a hierarchy of exocytotic Ca^{2+} sensors with distinct Ca^{2+} affinities. *EMBO J*, **21**, 270-280.

Sun JY, Wu XS and Wu LG (2002) Single and multiple vesicle fusion induce different rates of endocytosis at a central synapse. *Nature*, **417**, 555-559.

Swandulla D, Hans M, Zipser K and Augustine GJ (1991) Role of residual calcium in synaptic depression and posttetanic potentiation: fast and slow calcium signaling in nerve terminals. *Neuron*, **7**, 915-926.

Takahashi T, Nakajima Y, Hirokawa K, Nakajima S and Onodera K (1987) Structure and physiology of developing neuromuscular synapses in culture. *J Neurosci*, **7**, 473-481.

Takahashi T, Forsythe ID, Tsujimoto T, Barnes-Davis M, and Onodera K (1996) Presynaptic calcium current modulation by a metabotropic glutamate receptor. *Science*, **274**, 594-597.

Takeuchi A and Takeuchi N (1959) Active phase of frog's end-plate potential. *J Neurophysiol*, **22**, 395-411.

Talbot JD, David G and Barrett EF (2003) Inhibition of mitochondrial Ca^{2+} uptake affects phasic release from motor terminals differently depending on external $[\text{Ca}^{2+}]$. *J Neurophysiol*, **90**, 491-502.

Tanabe N and Kijima H (1992) Ca^{2+} -dependent and Ca^{2+} -independent components of transmitter release at the frog neuromuscular junction. *J Physiol*, **455**, 271-289.

Tang Y, Schlumberger T, Kim T, Lueker M and Zucker RS (2000) Effects of mobile buffers on facilitation: experimental and computational studies. *Biophys J*, **78**, 2735-2751.

Thaler C, Li W and Brehm P (2001) Calcium channel isoforms underlying synaptic transmission at embryonic *Xenopus* neuromuscular junctions. *J Neurosci*, **21**, 412-422.

Thompson S (1982) Aminopyridine block of transient potassium current. *J Gen Physiol*, **80**, 1-18.

Thomsen RH and Wilson DF (1983) Effects of 4-aminopyridine and 3,4-diaminopyridine on transmitter release at the neuromuscular junction. *J Pharmacol Exp Ther*, **227**, 260-265.

Thomson AM (2000) Facilitation, augmentation and potentiation at central synapses. *Trends Neurosci*, **23**, 305-312.

Tim RW, Massey JM and Sanders DB (2000) Lambert-Eaton myasthenic syndrome: electrodiagnostic findings and response to treatment. *Neurology*, **54**, 2176-2178.

Tomizawa K, Ohta J, Matsushita M, Moriwaki A, Li ST, Taker K and Matsui H (2002) Cdk5/p35 regulates neurotransmitter release through phosphorylation and downregulation of P/Q-type voltage-dependent calcium channel activity. *J Neurosci*, **22**, 2590-2597.

Tong JJ (2007) Mitochondrial delivery is essential for synaptic potentiation. *Biol Bull*, **212**, 169-175.

Trifaro JM, Glavinovic M and Rose SD (1997) Secretory vesicle pools and rate and kinetics of single vesicle exocytosis in neurosecretory cells. *Neurochem Res*, **22**(7), 831-841.

Triggle DJ (2003) Drug targets in the voltage-gated calcium channel family: why some are and some are not. *Assay Drug Dev Technol*, **1**, 719-733.

Trussell LO and Fischbach GD (1989) Glutamate receptor desensitization and its role in synaptic transmission. *Neuron*, **3**, 209-218.

Trussell LO, Zhang S, and Raman IM (1993) Desensitization of AMPA receptors upon multiquantal neurotransmitter release. *Neuron*, **10**, 1185-1196.

Tsien RW, Lipscombe D, Madison DV, Bley KR and Fox AP (1988) Multiple types of neuronal calcium channels and their selective modulation. *Trends Neurosci*, **11**, 431-438.

Ubach J, Zhang X, Shao X, Sudhof TC, and Rizo J (1998) Ca^{2+} binding to synaptotagmin: how many Ca^{2+} ions bind to the tip of a C2-domain? *EMBO J*, **17**, 3921-3930.

Ullrich B, Li C, Zhang JZ, McMahon H, Anderson RGW, Geppert M, and Sudhof TC (1994) Functional properties of multiple synaptotagmins in brain. *Neuron*, **13**, 1281-1291.

Van der Kloot W and Molgo J (1993) Facilitation and delayed release at about 0 °C at the frog neuromuscular junction: effects of calcium chelators, calcium transport inhibitors, and okadaic acid. *J Neurophysiol*, **69**, 717-729.

Vincent A, Lang B and Newsom-Davis J (1989) Autoimmunity to the voltage-gated calcium channel underlies the Lambert-Eaton myasthenic syndrome, a paraneoplastic disorder. *Trends Neurosci*, **12**, 496-502.

Von Gersdorff H and Matthews G (1994) Dynamics of synaptic vesicle fusion and membrane retrieval in synaptic terminals. *Nature*, **367**, 735-739.

Von Gersdorff H and Matthews G (1997) Depletion and replenishment of vesicle pools at a ribbon-type synaptic terminal. *J Neurosci*, **17**, 1919-1927.

Vyshedskiy A, Allana T and Lin JW (2000) Analysis of presynaptic Ca^{2+} influx and transmitter release kinetics during facilitation at the inhibitor of the crayfish neuromuscular junction. *J Neurosci*, **20**, 6326-6332.

Wachman ES, Poage RE, Stiles JR, Farkas DL and Meriney SD (2004) Spatial distribution of calcium entry evoked by single action potentials within the presynaptic active zone. *J Neurosci*, **24**, 2877-2885.

Wang XY and Lambert NA (2000) GABA(B) receptors couple to potassium and calcium channels on identified lateral perforant pathway projection neurons. *J Neurophysiol*, **83**, 1073-1078.

Weldon PR and Cohen MW (1979) Development of synaptic ultrastructure at neuromuscular contacts in an amphibian cell culture system. *J Neurocytol*, **8**, 239-259.

Winslow JL, Duffy SN and Charlton MP (1994) Homosynaptic facilitation of transmitter release in crayfish is not affected by mobile calcium chelators: implications for the residual ionized calcium hypothesis from electrophysiological and computational analyses. *J Neurophysiol*, **72**, 1769-1793.

Wright SN, Brodwick MS and Bittner GD (1996) Calcium currents, transmitter release and facilitation of release at voltage-clamped crayfish nerve terminals. *J Physiol*, **496**, 363-378.

Wu LG and Saggau P (1994) Presynaptic calcium is increased during normal synaptic transmission and paired-pulse facilitation, but not in long-term potentiation in area CA1 of hippocampus. *J Neurosci*, **14**, 645-654.

Xu J, Mashimo T, Sudhof TC (2007) Synaptotagmin-1, -2, and -9: Ca²⁺ sensors for fast release that specify distinct presynaptic properties in subsets of neurons. *Neuron*, **54**(4), 567-581.

Xu T, Naraghi M, Kang H and Neher E (1997) Kinetic studies of Ca²⁺ binding and Ca²⁺ clearance in the cytosol of adrenal chromaffin cells. *Biophys J*, **73**, 532-545.

Xu W and Lipscombe D (2001) Neuronal $\text{Ca}_v1.3$ $\alpha(1)$ L-type channels activate at relatively hyperpolarized membrane potentials and are incompletely inhibited by dihydropyridines. *J Neurosci*, **21**, 5944-5951.

Xu-Friedman MA and Regehr WG (2004) Structural contributions to short-term synaptic plasticity. *Physiol Rev*, **84**, 69-85.

Yamaguchi S, Okamura Y, Nagao T and Adachi-Akahane S (2000) Serine residue in the IIIIS5-S6 linker of the L-type Ca^{2+} channel 1C subunit is the critical determinant of the action of dihydropyridine Ca^{2+} channel agonists. *J Biol Chem*, **272**(52), 41504-41511.

Yamaguchi S, Zhorov BS, Yoshioka K, Nagao T, Ichijo H and Adachi-Akahane S (2003) Key roles of Phe¹¹¹² and Ser¹¹¹⁵ in the pore-forming IIIIS5-S6 linker of L-type Ca^{2+} channel $\alpha 1C$ subunit (Ca_v 1.2) in binding of dihydropyridines and action of Ca^{2+} channel agonists. *Mol Pharmacol*, **64**(2), 235-248.

Yan Z, Chi P, Bibb JA, Ryan TA and Greengard P (2002) Roscovitine: a novel regulator of P/Q-type calcium channels and transmitter release in central neurons. *J Physiol (Lond)*, **540**, 761-770.

Yazejian B, DiGregorio DA, Vergara JL, Poage RE, Meriney SD and Grinnell AD (1997) Direct measurements of presynaptic calcium and calcium-activated potassium currents regulating neurotransmitter release at cultured *Xenopus* nerve-muscle synapses. *J Neurosci*, **17**, 2990-3001.

Yazejian B, Sun XP and Grinnell AD (2000) Tracking presynaptic Ca^{2+} dynamics during neurotransmitter release with Ca^{2+} -activated K^+ channels. *Nat Neurosci*, **3**, 566-571.

Yoshihara M, Adolfsen B, Galle KT and Littleton JT (2005) Retrograde signaling by Syt 4 induces presynaptic release and synapse-specific growth. *Science*, **310**, 858-863.

Yoshikami D, Balgabaldo Z and Olivera BM (1989) The inhibitory effects of omega-conotoxins on Ca channels and synapses. *Ann NY Acad Sci*, **560**, 230-248.

Zhang X, Rizo J, and Sudhof TC (1998) Mechanism of phospholipids binding by the C2A-domain of synaptotagmin I. *Biochemistry*, **37**, 12395-12403.

Zucker RS and Fogelson AL (1986) Relationship between transmitter release and presynaptic calcium influx when calcium enters through discrete channels. *PNAS*, **83**, 3032-3036.

Zucker RS, Delaney KR, Mulkey R and Tank DW (1991) Presynaptic calcium in transmitter release and posttetanic potentiation. *Ann NY Acad Sci*, **635**, 191-207.

Zucker RS and Regehr WG (2002) Short-term synaptic plasticity. *Annu Rev Physiol*, **64**, 355-405.